Design of LP_{01} to LP_{lm} Mode Converters for Mode Division Multiplexing

Hakim Mellah

A Thesis

In the Department

of

Electrical and Computer Engineering

Presented in Partial Fulfillment of the Requirements

For the Degree of

Doctor of Philosophy (Electrical and Computer Engineering) at

Concordia University

Montreal, Quebec, Canada

June 2018

CONCORDIA UNIVERSITY

School of Graduate Studies

This is to certify that the thesis prepared

By: Hakim Mellah

Entitled: Design of LP_{01} to LP_{lm} Mode Converters for Mode Division Multiplexing

and submitted in partial fulfillment of the requirements for the degree of

Doctor of Philosophy (Electrical and Computer Engineering)

complies with the regulations of the University and meets the accepted standards with respect to originality and quality.

Signed by the final Examining Committee:

_____ Chair
Dr. S. Samuel Li

_____ External Examiner
Dr. Lawrence R. Chen

_____ External to Program
Dr. Pablo Bianucci

_____ Examiner
Dr. Ahmed A. Kishk

_____ Examiner
Dr. Christopher W. Trueman

_____ Thesis Supervisor
Dr. John Xiupu Zhang

Approved by _____
Dr. Mustafa K. Mehmet Ali, Graduate Program Director

Thursday, August 30, 2018 _____

Dr. Amir Asif, Dean
Faculty of Engineering & Computer Science

ABSTRACT

Design of LP_{01} to LP_{lm} Mode Converters for Mode Division Multiplexing

Hakim Mellah, Ph.D.

Concordia University, 2018

Mode division multiplexing (MDM) over few mode fiber (FMF) has been proposed as an alternative solution to tackle the capacity limitations of optical networks based on standard single mode fiber (SMF). These limitations are caused by the fiber nonlinear effects. MDM is realized through excitation of different fiber spatial modes, each mode being an independent transmission channel. Therefore, MDM over FMF requires mode conversion (basically from fundamental mode to higher order modes and vice versa) as well as mode multiplexing and demultiplexing.

Mode conversion, multiplexing and demultiplexing can be realized through different techniques. It can be achieved using free-space optics based on matching the profile of an input mode to the profile of an output mode using phase mask or spatial light modulator. Mode conversion and (de)multiplexing can also be achieved using waveguide structures. These mode converters and (de)multiplexers are mainly based on optical fiber and planar waveguide, which include fiber grating, tapering, lanterns, planar lightwave circuit (PLC), photonic crystal fiber (PCF), mode selective coupler (MSC) and Y-junction. It is worth mentioning that more than one technique may be applied to realize a specific converter/ (de)multiplexer for a specific mode.

In general, Mode converters and (de)multiplexers based on free space optics are polarization insensitive and wavelength independent, but they result in high insertion loss and are bulky. On the other hand, all-waveguide mode converters and (de)multiplexers have high mode conversion efficiency (less insertion loss and high extinction ratio) and are compact, but they are wavelength dependent.

Recently, many research works demonstrate the design, analysis and fabrication of several types of mode converters and (de)multiplexers. However, almost all the proposed devices are specific to a certain number of modes, therefore, they result in mode-specific designs.

The explosive growth of traffic over telecommunication networks, especially in the access networks mandates that more and more modes would be (de)multiplexed to respond to the high traffic demands. As a result, proposing a universal mode converter and (de)multiplexer, that can convert and (de)multiplex any required number of modes is needed.

In this thesis, mode converters and (de)multiplexers are thoroughly investigated. A universal LP_{01} to LP_{lm} mode converter and (de)multiplexer is proposed. The mode converter is based on tapered circular waveguides and the (de)multiplexer is based on symmetric directional couplers.

An LP_{01} to LP_{02} is first introduced. It consists of a tapered circular waveguide followed by a non-tapered circular waveguide. Inside the second waveguide, a circular tapered element is inserted. The initial tapered waveguide allows excitation of LP02 mode as well as other LP0m modes (m > 2). The second waveguide (comprising the circular section and the inner tapered element) is used to make conversion to be mainly from LP01 to LP02. Simulation shows that conversion efficiency of almost 100% at the central wavelength of O- S- and C-band, and above 98% over the S- and C-band is achieved. Moreover, suppression of non-desired higher order modes is more than 10 dB over the whole O-, S- and C-band. In particular, suppression is more than 19 dB over the entire C-band. The analysis also shows that the performance of the mode converter is not sensitive to slight variations of the converter's parameters. In addition, the same converter can be used for converting LP_{02} back to LP_{01}. Further, a (de)multiplexer for an LP_{02} and an LP_{01} mode is designed using the mode converter combined with a symmetric directional coupler. The multiplexer is broadband and has insertion loss less than 0.5 dB over the C-band.

The proposed design is fabricated by inscribing it in the bulk of a borosilicate glass using a femtosecond laser. The converter has an insertion loss of less than 1 dB for the entire C-band and a total length of 2.22mm. this fabricated prototype validates the proposed mode converter design.

The LP_{01} to LP_{02} mode converter structure can also be used to convert to other LP_{0m} mode by proper tuning its parameters. After extensive simulations and optimizations, an LP_{01} to LP_{0m} mode converter is proposed. The proposed converter structures are designed not only to provide high performances (low insertion losses and high extinction ratios), but also to be able to be fabricated by respecting the fabrication requirements (in terms of lengths and refractive indices). As a case study, six mode converters, converting LP_{01} to LP_{0m}, with m = 2 to 7 are reported. The structures have insertion losses ranging from 0.1 dB to 2.5 dB. These performance results outperform all reported similar mode converters.

To (de)multiplex the resulting LP_{0m} modes, a (de)multiplexer based on symmetric directional couplers is proposed. This kind of devices are easy to design and fabricate and provide low insertion loss and cross talk. As an example, the first five modes (LP_{01} to LP_{05}) are (de)multiplexed with an insertion loss less than 2.5 dB and cross talk less than -15 dB at the design wavelength. These results outperform the reported results for similar devices.

The LP_{01} to LP_{0m} mode converter structure is modified by inserting more inner elements to be able to convert to any LP_{lm} mode. Therefore, a universal LP mode converter structure is proposed. The number and parameters of these inner elements depend on the desired LP_{lm} mode. For instance, structures to convert LP_{01} to LP_{11}, LP_{21} and LP_{31} are provided. These modes require between 5 to 6 inner elements with different radii and lengths. The simulation results for these three structures shows that an insertion loss less than 1.9 dB and an extinction ratio higher than 10 dB are achieved for the three modes at the design wavelength of 1550nm.

Furthermore, the three modes (LP_{11}, LP_{21} and LP_{31}) are (d)multiplexed using a symmetric directional coupler with an insertion loss less than 0.9 dB and a cross talk below -17 dB for the three modes at the design wavelength.

All the parameters of the presented mode converters and (de)multiplexers are designed to allow them to be fabricated using 3D femtosecond laser inscription technique.

Acknowledgments

I would like to express my sincere gratitude to my supervisor Prof. John Xiupu Zhang for his continuous help, advice and support for me to finish this thesis.

I am grateful my parents for their unconditional love, guidance and endless support.

I would like to thank my wife and my children for being patient with me during my endless hours of work.

I would also like to thank all my colleagues who were an inspiration for me throughout my research journey at Concordia university.

TABLE OF CONTENTS

List of Figures

List of Tables

List of Abbreviations

dB	Decibel
DC	Directional Coupler
DEMUX	Demultiplexer
DSP	Digital Signal Processing
EME	Eigen Mode Expansion
ER	Extinction Ratio
FCF	Few-Core Fiber
FMA	Few Mode Amplifier
FMF	Few-Mode Fiber
FWHM	Full-Width at Half Maximum
IL	Insertion Loss
LCoS	Liquid Crystal on Silicon
LP	Linearly Polarized
LPFG	Long Period Fiber Grating
MC	Mode Converter
MDM	Mode Division Multiplexing
MFD	Mode Field Diameter
MIMO	Multi-Input Multi-Output

MMF	Multi-Mode Fiber
MMI	Multi-Mode Interference
MSC	Mode Selective Coupler
MUX	Multiplexer
NA	Numerical Aperture
PCF	Photonic Crystal Fiber
PLC	Planar Lightwave Circuit
QPSK	Quadrature Phase Shift Keying
SDM	Space Division Multiplexing
SLM	Spatial Light Modulator
SMF	Single-Mode Fiber
SOI	Silicon-On-Insulator
TE	Transverse Electric
TM	Transverse Magnetic
WDM	Wavelength Division Multiplexing

List of Symbols

β	Mode propagation constant
Δn	Difference in refractive indices
λ	Wavelength
κ	Coupling coefficient
e_a	Electric field of modes *a*
ER	Extinction ratio
IL	Insertion loss
$J_n()$	n^{th} order Bessel function
k	The wavenumber
$K_n()$	n^{th} order Modified Bessel function
L_i	Length of section *i* in μm
NA	Numerical aperture
n_{eff}	Effective refractive index
n_i	Refractive index of section *i*
P_{in}	Optical input power
P*out*	Optical output power
r_i	Radius of section *i* in μm
V	Normalized frequency

Chapter 1: Introduction

1.1 Mode Division Multiplexing Systems

The explosive growth of communication traffic has pushed optical transport networks, which are based on standard single mode fiber (SMF), to reach the capacity limits of the SMF due to Kerr fiber nonlinearity effect. Even if substantial reduction in losses and nonlinear effects in SMF are obtained, it is expected that the resulting increase in the SMF capacity will not be significant[1]–[4].

Optical space and mode division multiplexing (SDM/MDM) [5]–[7], a new multiplexing dimension for optical fiber links, has received recently increasing attention by the researchers' community as well as the industry players [8]–[11]. It is a promising technique to increase fiber link throughputs and overcome the capacity limitations of the SMF and enable the implementation of optical multiple-input and multiple-output (MIMO) systems with a single wavelength [12]–[16].

SDM transmissions are based on fibers that are supporting multiple spatial modes, which can be deployed using few mode fiber (FMF), or based on few core fiber (FCF) [6], [7], [17]–[24].

In SDM over FCF [25]–[27], suppression of coupling between modes is required to minimize the crosstalk. This is achieved by making large separations between cores. However, this requirement limits the spatial density of cores and makes the fabrication of such fibers challenging. Each core (typically a single mode) is an independent channel; therefore, the capacity of the system is scaled with the number of cores inside the same fiber. The performance of SDM over FCF is limited by the crosstalk between the different cores and depends also on cores configuration [25], [28]–[30].

In SDM over FMF, i.e. MDM, coupling between modes is permitted, which lowers the fabrication requirements but requires the use of some forms of MIMO signal processing at the receiver [16].

Figure 1-1. shows a typical block diagram of an optical transmission system using MDM over FMF, where six modes are considered as an example. At the transmitter side, six transmitters (e.g., lasers) are used; and each one excites the fundamental mode (e.g., the LP_{01}) of a SMF. All transmitters use the same wavelength (which simplifies the design). Five of these transmitters are connected to mode converters to convert each of the LP_{01} modes to a higher order mode (here, LP_{11a}, $LP_{11b,}$ LP_{21a}, LP_{21b} and LP_{02}) of an FMF. These six modes (having different field profiles and/or propagation constants and/or different polarization) are multiplexed (by the MUX) into a 4-mode FMF. At the receiver side, the demultiplexer (DEMUX) separates the different spatial modes. For simplifying the design, each of the higher order mode is converted back to the fundamental LP_{01} mode, so that all the receivers are similar, and then received by six receivers. Other functions, such as amplification (using the few mode amplifier FMA) and MIMO processing, are also part of the system. Usually, the mode converter and (de)multiplexer together are called mode (de)multiplexer, in which the mode conversion is the key for mode multiplexing and demultiplexing.

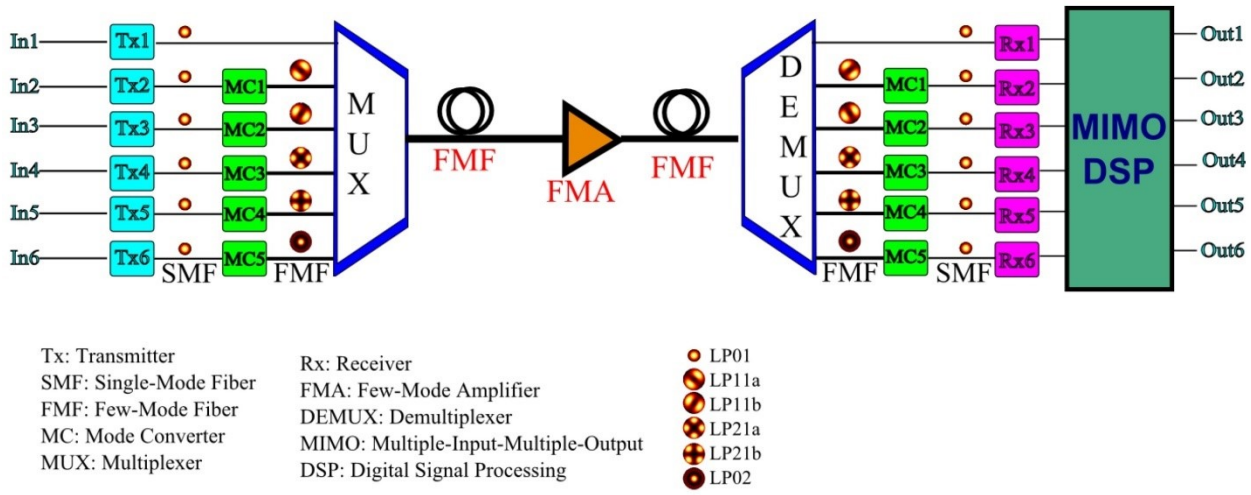

Figure 1-1: Block Diagram of MDM System

Several experiments have been reported demonstrating the SDM over FMF and FCF. For instance, a transmission of six independent (spatial and polarization modes) QPSK signals with data rate of 40Gbps over 96km using three-mode fiber was reported in [31]. In another experiment

[32], two channels each carrying 100Gbps QPSK signals for 100km over a two-mode fiber was demonstrated.

Despite the complex MIMO and DSP processing at the receiver using FMF and the fabrication requirements for FCF, such experiments are more than a proof of concept of the viability of MDM over FMF and SDM over FCF and their potentials for long haul telecommunications systems.

Using FMF for carrying more than one signal (using a single wavelength) requires the use of different spatial modes, which are (de)multiplexed at certain points in the link. Higher order modes can either be excited directly inside the fiber or result from the conversion of another mode (basically the fundamental mode). Therefore, mode conversion (MC) and (de)multiplexing (MUX/DEMUX) are very important functions in transmission systems using FMF. The different techniques used for mode conversion and (de)multiplexing are presented in the next chapter.

1.2. Motivations and Contributions

Mode and space division multiplexing (MDM/SDM) are based on mode converters and mode (de)multiplexers. These devices are an integral part of any MDM/SDM system and their performances, in terms of insertion loss, extinction ration, size and crosstalk, affect the implementation of these systems.

Most designs of mode converters and (de)multiplexers are based on waveguide structures. This type of devices provides low losses and crosstalk and result in small size structures.

Waveguide-based mode converters and (de)multiplexers tend to be wavelength sensitive, which means they can operate in a narrow wavelength bandwidth, however, some design can result in a broadband operation.

In this thesis, the research focuses mainly on the design and analysis of a tapered-based mode converter structure that can convert LP_{01} mode to any LP_{lm} mode. Furthermore, the main contributions of this work include:

1) The design, performance analysis and fabrication of an LP_{01} to LP_{02} mode converter based on a tapered waveguide structure. The device can operate over the entire C-Band (from 1530nm to 1565nm) with an insertion loss less than 0.5dB and an extinction

ration above 15dB. These two modes are then (de)multiplexed using symmetric directional couplers.

2) The design and performance analysis of an LP_{01} to LP_{0m} mode converter and (de)multiplexer. The converter structure is based on the LP_{01} to LP_{02} structure and the (de)multiplexer is based on directional couplers. By choosing the correct structure parameter, the desired LP_{0m} mode converter can be obtained. Optimization algorithms can be applied to optimize the structure parameters for a desired LP_{0m} mode.
3) The LP_{01} to LP_{0m} mode converter structure is further modified to allow conversion from LP_{01} to any LP_{lm} mode. The proposed converter structure can be used as a framework and its parameters can be optimized for any desired output LP_{lm} mode.

1.3. Organization of the Thesis

In this chapter, a brief introduction about mode and space division multiplexing systems has been introduced. The different components of such systems have been briefly stated. The motivations and contributions of this research have been outlined.

In chapter 2, the background and literature review of mode division multiplexing components, especially mode converters and mode (de)multiplexers are given.

In chapter 3, the design, performance analysis and fabrication results of the proposed LP_{01} to LP_{02} mode converter is presented. The design and simulation results of a symmetric directional coupler to (de)multiplex the LP_{01} and LP_{02} modes are also provided.

In chapter 4, an LP_{01} to LP_{0m} mode converter is designed and its performances are analyzed. A mode (de)multiplexer is also presented and its performances are evaluated.

In chapter 5, a more general mode converter structure is proposed. It can convert LP_{01} mode to any desired LP_{lm} mode.

In chapter 6, the summary of the research is provided and future works on mode converters and (de)multiplexers for mode division multiplexing systems are suggested.

Chapter 2: Literature Review

2.1 Introduction

Mode division multiplexing (MDM) uses the orthogonal guided optical modes of the few mode fibers to carry different optical signals, i.e. one mode corresponding to one optical channel [33]. Therefore, mode converters/(de)multiplexers are required at optical transmitters and receivers. In other words, mode conversion from fundamental to higher order modes is required at optical transmitters, while mode conversion from higher-order modes to the fundamental modes is usually required at optical receivers [17].

Mode converters and (de)multiplexers can be classified into two big classes: free-space optics-based and waveguide-based (including fiber based). The details of these two classes are outlined in the next sections.

2.2. Free-Space Optic Mode Converters

Free-space optic mode converters are based on matching the profile of an input mode to the profile of an output mode. This profile matching can be achieved using a phase mask or a spatial light modulator (SLM) [34]–[36]. For example, a mode converter and a multiplexer based on liquid crystal on silicon (LCoS) spatial modulator were demonstrated in [32]. Figure 2-1 shows the setup to convert LP_{01} to LP_{11a} and LP_{11b}, with about 9 dB conversion loss (insertion loss) and an additional 16 dB loss for multiplexing the modes in an FMF.

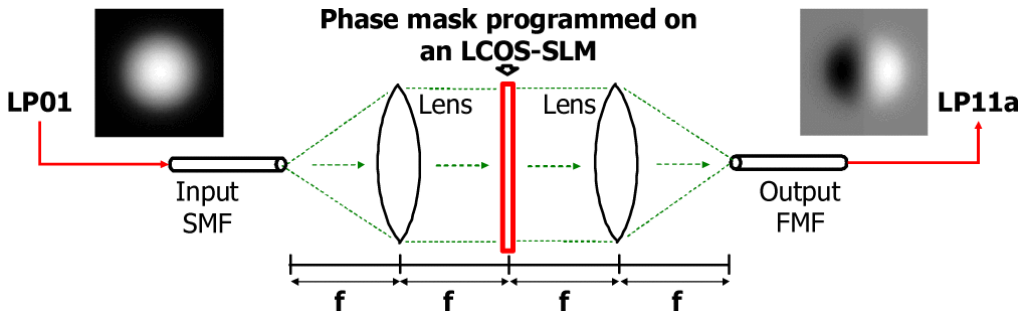

Figure 2-1: Liquid Crystal on Silicon (LCoS) mode converter [32]

Another free-space mode converter and multiplexer using phase plates, beam splitters, mirrors and lenses was presented in [31] and shown by Figure 2-2. Phase plate was used to convert each of the two linearly polarized LP_{01} modes (LP_{01x} and LP_{01y}) to two LP_{11} modes (LP_{11a} and LP_{11b}), with high extinction ratio at 1550 nm (higher than 28 dB), and high loss (9 dB for LP_{01}-LP_{11a} conversion and 7.8 dB for LP_{01}-LP_{11b} conversion).

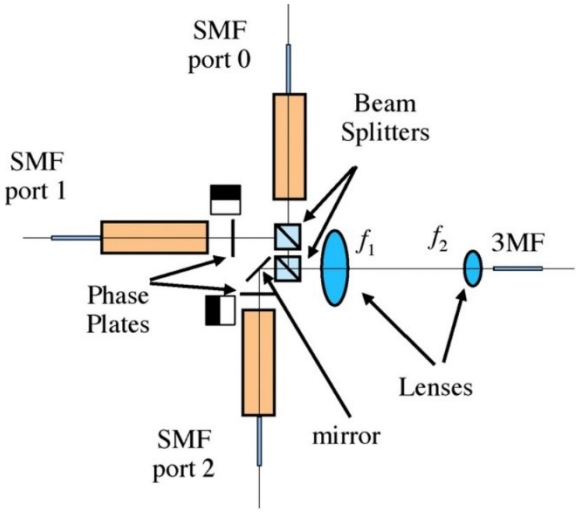

Figure 2-2: Mode converter based on phase plate s and lenses [31]**.**

Free space mode converters and (de)multiplexers can have the features of insensitivity to polarization and independence of wavelength, i.e. they can be broadband. However, their main drawbacks are high insertion loss and they result in bulky structures, thus they are difficult to be integrated.

2.3. Waveguide-based Mode Converters:

Waveguide mode converters and (de)multiplexers are mainly based on optical waveguides which can be either circular or planar [7]. They may be realized through several techniques such as grating [37], tapering [38], lanterns [39], planar lightwave circuit (PLC) [40], photonic crystal fiber (PCF), mode selective coupler (MSC) and Y-junction [41]. It is worth mentioning that more than one technique may be applied to realize a specific converter/(de)multiplexer for a specific

mode. For example, mode conversion can be based on fiber grating and multiplexing/demultiplexing on mode selective optical coupling [42].

In [43], a mode converter for converting LP_{01} to LP_{11} using long period fiber grating (LPFG) was proposed and demonstrated. The mode converter is illustrated by Figure 2-3 and the grating was obtained by applying a mechanical pressure on the fiber. The converter has 22 dB extinction ratio and 1.5 dB insertion loss at 1550 nm, in addition the converter has a very narrow bandwidth (13 nm centered at 1551 nm).

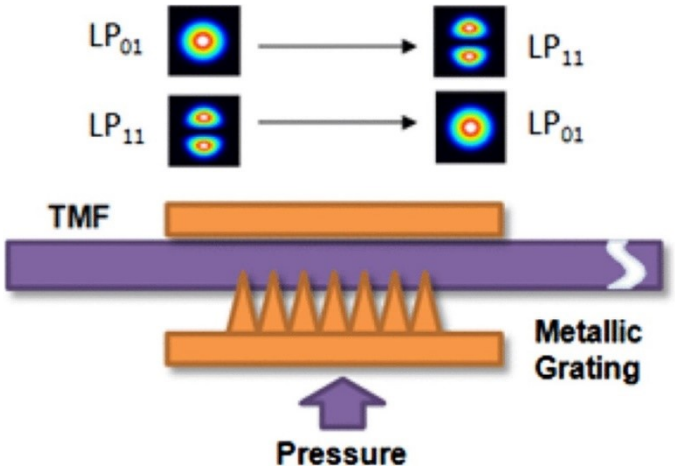

Figure 2-3: Mode converter based on Long Period Fiber Grating (LPFG) [43]**.**

Using multimode interference, an all-fiber mode converter converting LP_{01} to LP_{02} was demonstrated, in which a multimode fiber (MMF) is used to interconnect a SMF to an FMF as shown in Figure 2-4. The converter has an extinction ratio higher than 55 dB and insertion loss more than 1.8 dB at 1550nm (equivalent to less than 66% conversion efficiency) [44].

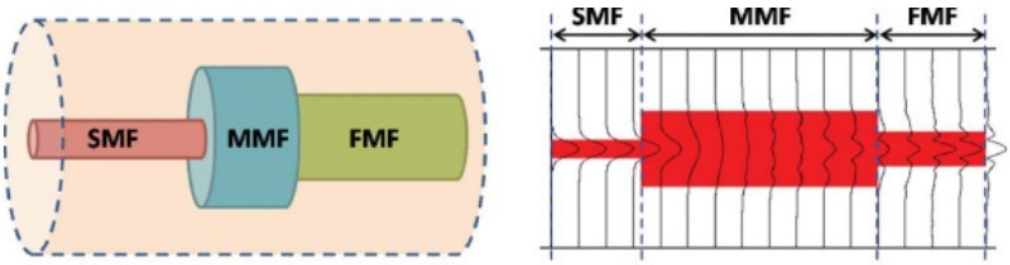

Figure 2-4: Mode converter based on multimode interference (MMI) [44]

Silicon based asymmetrical directional couplers were also proposed and demonstrated to convert and multiplex eight guided modes (TE_i and TM_i, i=0…3) [45]. The multiplexer chip has low excess loss (0.5 dB) and high extinction ratio (20 dB) at the central wavelength of 1555 nm, in addition to that the structure has a coupling loss of 12 dB to couple from the chip to the fiber.

Mode conversion and multiplexing based on optical coupling were investigated theoretically in [46]. A two-mode multiplexer using optical coupling was demonstrated [47], and it was shown that a broadband (1500-1600 nm), low insertion loss (0.3 dB) and high extinction ratio (36 dB) can be obtained. The multiplexer is composed of two parallel rectangular waveguides. Two optical modes (even and odd) are injected at the input, one on each waveguide. In the multiplexing region, the two waveguides are separated by a gap (G) as shown in Figure 2-5.

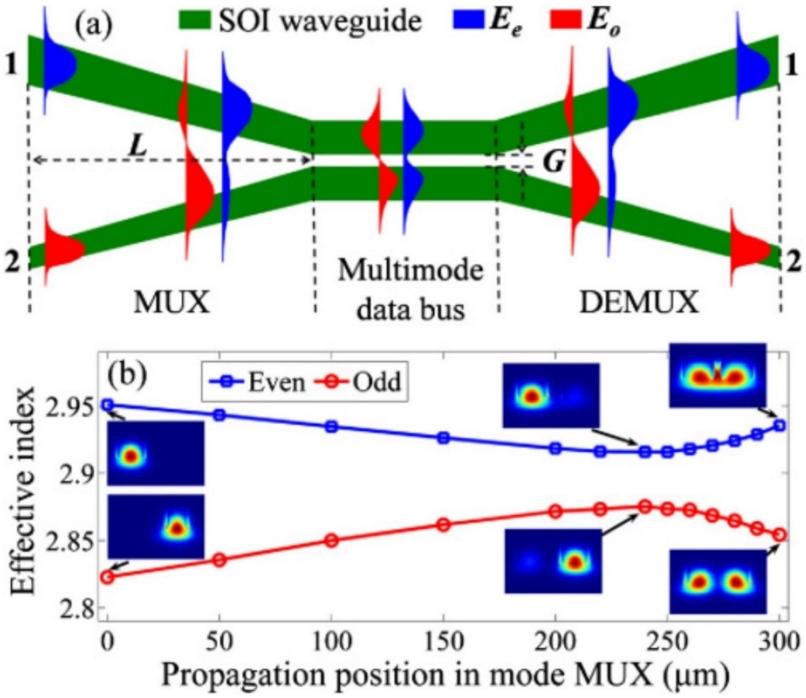

Figure 2-5: Mode converters based on optical coupling [47]

Using Silicon grating couplers, a six-polarization mode multiplexer (LP_{01x}, LP_{01y}, LP_{11ax}, LP_{11ay}, LP_{11bx} and LP_{11by}), was demonstrated, showing broadband operation with high insertion loss (23 dB) [48].

Using cascaded optical fiber couplers, low insertion loss mode conversion and multiplexing for LP_{01}, LP_{11}, LP_{21} and LP_{02} were achieved [49]. Similarly, a two-mode multiplexer (for TE_0 and TE_1) based on an asymmetrical coupler was analyzed using plasmonic waveguide as shown in Figure 2-6, with features of broadband (100 nm), low insertion loss (0.35 dB), and high extinction ratio (17 dB) [50].

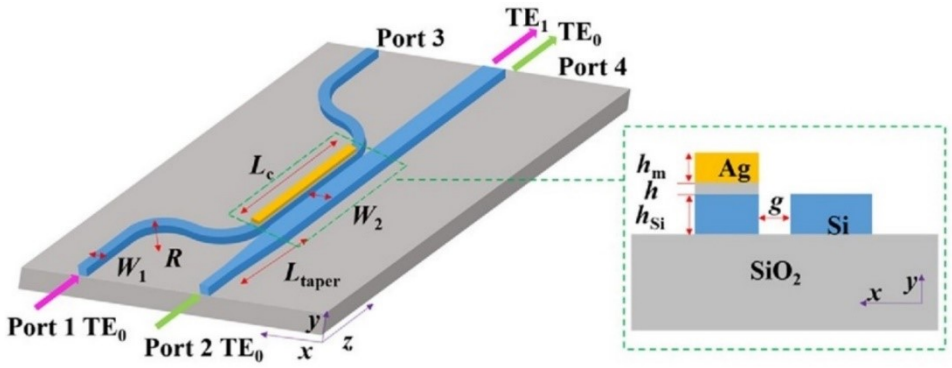

Figure 2-6: Two mode multiplexer based on asymmetric coupler [50]

Silica based planar lightwave circuits (PLC) have been also used to design and fabricate mode converters and multiplexers, such as the works introduced in [51] and [52] illustrated in Figure 2-7, where two and three mode multiplexers for the C-band were demonstrated using asymmetrical couplers respectively.

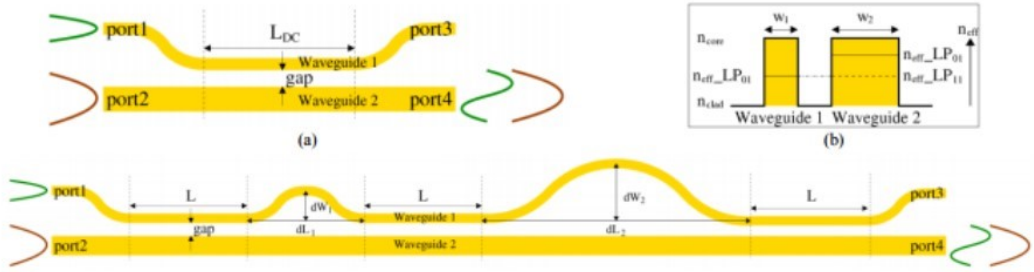

Figure 2-7: Silica based planar lightwave circuit (PLC) [51]

In [51], two modes (LP_{01} and LP_{11}) were multiplexed through directional couplers. The multiplexer has an insertion loss less than 0.5 dB over S, C and L bands, with 2.5 dB extra loss due to mode field diameter mismatch between the circular fiber and the rectangular waveguide. In [52], three-mode (LP_{01}, LP_{11} and LP_{21}) multiplexer was designed using parallel waveguides for C-band. Conversion is achieved through matching effective index of one mode in one waveguide to

the other mode in the other waveguide, achieving conversion efficiency higher than 90% over the C-band with a high insertion loss of 10 dB for the LP_{21} mode.

All-waveguide mode converters can also be realized using optical tapers, photonic crystal fibers, optical Y-junctions or optical lantern structures [53]–[65]. For instance, based on tapered submicron silicon ridge optical waveguide, mode conversion from TM_0 to TE_1 and TE_3 was proposed and demonstrated in [59]. It was shown that the converter has a high conversion efficiency (more than 90%). However, interfacing to a circular waveguide such as fiber may result in high insertion loss.

In [60] and [61], the design and fabrication of a mode (de)multiplex based on all-waveguide tapered mode-selective couplers was presented. The fabrication of such a mode (de)multiplexer was using femtosecond laser direct-write technique. The (de)multiplexer can be used in a wide bandwidth (more than 400nm from 600nm to 1000nm) with a low insertion loss (below 2dB) and high extinction ration (above 20dB). Figure 2-8 shows the schematic diagram of such fabricated device.

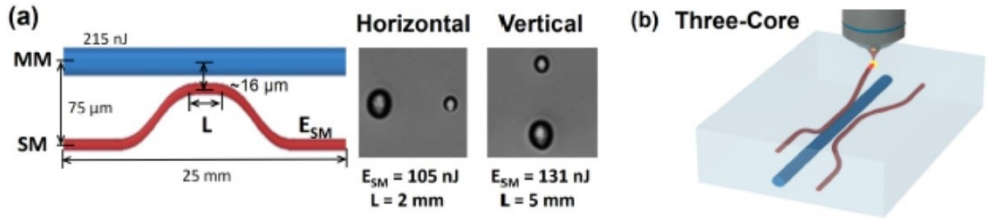

Figure 2-8: All-waveguide tapered mode-selective couplers mode (de)multiplexer [61]**.**

A fiber based photonic lantern was obtained for three mode multiplexing (LP_{01}, LP_{11a} and LP_{11b}) [62]. The multiplexer is obtained by adiabatically fusing three single mode fibers through a capillary to form a few-mode fiber as depicted by Figure 2-9. The lantern achieved an insertion loss of less than 2dB over a wideband (from 1510nm to 1620nm).

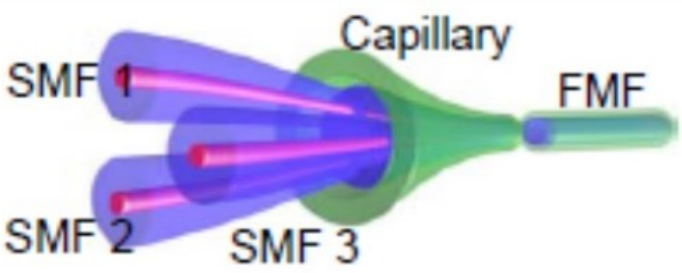

Figure 2-9: Fiber based photonic lantern mode multiplexer [62]

Another all-optical mode converter using photonic crystal fiber (PCF) and optical taper was also introduced in [63]. It converts LP_{01} to LP_{11} with an insertion loss of 0.3 dB and extinction ratio of 20 dB at 1550 nm. The schematic diagram of the device is given in Figure 2-10.

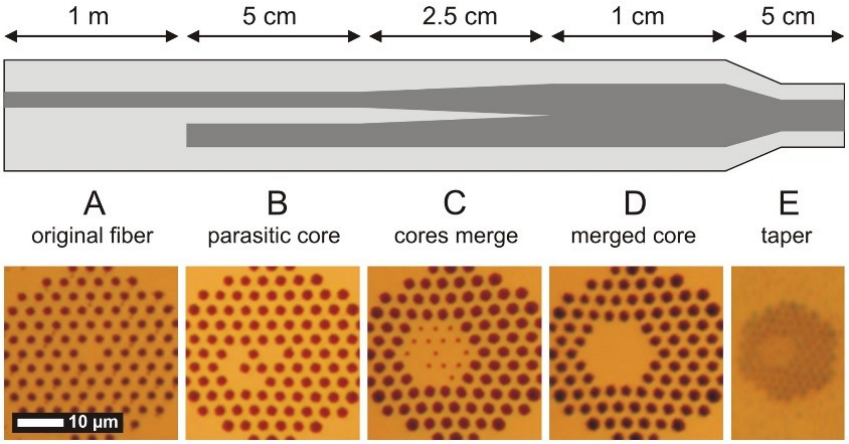

Figure 2-10: All-fiber LP_{01} to LP_{11} mode converter [63]**.**

A broadband mode converter between LP_{01} and LP_{02} was proposed and demonstrated in [64], in which photonic crystal fiber with pressurized holes inflated but the plugged holes collapsed to form a new annular core around the original core was used to achieve the mode conversion. Similarly, based on the same principle a three-mode multiplexer was demonstrated in [65].

A wide divergence angle asymmetric Y-junction mode (de)multiplexer for modes TE_0 and TE_1 was proposed in [53] as shown by Figure 2-11. The insertion loss was less than 1dB and the crosstalk less than –24 dB from 1530 nm to 1590 nm. Furthermore, the proposed scheme could also be expanded to include more modes.

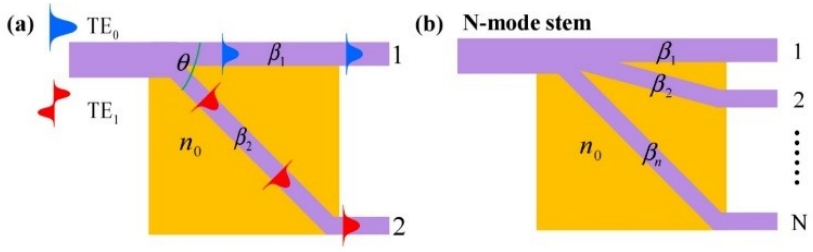

Figure 2-11: Y-Junction mode (de)multiplexer [53]

Table 2-1 summarizes some different all-fiber techniques that have been reported to achieve mode conversion (MC) and/or mode (de)multiplexing (MUX) with their brief performance (insertion loss, extinction ratio and bandwidth or design wavelength).

Generally speaking, all-waveguide mode converters and multiplexers have high mode conversion efficiency (80%–90%) [66], and are compact, but they are wavelength dependent.

Table 2-1: Summary of different all-fiber techniques to achieve mode conversion (MC) and/or mode multiplexing (MUX) with their brief performance

Technique	Example	IL (dB)	ER (dB)	λ or BW (nm)
Fiber Grating	[43] LP_{01} to LP_{11} MC	1.5 to 2.5	22	13 (C-Band)
	[67] LP_{01} to LP_{11} MC	2.8 – 4	20	At 1550
Taper	[60] LP_{01}, LP_{11a} and LP_{11b} MUX	< 2	20	600–1000
	[68] TE_0, TE_1 and TE_2 MUX	< 0.1	20	Broadband
	[69] LP_{01} and two-LP_{11} MUX	0.6 – 0.7	17.3 – 19.1	At 1310
Photonic Lanterns	[17]LP_{01}, two LP_{11} MC and MUX	6.5	NA	100
	[64] LP_{01} to LP_{11} MC	0.3	20	At 1550
	[70] LP_{01}, two LP_{11}, two LP_{21}, LP_{02} MC and MUX	0.6 – 0.7	NA	At 1550
Planar Lightwave Circuits (PLC)	[51]LP_{01}, LP_{11} and LP_{21} MUX	0.5 – 10	NA	60 (C-band)
	[71]LP_{01} and LP_{11} MC and MUX	1.2	NA	100 (1500–1600)
	[65] LP_{01} to LP_{02} MC	0.1	15	Broadband
	[72] LP_{01}, LP_{11a}, LP_{11b}, LP_{21a} MC and MUX	1.1 – 0.5	12 – 20	1530 – 1560
Photonic Crystal Fiber (PCF) Mode Selective Couplers (MSC) Y-Junction	[49] LP_{01}, LP_{11}, LP_{21} and LP_{02} MUX	0.4 – 1.5	NA	1543.5
	[45] TE_i and TM_i, i=0…3 MC and MUX	0.2 – 2	11 – 20	1555 (C-Band)
	[73] TM_0 and TE_0	0.7	22	1450– 1750
	[47] 2-modes MUX	0.3	36	100 (1500-1600)
	[50] TE_0 and TE_1 WG MUX	0.35	17	100 (C-Band)
	[74] LP_{01}, LP_{11a}, LP_{11b}, LP_{21a}, LP_{21b}, LP_{02} MUX	1.4 – 1.8	20	C-band

Chapter 3: LP_{01} to LP_{02} Mode Converter and (de)Multiplexer for the O, S and C-Band

3.1 Introduction

Mode converters and (de)multiplexers are key components for enabling mode and space division multiplexing (MDM/SDM). These devices can be designed based on free space optics or based on waveguides. There exist a large flavor of such devices, especially those based on waveguides because they provide mode conversion and (de)multiplexing with a low insertion loss and result in small size components allowing them to be easily integrated with other optical devices [17], [49], [75], [76]. The basic idea behind waveguide-based mode converters and (de)multiplexers is to introduce some physical or structural perturbation to the device such as changing its physical dimensions or refractive index profile. For instance, a tapered-based mode converter is achieved by gradually increasing the cross-section of the waveguide. This tapering may result in a waveguide section that starts as a single mode (can support only the fundamental LP_{01} mode) and ends as a few or multimode (supporting LP_{01} mode and other higher order modes).

In this chapter, a waveguide-based doubly tapered mode converter that converts LP_{01} to LP_{02} for the O, S and C-band is proposed [42]. The subsequent sections outline the design, performance analysis and fabrication results of the proposed mode converter structure.

3.2. The Proposed Mode Converter Structure

3.2.1. The Structure

The proposed structure of the mode converter is shown in Figure 3-1. It consists basically of two tapered circular sections (AB and CF) connected by a straight circular section (BC). The first taper (AB) has a length L_1, a starting radius r_1 and an ending radius r_2. The tapering follows an exponential function to make transition smooth and reduce losses. The core refractive index is n_1, whereas the cladding refractive index is n_2. This taper is followed by a few-mode circular section of length L_2 and core radius r_2. Then, a second inner core is introduced (with a refractive index $n_3 < n_1$) (CF) which is tapered from both ends with a radius starting with zero (at C) to r_4 (section DE) and back to zero (at F). This second taper forms a ring index profile [65] as depicted by the transversal refractive index distribution in Figure 3-1. The outer cladding of the structure has a radius r_3 and index n_2.

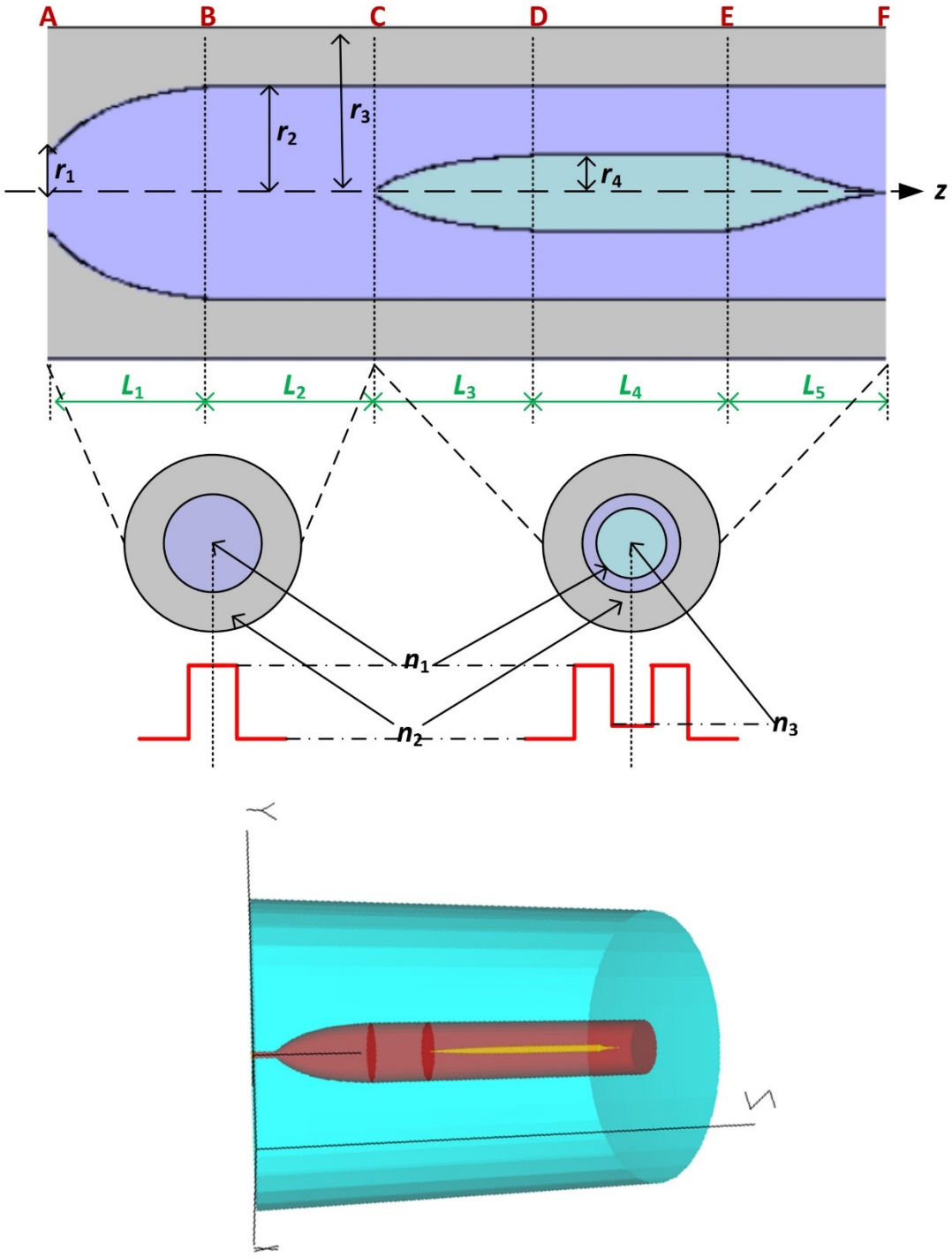

Figure 3-1: Schematic diagram of the proposed mode converter

3.2.2. *The Operating Principle*

The proposed mode converter structure operates as follows. The fundamental mode (LP_{01}) is injected at the left port of the converter at the beginning of the first taper (A). The changing radius of this taper (from r_1 to r_2) causes excitation of higher order modes and power coupling from LP_{01} mode to some higher order modes. The strength of power transfer (mode conversion efficiency) in this section depends on the parameters of this taper (r_1, r_2, L_1, n_1 and n_2). For instance, injecting the LP_{01} mode at the starting of section AB can excite different higher order LP_{0m} modes throughout the section and causing power transfer (or mode conversion) from the injected LP_{01} to a higher order mode. By carefully tuning the parameters of the AB tapered section, the power transfer can be made to occur mostly from LP_{01} to the desired LP_{02}. However, some other higher order modes (especially those LP_{0m}, $m > 2$ modes) can still have significant amount of power in this section. Figure 3-2 shows the normalized power of the injected fundamental mode LP_{01} and some higher order modes throughout the tapered AB section at the wavelength of 1310 nm (the center of the O-Band) for some fixed length L_1 and radius r_2.

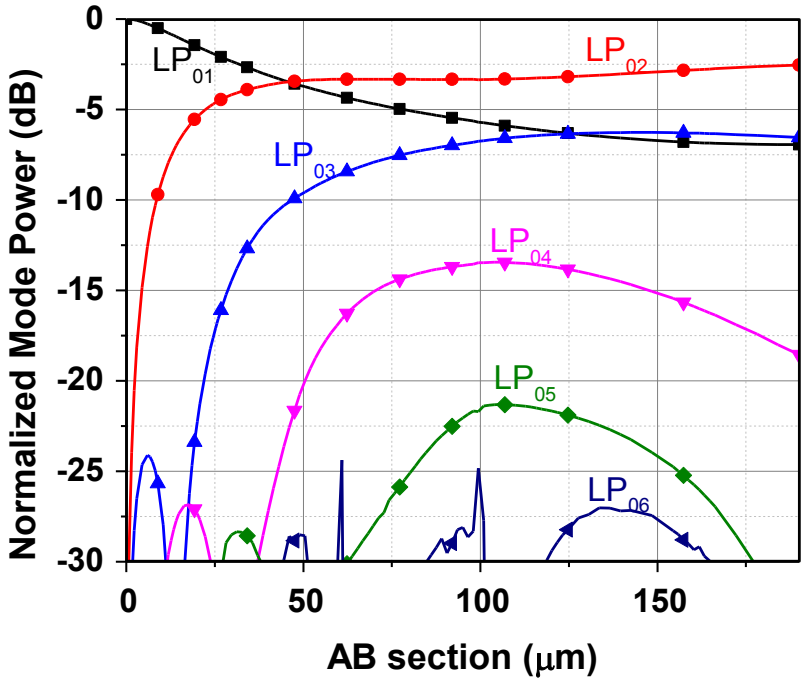

Figure 3-2: Normalized power along AB section

It is clearly shown that almost all the power is distributed among the four modes, LP_{01}, LP_{02}, LP_{03}, and LP_{04}. In other words, the rest of higher order modes occupy negligible power. It is obvious from the figure that most of the input LP_{01} power is converted to LP_{02} mode. However, limited conversion efficiency is obtained if only one taper (the AB section) is used. Therefore, a second section (CF) is added to improve the conversion efficiency. It is worth mentioning that the circular BC section does not introduce power transfer (mode conversion), but it allows tuning the phases of the different modes. Thus, the maximum mode power transfer from LP_{01} and LP_{02} can be achieved, as well as reducing the power transfer to non-desired modes.

The second section (CF) is formed by inserting an inner tapered element with a refractive index n_3 that is smaller than the index of the core n_1 ($n_3 < n_1$). This inner taper should be chosen not only to maximize the power conversion from LP_{01} to LP_{02} mode but also to minimize the power reflection, loss and power leakage to other non-desired modes.

In order to tune the parameters of the proposed mode converter structure to achieve high mode conversion efficiency from LP_{01} to LP_{02} mode, we have performed extensive simulation using a vector mode solver, which is based on Eigen Mode Expansion (EME) [66] method to find the modes inside the waveguide.

To evaluate the performance of the mode converter, two performance parameters are used [44], which are the insertion loss (IL) of LP_{02} mode and the mode extinction ratio (ER), defined as:

$$\mathrm{IL} = 10\mathrm{Log}_{10}\left(\frac{\mathrm{P}_{\mathrm{LP}_{01},\mathrm{in}}}{\mathrm{P}_{\mathrm{LP}_{02},\mathrm{out}}}\right) \qquad (3.1)$$

$$\mathrm{ER}_{2\mathrm{m}} = 10\mathrm{Log}_{10}\left(\frac{\mathrm{P}_{\mathrm{LP}_{02},\mathrm{out}}}{\mathrm{P}_{\mathrm{LP}_{0\mathrm{m}},\mathrm{out}}}\right) \qquad (3.2)$$

where, $\mathrm{P}_{\mathrm{LP}01,\mathrm{in}}$ and $\mathrm{P}_{\mathrm{LP}_{0\mathrm{m}},\mathrm{out}}$ are the optical input power of LP_{01} mode at point A and the optical output power of mode LP_{0m}, (m = 1, 2, …) at the output of the mode converter (F), respectively. For the extinction ratio, we have considered only the LP_{01}, LP_{03} and LP_{04} modes because they were the modes carrying the highest powers at the output among all non-desired modes. Note that the insertion loss is corresponding to conversion efficiency, i.e. less insertion loss means high conversion efficiency. Even though in general situations, insertion loss and conversion efficiency may result in different measurements, in this thesis we use them interchangeably. This is due to the short length of our designed devices. The extinction ratio measures the strength of the output

LP_{02} mode with respect to the remaining non-desired modes, i.e. higher extinction ratio means higher suppression of non-desired modes. In other words, the higher the extinction ratio the lower the crosstalk between modes.

3.3. Mode converter for O-, S- and C-band

To identify the optimal structure parameters, we carried out extensive simulation. The final parameters of the mode converter for the O-band (1260 – 1360 nm), the S-band (1460 – 1530 nm) and the C-band (1530 – 1565 nm) are given in Table 3-1. Figure 3-3(a), (b) and (c) illustrate the extinction ratio (ER) and insertion loss (IL) of our proposed mode converter in the O- S- and C-band, respectively. Figure 3-3(a) shows that the insertion loss of the LP_{02} mode is less than 1.2 dB over the entire O-band and a minimum IL = 0.004 dB is obtained at the central wavelength (λ_0=1310 nm), which is equivalent to a conversion efficiency of 99.9%. The maximum IL on the O-band is 1.2 dB, i.e. 75% conversion efficiency. The mode extinction ratio, which represents power ratio of the LP_{02} mode to the remaining non-desired modes, remains above 10 dB for the entire O-band and more than 30 dB at the central 1310 nm wavelength. Figure 3-3(b) shows the IL and ER in the S-band (between 1460 nm and 1530 nm, centered at λ_0=1500 nm). The IL is less than 0.08 dB, i.e. more than 98% conversion efficiency; and the ER is above 20 dB, over the entire S-band. At the central wavelength of 1500 nm, the IL = 0.002dB (99.95% conversion efficiency) and ER > 30dB are achieved. For the C-band (from 1530 nm to 1565 nm and centered at 1550 nm), the insertion loss and extinction ratio are illustrated in Figure 3-3(c). Over this entire C-band, an IL of less than 0.06 dB (conversion efficiency of more than 98%) and an ER of above 19 dB are achieved. At the central wavelength of 1550 nm, conversion efficiency of 99.6% (0.02dB) and ER of greater than 26 dB are attained. Note that Figure 3-3(b) shows the performance of the mode converter for the entire S- and C- bands, i.e. the wavelength from 1360 to 1565 nm, in which the mode converter is optimized at the wavelength of 1500 nm. It is seen that the conversion efficiency of more than 90% and extinction ratio of more than 10 dB are achieved. This suggests that the same mode converter can be used for the two bands.

Table 3-1: List of the parameters used in Figure 3-3 (lengths and radii are in μm)

Symbol	Definition	Values		
		O-Band	**S-band**	**C-Band**
n_1	Ref. index of core	1.49	1.5	1.5
n_2	Ref. index of outer clad	1.45	1.4535	1.4505
n_3	Ref. index of inner clad	1.4686	1.4555	1.4519
L_1	Length of 1st taper (AB)	181	182	191
L_2	Length of segment (BC)	1497	428	400
L_3	Length of segment (CD)	60	166	370
L_4	Length of segment (DE)	46	0	712
L_5	Length of segment (EF)	536	432	360
r_1	Radius of initial core	4	4	4
r_2	Radius of (BC)	15	15	15
r_3	Radius of outer cladding	40	40	40
r_4	Radius of (DE)	3	3	3
λ_0	Center wavelength	1310	1500	1550
C_{eff}	Conversion eff. at λ_0	99.9%	99.9%	99.6%

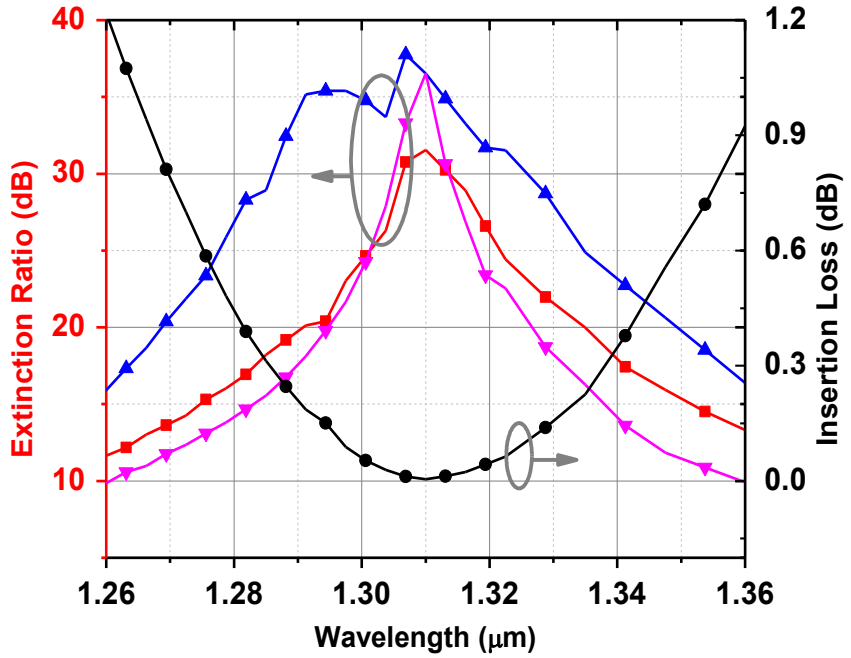
Extinction Ratio (dB)
Insertion Loss (dB)
Wavelength (μm)
40
30
20
10
1.2
0.9
0.6
0.3
0.0
1.26
1.28
1.30
1.32
1.34
1.36

(a)

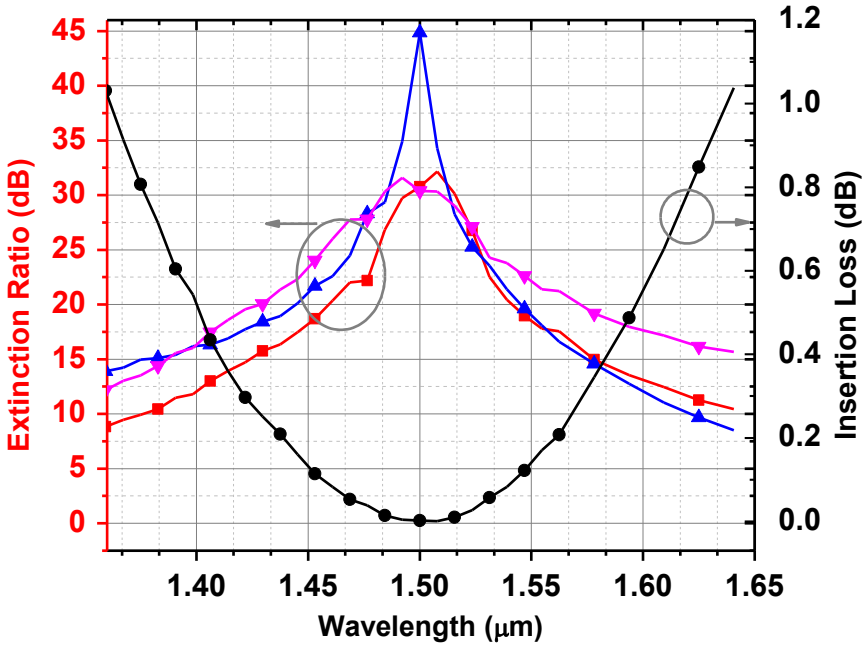
Extinction Ratio (dB)
Insertion Loss (dB)
Wavelength (μm)
45
40
35
30
25
20
15
10
5
0
1.2
1.0
0.8
0.6
0.4
0.2
0.0
1.40
1.45
1.50
1.55
1.60
1.65

(b)

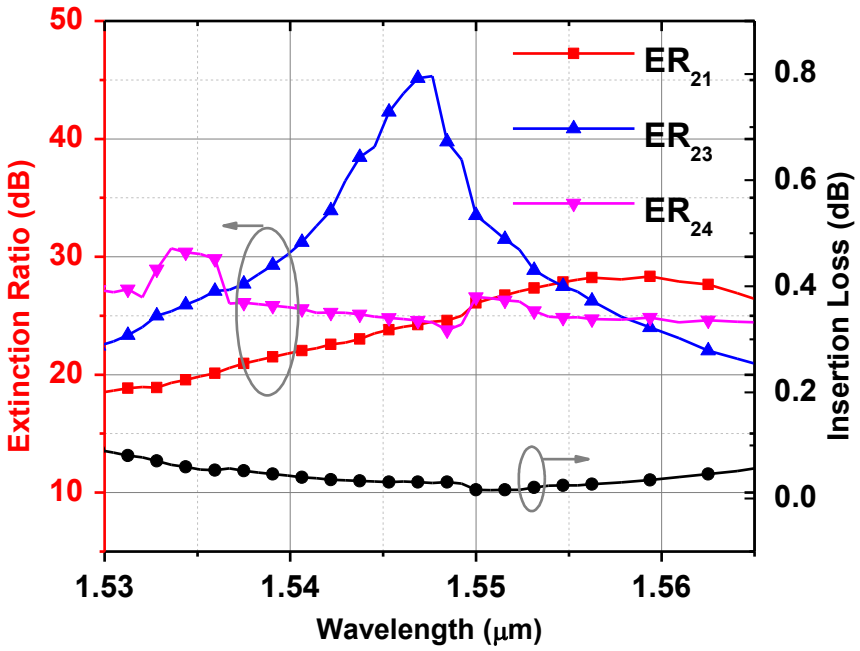

(c)

Figure 3-3: Extinction ratio and insertion loss achieved by the proposed mode converter in (a) O-band, (b) S-band and (c) C-band

Table 3-2 summarizes the obtained results for the three bands. Except 75% conversion efficiency for a few shorter and longer wavelengths in the O-band, the conversion efficiency is greater than 98% over the O-, S- and C-band, which are the mostly used wavelength bands for telecommunication systems using optical fibers, particularly C-band.

Table 3-2: Maximum and minimum IL(dB) and ER (dB) in O-, S- and C-band

	Max IL	Min IL	Min ER at Central λ	Min ER over entire band
O-Band	**1.2**	**0.004**	**30**	**10**
S-Band	**0.08**	**0.002**	**30**	**20**
C-Band	**0.06**	**0.016**	**26**	**19**

3.4. Analysis of the Designs

To investigate the stability of the previous designs in Table 3-2 as well as their tolerances for fabrication purposes, this section presents an analysis of the effects of the mode converter parameters. We consider the C-band mode converter only as an example, and the analysis for O- and S-band should be similar.

3.4.1. Effect of the lengths

Figure 3-4 shows the effect of lengths L_i (i = 1…5) on the IL and ER at the central wavelength of 1550 nm. Figure 3-4(a) shows that the tolerance range of L_1 from the nominal value is ±36 μm (L_1 = 191 ± 36 μm) for a conversion efficiency greater than 80% and ER greater than 10 dB. The tolerance range of L_2 is ±57 μm, given by Figure 3-4(b), for the conversion efficiency of 80% and ER of 10 dB. Moreover, the conversion efficiency and extinction ratio are not sensitive to L_3, L_4, and L_5 as depicted in Figure 3-4(c), (d), and (e). It is seen that L_3 = 370 ± 75 μm results in efficiency higher than 95% and ER higher than 20 dB, L_4 = 712 ± 66 μm leads to efficiency higher than 97% and ER higher than 18 dB, and L_5 = 360 ± 97 μm results in efficiency higher than 98% and ER higher than 20 dB. Based on these results, it is obvious that the converter can tolerate deviations of the lengths L_1, L_2, L_3, L_4 and L_5 from their nominal values with a small penalty on the conversion efficiency.

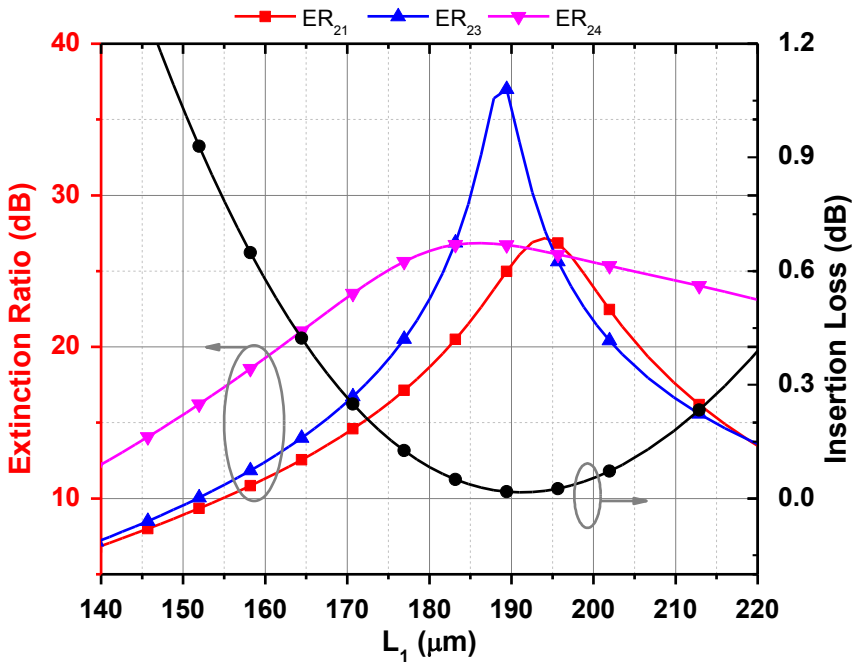
ER21
ER23
ER24
Extinction Ratio (dB)
Insertion Loss (dB)
L1 (μm)
40
30
20
10
1.2
0.9
0.6
0.3
0.0
140
150
160
170
180
190
200
210
220

(a)

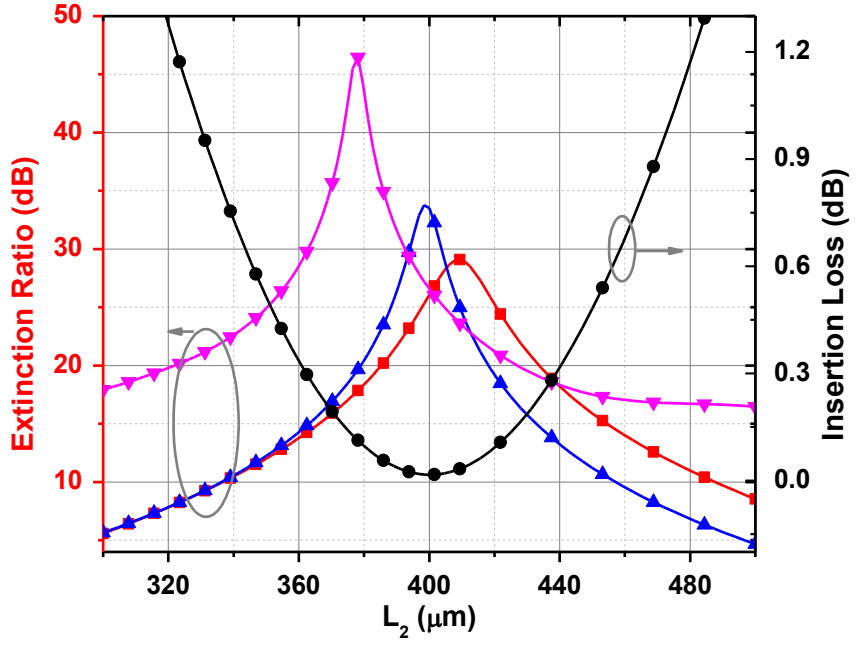
Extinction Ratio (dB)
Insertion Loss (dB)
L2 (μm)
50
40
30
20
10
1.2
0.9
0.6
0.3
0.0
320
360
400
440
480

(b)

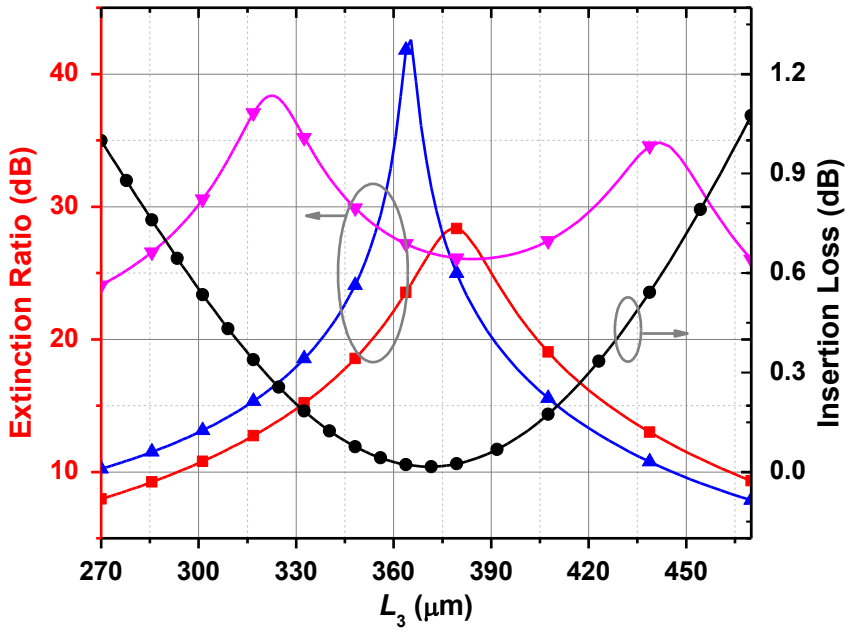
Extinction Ratio (dB)
Insertion Loss (dB)
40
30
20
10
1.2
0.9
0.6
0.3
0.0
270
300
330
360
390
420
450
L_3 (μm)

(c)

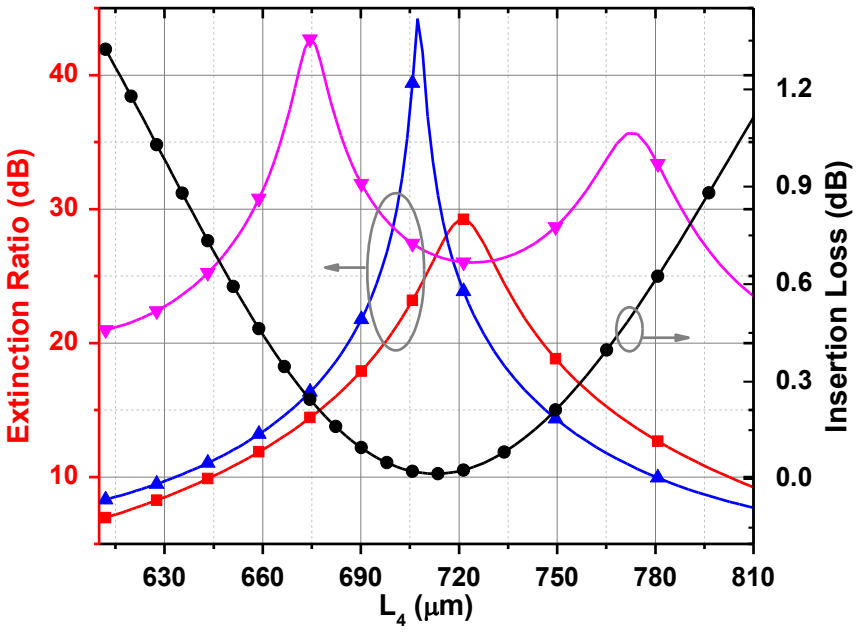
Extinction Ratio (dB)
Insertion Loss (dB)
40
30
20
10
1.2
0.9
0.6
0.3
0.0
630
660
690
720
750
780
810
L_4 (μm)

(d)

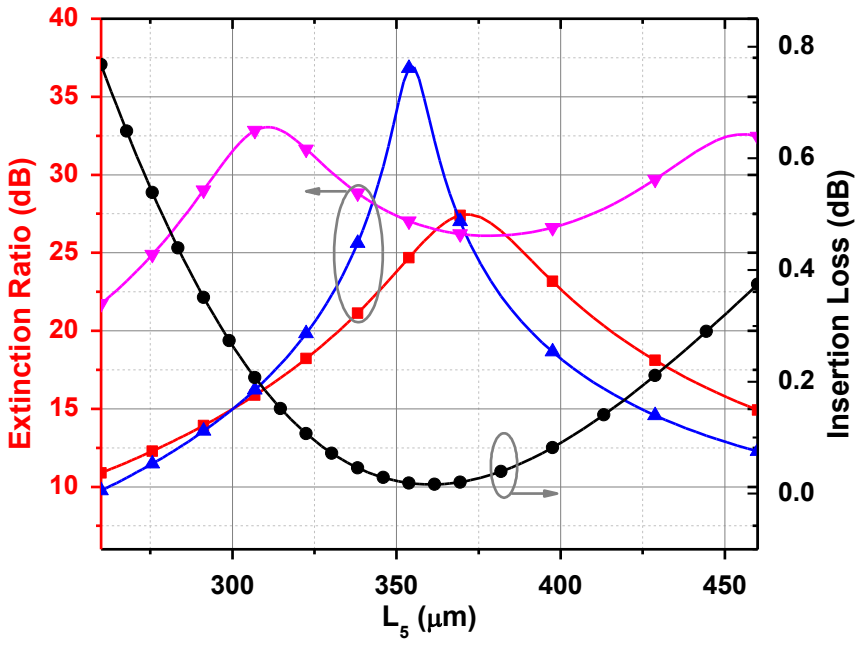

(e)

Figure 3-4: Effect of the lengths L_i (i=1…5) on conversion efficiency and extinction ratio in the C-band.

3.4.2. Effect of the radii

The tolerances to the deviation in the radii are tighter than the tolerances to the deviations in the lengths. Figure 3-5(a), (b), (c) and (d) show the impact of the radii r_1, r_2, r_3 and r_4 on the performance of the mode converter, respectively. As shown in Figure 3-5(a), the staring radius of the first taper r_1 may deviate by ±2 μm from its nominal value and can still result in an efficiency higher than 80% and ER higher than 10 dB. Figure 3-5(b) shows that the radius of the circular section r_2 can deviate by only about ±0.3 μm from its nominal value (15 μm). Unlike r_2, the converter is much less sensitive to the outer cladding radius r_3, and r_3=40 ± 20 μm still results in more than 98% conversion efficiency and 23 dB ER. For the radius of the inner element r_4 as shown in Figure 3-5(d), r_4=3 ± 0.3μm leads to a conversion efficiency more than 80% and ER larger than 10 dB. Therefore, the converter is more sensitive to r_2 and r_4 than to r_1 and r_3. As a

matter of fact, r_1 and r_3 can deviate by 50% from their nominal values and the converter can still achieve a conversion efficiency of more than 80%. However, r_4 can tolerate a deviation of 10% from its nominal value to insure a conversion efficiency greater than 80%. Furthermore, r_2 has the tightest tolerance, since a deviation of 2% is required to keep conversion efficiency within the 80% range.

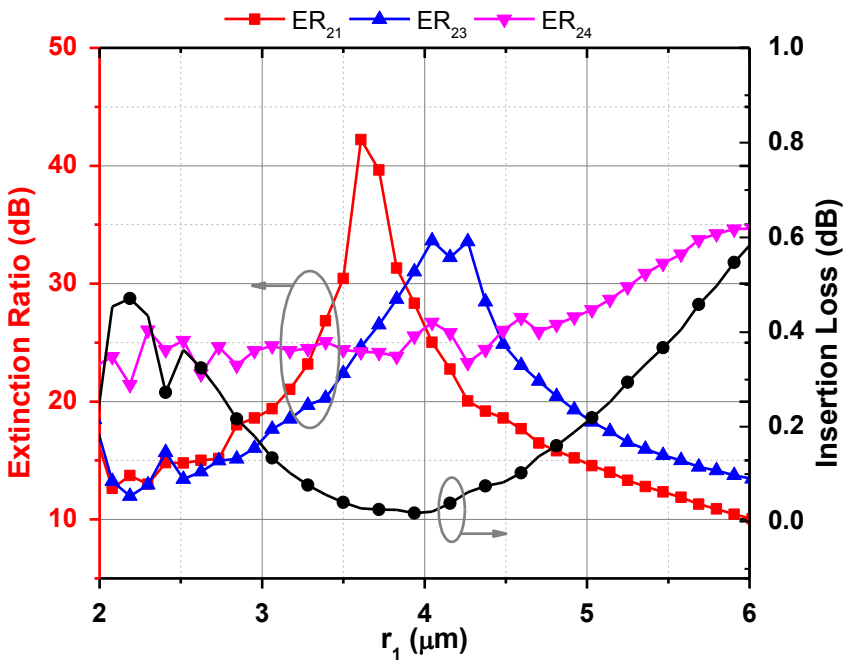

(a)

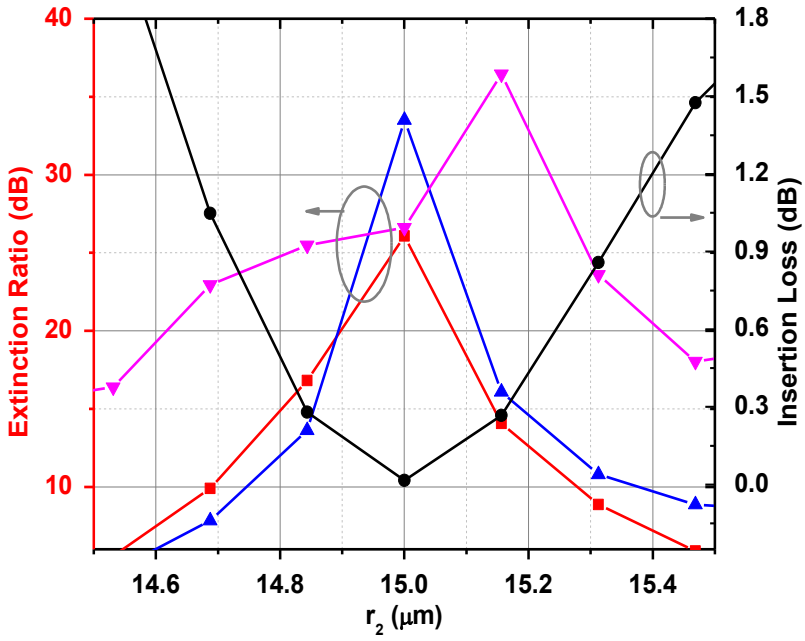
Extinction Ratio (dB)
Insertion Loss (dB)
r2 (μm)
40
30
20
10
1.8
1.5
1.2
0.9
0.6
0.3
0.0
14.6
14.8
15.0
15.2
15.4

(b)

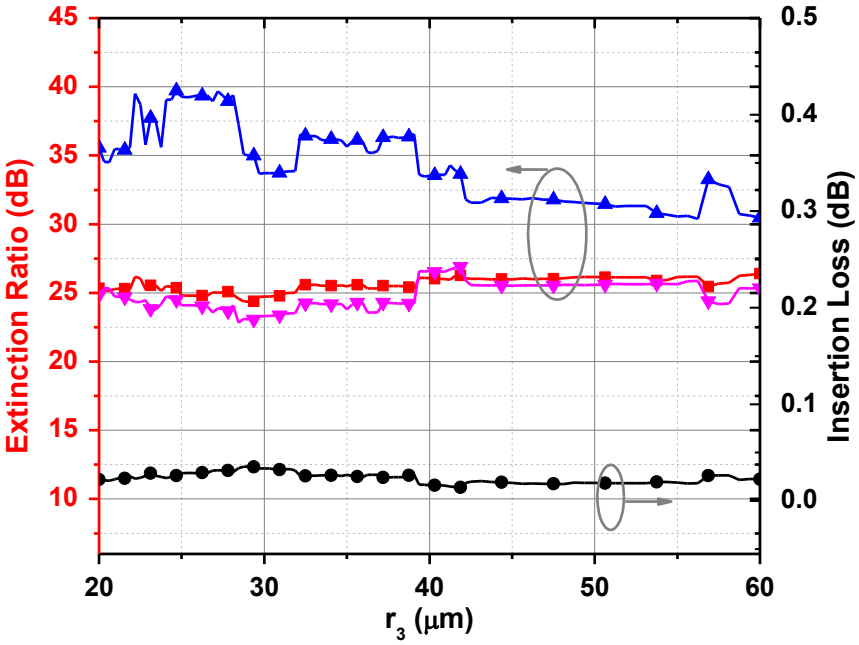
Extinction Ratio (dB)
Insertion Loss (dB)
r3 (μm)
45
40
35
30
25
20
15
10
0.5
0.4
0.3
0.2
0.1
0.0
20
30
40
50
60

(c)

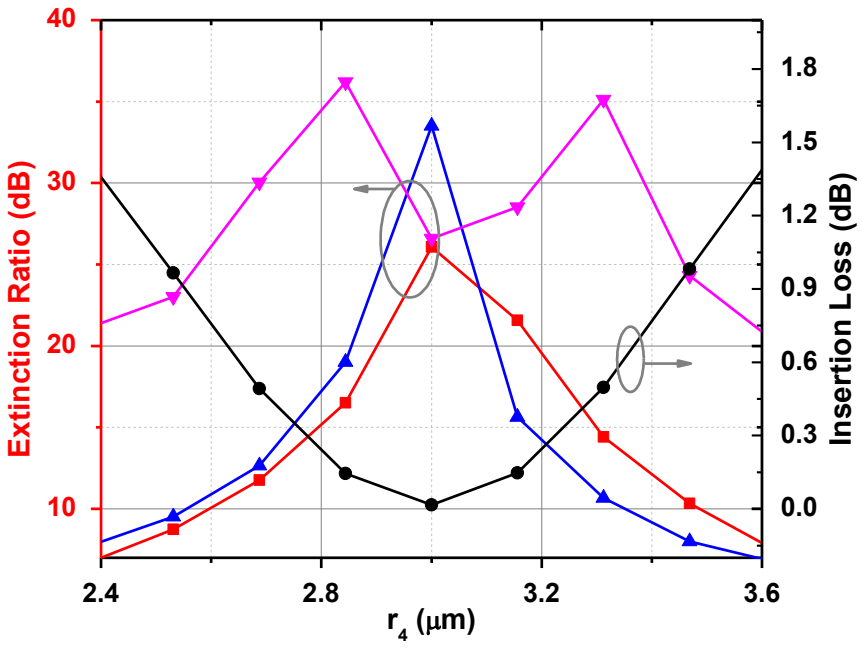

(d)

Figure 3-5: Effect of the radii r_i (i=1...4) on conversion efficiency and extinction ratio in the C-band.

It is shown that the impact of the lengths and radii deviation is roughly symmetrical with respect to the nominal value. However, the impact of refractive index deviation from the nominal value is quite different from that of the lengths and radii, as shown in Figure 3-6. This is because the light guiding mechanism inside the fiber is governed by the refractive index difference between the core and the cladding. Therefore, the core must always have a refractive index higher than the cladding ($n_1 > n_2$).

To keep the conversion efficiency higher than 80% and ER higher than 10 dB, the indices of refractions must be within the ranges of $1.483 \le n_1 \le 1.7$, $1.408 \le n_2 \le 1.47$ and $1.35 \le n_3 \le 1.473$.

As a conclusion, the proposed mode converter structure can tolerate some variations of the design parameters from their nominal values for a target insertion loss of less than 1dB. As a result, the structure can be fabricated using current fabrication processes based on femtosecond laser direct inscription [77], [78].

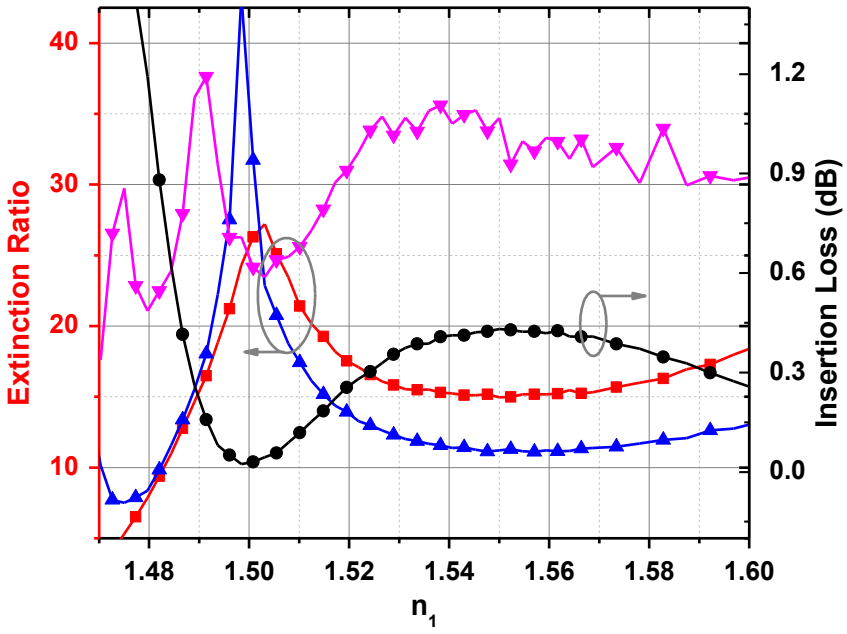
Extinction Ratio
Insertion Loss (dB)
n1
40
30
20
10
1.2
0.9
0.6
0.3
0.0
1.48
1.50
1.52
1.54
1.56
1.58
1.60

(a)

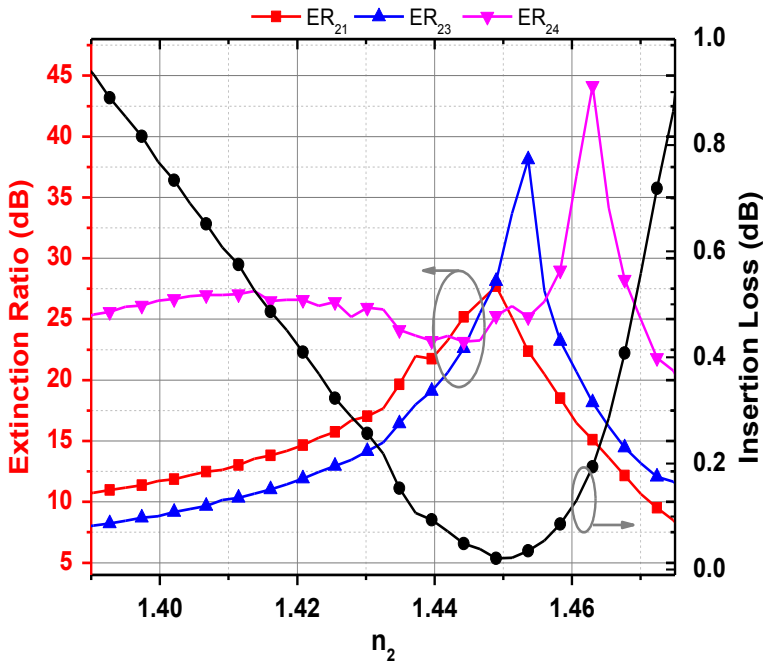
ER21
ER23
ER24
Extinction Ratio (dB)
Insertion Loss (dB)
n2
45
40
35
30
25
20
15
10
5
1.0
0.8
0.6
0.4
0.2
0.0
1.40
1.42
1.44
1.46

(b)

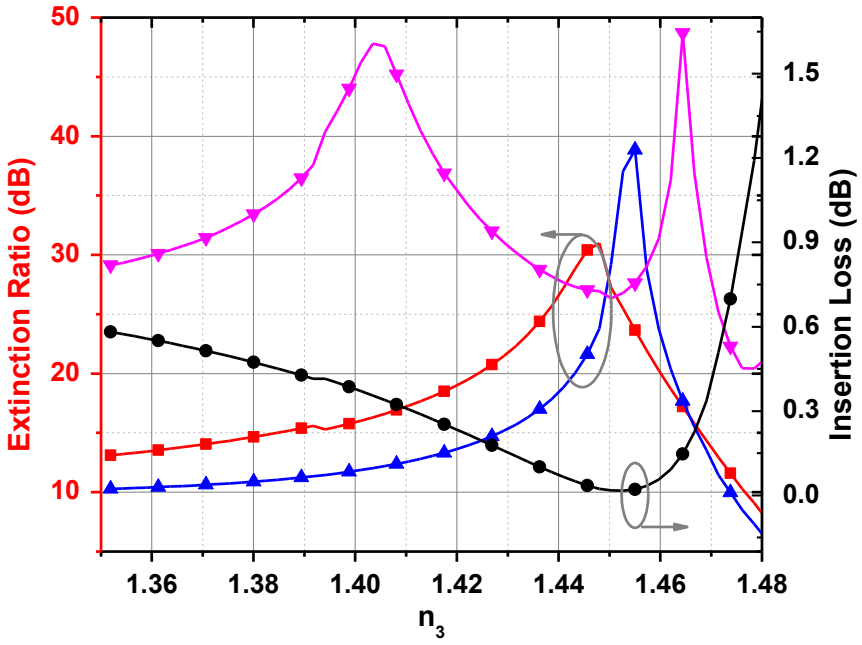

(c)

Figure 3-6: Effect of the refractive indexes n_i (i=1...3) on conversion efficiency and extinction in the C-band.

3.5. Conversion from LP_{02} to LP_{01}

The proposed mode converter can be also used at the receiver side for reciprocal operation, converting LP_{02} back to LP_{01}. Using the same parameters in Table 3-1, Figure 3-7 shows the extinction ratio (between LP_{01} and LP_{02}) and IL of LP_{01} (conversion efficiency from LP_{02} to LP_{01}) for the reciprocal operation, i.e. LP_{02} is injected at F (see Figure 3-1) and LP_{01} is output at point A, for the three bands (O, S and C). Here we only consider the ER between LP_{01} and LP_{02} because the other higher order modes (LP_{03} and LP_{04}) are not supported at the output due to the ending radius of the structure (r_1). It is clearly observed that for the reciprocal operation more than 99% conversion efficiency and higher than 30 dB ER can be achieved at the central wavelength in O-, S- and C-bands. For the entire bands, the minimum ER is 16 dB and 17 dB for S- and C-band, respectively. furthermore, the performance in the C-band does not have strong dependence on wavelength.

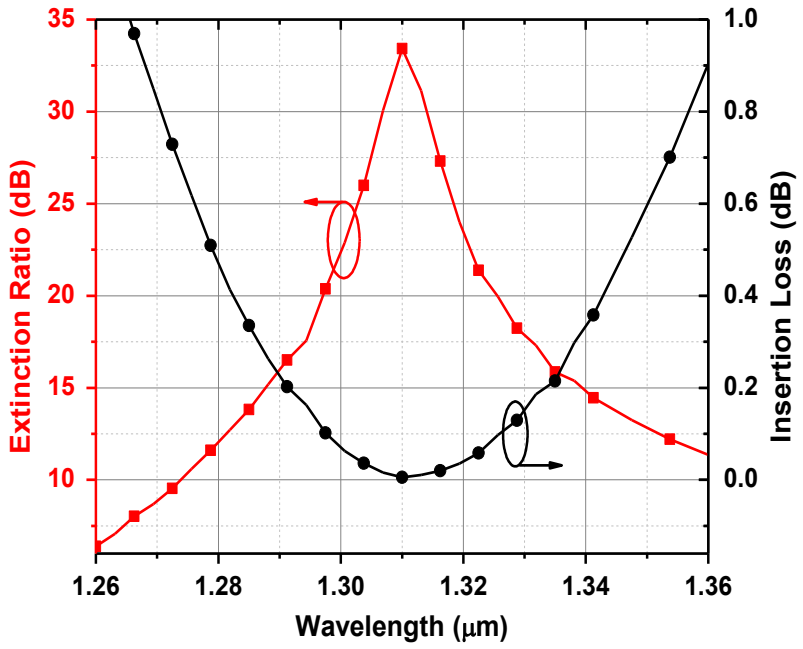
Extinction Ratio (dB)
Insertion Loss (dB)
Wavelength (μm)
35
30
25
20
15
10
1.0
0.8
0.6
0.4
0.2
0.0
1.26
1.28
1.30
1.32
1.34
1.36

(a)

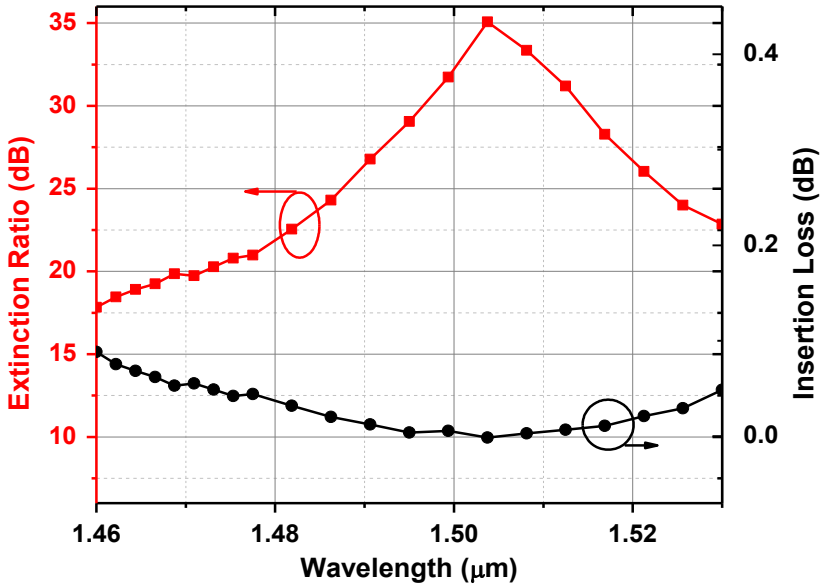
Extinction Ratio (dB)
Insertion Loss (dB)
Wavelength (μm)
35
30
25
20
15
10
0.4
0.2
0.0
1.46
1.48
1.50
1.52

(b)

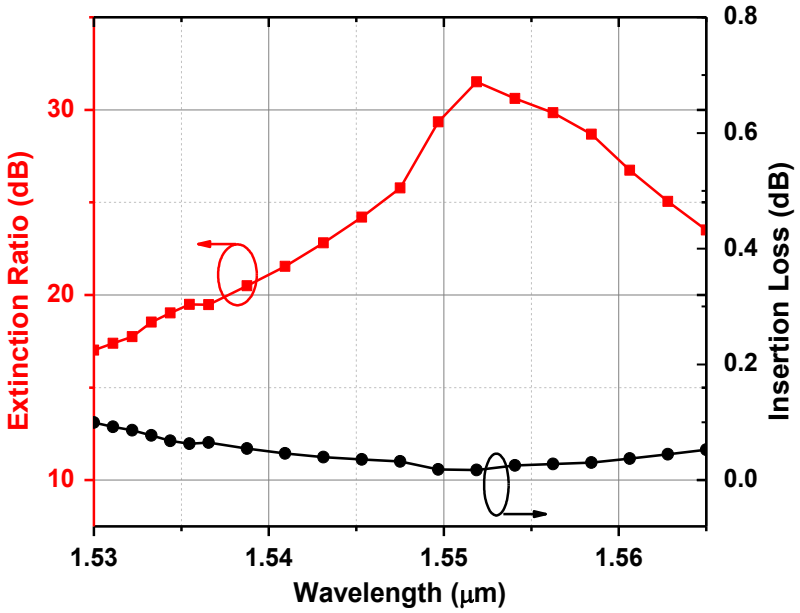

(c)

Figure 3-7: Extinction ratio (ER_{12}) and insertion loss of LP_{02} converted to LP_{01} in the a) O-band, b) S-band, and c) C-band

3.6. The (de)multiplexer:

To (de)multiplex LP01 and LP02, we design a symmetrical circular directional coupler (DC) as shown in

Figure 3-8. Such a (de)multiplexer can be made easily broadband. The coupler has two input ports (P1 and P2) and two output ports (P3 and P4). The waveguides forming the two arms of the coupler have the same radius rc. The refractive index of the two cores is n1 (the same as the refractive index of the core in the mode converter) and the refractive index surrounding the two waveguides is n2. The two waveguides are separated by a distance d1 at the input and a distance dc at the coupling region.

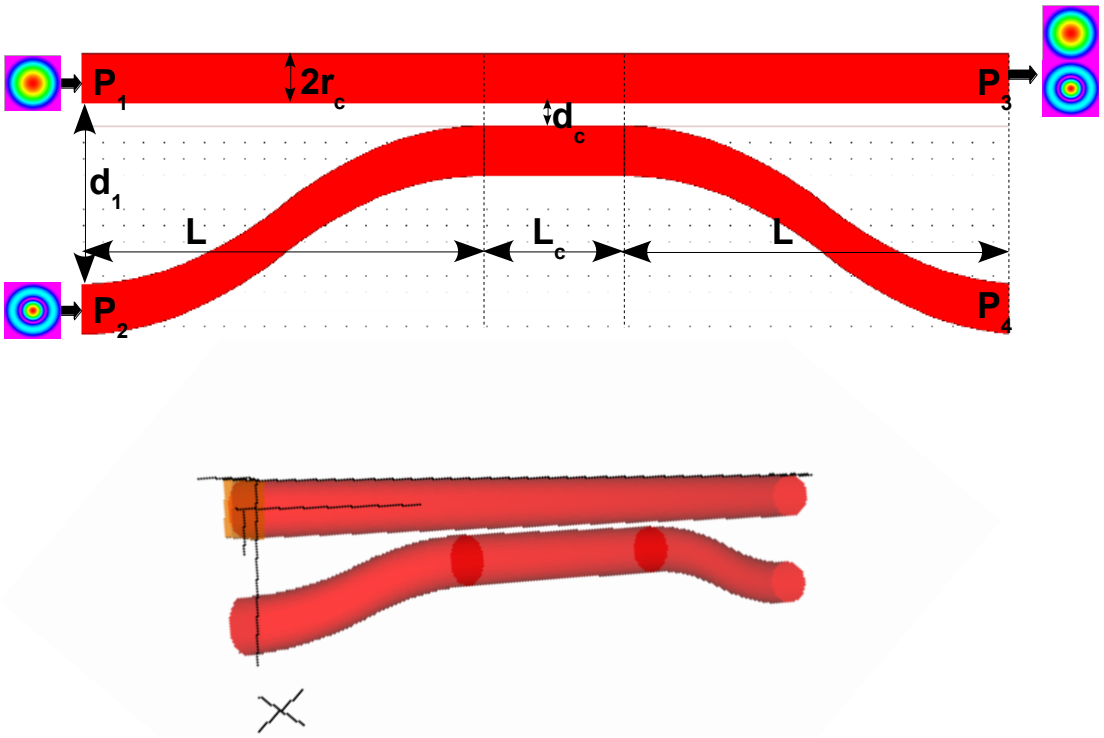

Figure 3-8: Symmetrical directional coupler

In general, if mode *b* from port 2 is to be multiplexed with mode *a* from port 1, the minimum coupling distance L_c is given by: $L_c = \frac{\pi}{2\kappa}$, where κ is the coupling coefficient between the two modes *a* and *b*, and it is given by [79]:

$$\kappa = \frac{\omega}{4}\varepsilon_0 \int\int e_a^* . \Delta n^2 . e_b \, dx \, dy \qquad (3.1)$$

Where e_a and e_b are the electric field of modes *a* and *b* respectively. Δn represents the difference in refractive indices.

In the case of coupling to the same mode (i.e., $a = b$), the coupling coefficient is inversely proportional to the mode propagation constant β, which is proportional to the mode order ($\beta_{LP01} > \beta_{LP02} > \beta_{LP03} > \ldots$). Therefore, the coupling distance is inversely proportional to the mode order ($L_{c,LP01} > L_{c,LP02} > L_{c,LP03} > \ldots$). This is why we have chosen to input mode LP_{01} from port P_1 and mode LP_{02} from port P_2 to minimize the coupling distance L_c. Table 3-3 illustrates the values of the DC parameters optimized for the C-band.

Table 3-3: The optimized parameters of the DC

Parameter	Value (mm)
r_c	5
L	1000
L_c	1060
d_1	10
d_c	0

Figure 3-9 shows the insertion loss (IL) of modes LP_{01} and LP_{02} along the multiplexer when both modes are input (LP_{01} at P_1 and LP_{02} at P_2). The figure (with the zoomed inset) shows clearly that both modes are output at the same port P_3 with 0.45dB and 0.1dB insertion loss for modes LP_{01} and LP_{02} respectively. The IL of LP_{02} is chosen to be lower than that of LP_{01} to compensate for the IL generated by the mode converter.

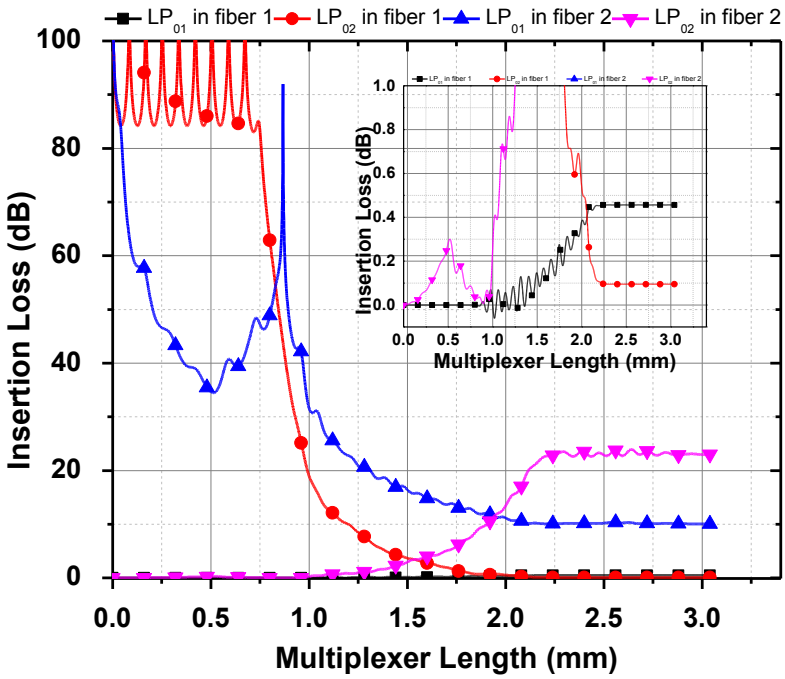

Figure 3-9: IL of LP_{01} and LP_{02} mode when both modes are input to the multiplexer

Figure 3-10 shows the IL when a single mode is input to the multiplexer and Figure 3-11 illustrates the electric field profile along the multiplexer in the case when both modes are input as well as a single mode is input.

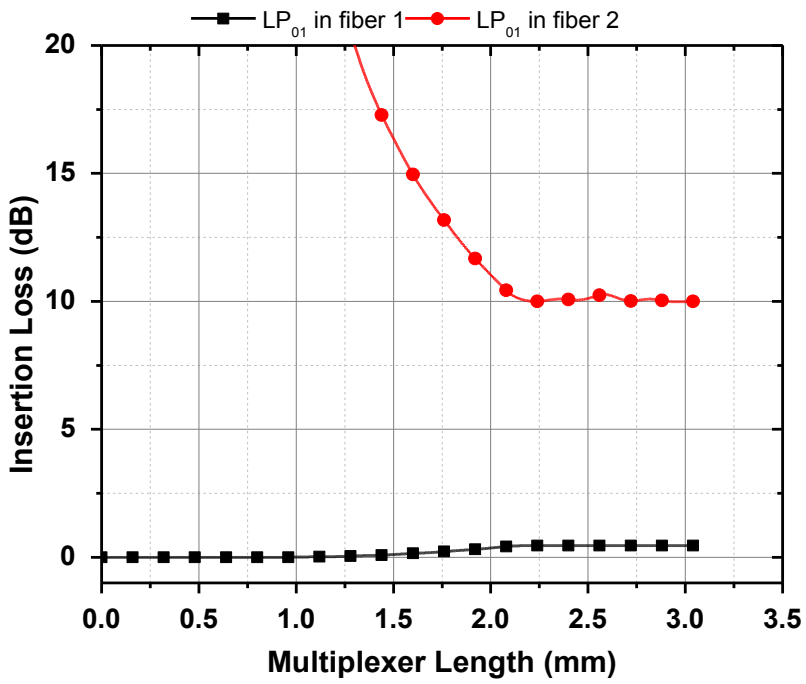

(a)

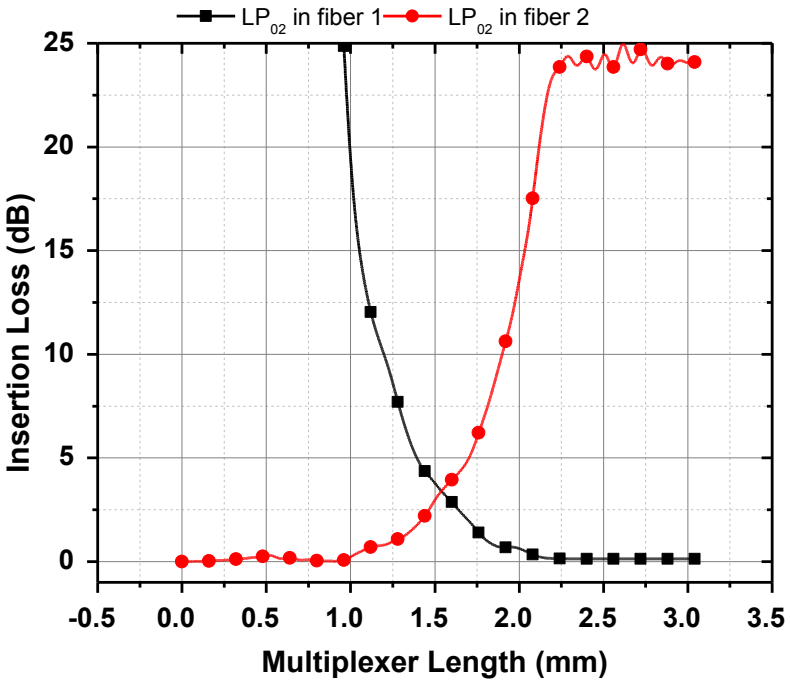

(b)

Figure 3-10: IL of (a) LP_{01} and (b) LP_{02} mode when a single mode input to the multiplexer

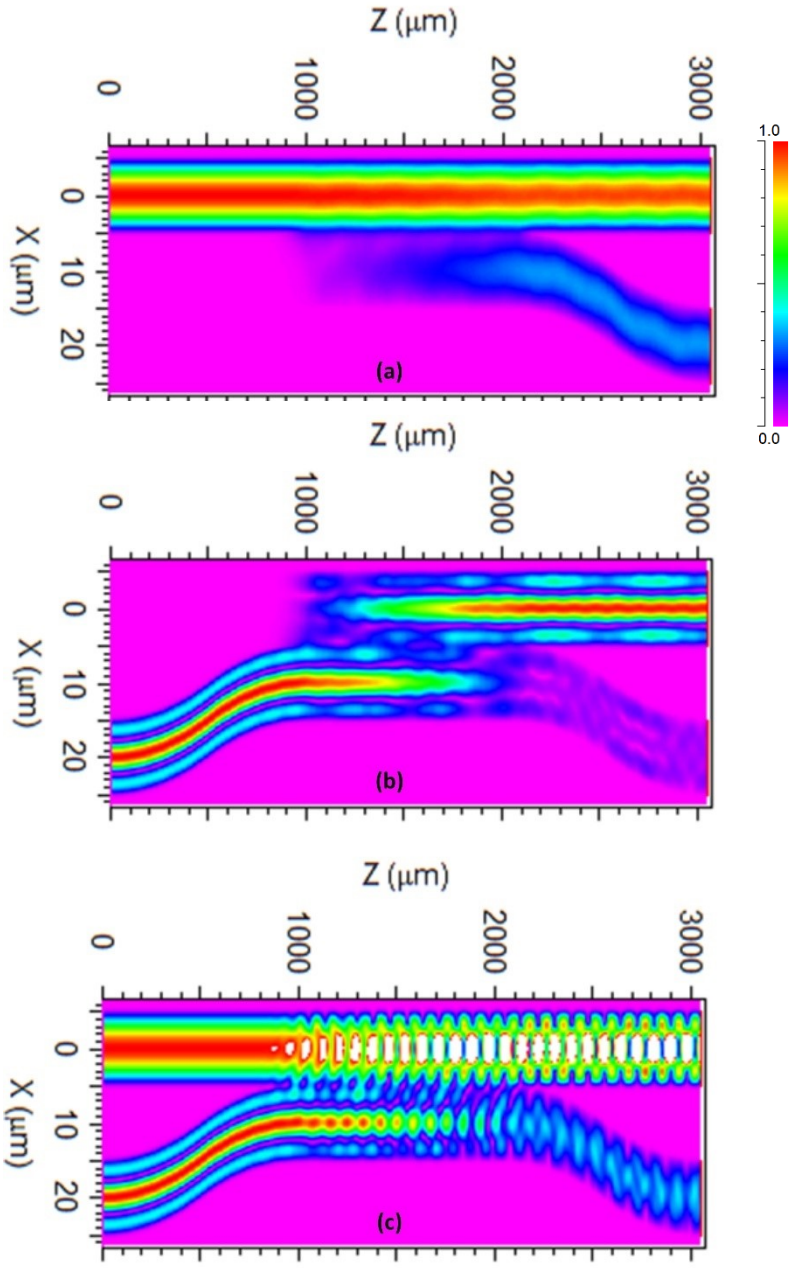

Figure 3-11: Electric field profile of (a) LP_{01}, (b) LP_{02} and (c) both LP_{01} and LP_{02} modes

Figure 3-12 with the inset shows the insertion loss when both modes are input versus the wavelength. We can see clearly that even though the multiplexer was designed for the C-band, it is broadband stretching to cover the O and S bands with a small additional loss (less than 1.5dB).

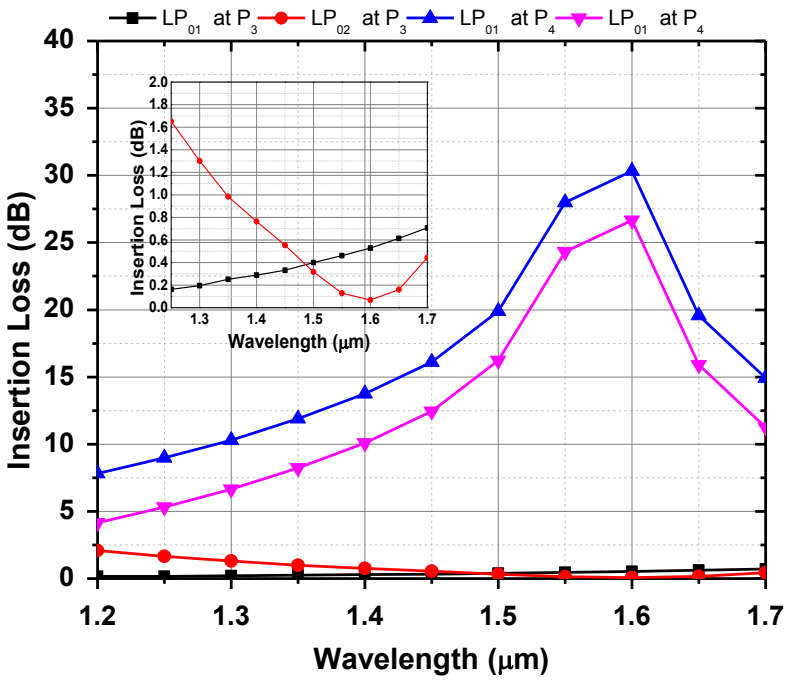

Figure 3-12: Insertion Loss of the multiplexer over a very wide band of wavelengths

The coupler is symmetric, so it can be used to multiplex and demultiplex LP_{01} and LP_{02} modes as shown in Figure 3-13.

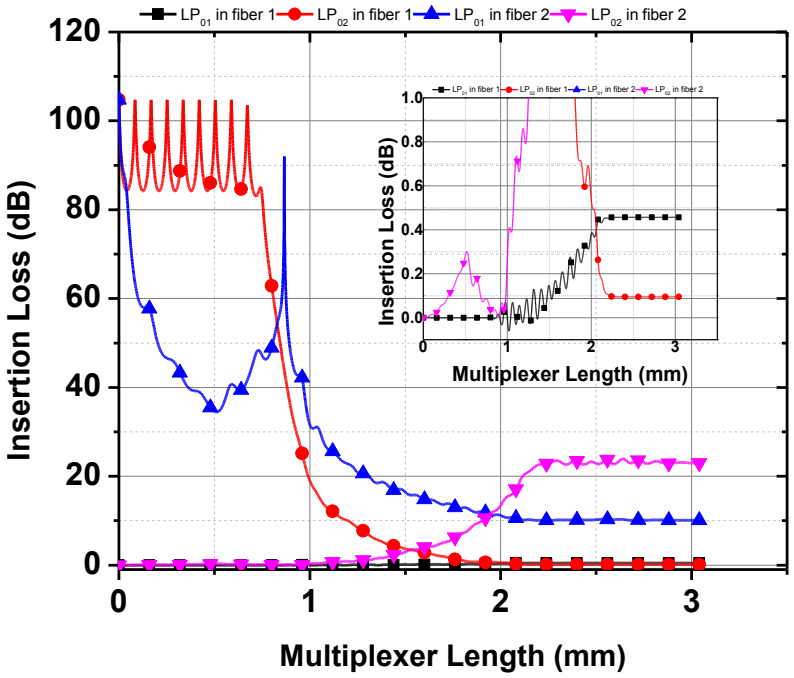

(a)

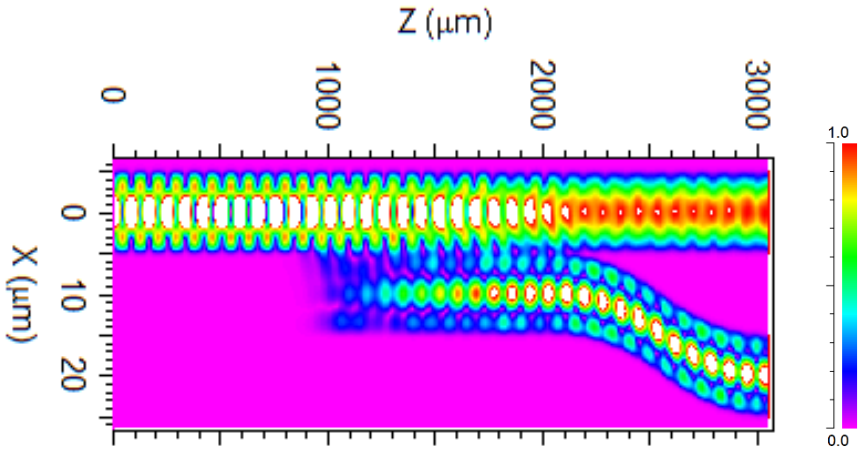

(b)

Figure 3-13: Insertion Loss and electric field profile of the demultiplexer

Now, it is time to put the two devices together (converter and multiplexer). At the transmitter side, mode LP_{01} is directly injected to the multiplexer at port P_1, whereas LP_{02} is resulted from mode converter. There is also a radius adaptation step between the output of the mode converter and the input of the mode multiplexer at port P_2 (this adapter is realized using a tapered section with an initial radius equal to the output radius of the mode converter and a final radius equal to the radius of the waveguide of the mode multiplexer). The complete device is shown in Figure 3-14.

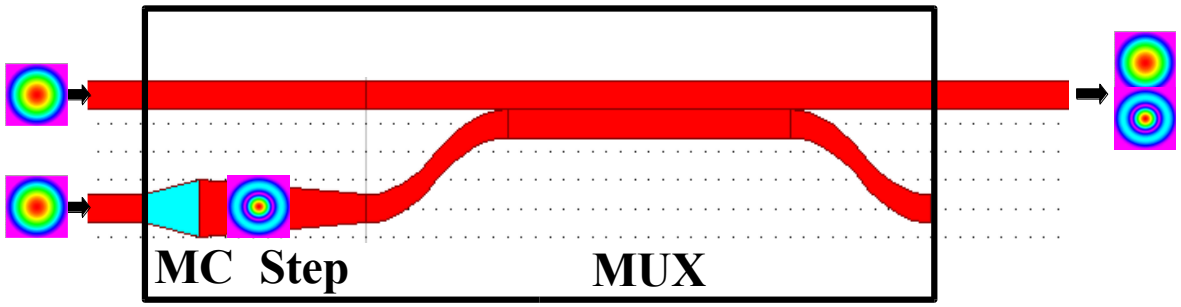

Figure 3-14: Schematic diagram of the complete device (Mode converter (MC), step and multiplexer (MUX))

Table 3-4 gives the IL of the output modes LP_{01} and LP_{02} using the complete device in the center of C-band.

Table 3-4: IL of the complete device in C-band

Mode	In MC	In step	In MUX	Total
LP_{01}	0	0	0.46dB	0.46dB
LP_{02}	0.016dB	0.3	0.1dB	0.416dB

3.7. Fabrication of a LP_{01} to LP_{02} mode converter

The proposed device is based on an axially-varying profile waveguide. This type of circular tapers would be difficult to realize with traditional fiber drawing techniques, such as those techniques using planar geometry to realize tapers. Recently, advances in femtosecond laser pulses to inscribe a 3D photonic device inside a transparent glass have received full attention from designers and researchers. This technique allows the fabrication of passive and active integrated photonic devices by focusing the light of a laser beam to induce a local refractive index change through multiphoton interaction [77], [78], [80], [81]. This technique has also a great flexibility with the type of glasses in which inscription is performed since it does not require UV sensitive glasses like continuous-wave or quasi-continuous-wave UV exposure techniques [82]. With proper displacement, rotation and translation of the glass, almost any arbitrary shape can be written (taper, Y-junction, S-section, etc.). Moreover, different devices could be written sequentially or in parallel, allowing the integration of complex photonic devices and systems.

To fabricate the proposed mode converter embedded in a bulk glass using femtosecond direct inscription, the device parameters have been re-tuned to fit the fabrication requirements. The values of the mode converter parameters are given in Table 3-5.

Table 3-5: Parameters of the fabricated mode converter (L_i and r_i in μm)

Parameters	L_1	L_2	L_3	L_4, L_5	n_1, n_3	n_2	r_0	r_1	r_2
Value	1200	0	1020	0	1.4877	1.4907	5	39	4

The converter has a total length of about 2.22 mm, an initial diameter of 10 microns and a final diameter of 78 microns. The input of the converter can be easily coupled to a single mode fiber (Corning SMF-28), which has a typical mode field diameter (MFD) of about 10.4 microns.

The mode converter was inscribed in a 1.1 mm thick bulk glass sample (top surface of 2×10 mm^2, Corning Eagle2000) using a Ti:sapphire laser system (Coherent RegA). The system was operated at a wavelength of 790 nm and a repetition rate of 250 kHz. The temporal full-width at

half maximum (FWHM) of the pulses was measured to be ~65 fs at the laser output and estimated at 85 fs on the sample. The beam was focused beneath the surface of glass samples using a 50× (Edmunds M Plan APO LWD, f = 4 mm, 0.55 NA) microscope objective. A cylindrical lens telescope was used to produce an astigmatic beam and shape the focal volume in such a way as to form traces with circular cross sections [83], [84]. The samples were translated at a speed of 3mm/s, across the focal point, perpendicular to the laser beam using motorized mechanical stages (Newport XML210 and GTS30V). In order to fabricate the mode converter, an approach similar to Gosh et al. [85], [86] was used. The beam was scanned multiple times (314 times) while following slightly displaced trajectories (with 2 microns space between each adjacent trajectory) was used to fill in the contour of the design. After the inscription process, photo-inscribed devices were examined under an optical microscope (Olympus STM6). Figure 3-15 shows the top view, the input face as well as the output face of the fabricated mode converter.

Figure 3-15(a) shows the left part of the fabricated device (mainly section L_1 as shown in Figure 3-1). At the left, a circular section is inserted with a diameter of ~10 microns and a length of ~47 microns. This section is used for input LP_{01} mode to be coupled to a SMF. The right section depicts clearly the tapered segment L_1. The resulting inscribed taper and core-cladding refractive index contrast follow our design. Figure 3-15(b) illustrates the input beam of the laser to be used for inscription. Unfortunately, the beam has a principal (desired) focus and a second (non-desired) focus. Moreover, the shape of the principal focus deviates from the targeted shape, since it does not have a perfect circular form (in fact, it has a D shape) and its radii are slightly above the desired 10 micron). Figure 3-15(c) shows that there is an unwanted structure formed underneath the desired structure. This structure is due to the second focus of the astigmatic input beam [83]. The image of the input face of the bream (Figure 3-15(b)) clearly shows that defect exists (not perfect fundamental mode). As a result, a region in which the refractive index difference is slightly higher than the rest of the structure is formed where the unwanted and desired structures overlapped. Therefore, the output LP_{02} mode is more confined in the overlap region than the rest as shown by Figure 3-16.

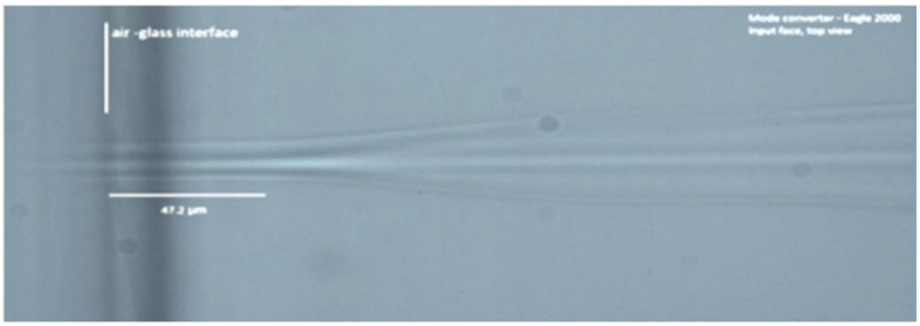

(a) Top view

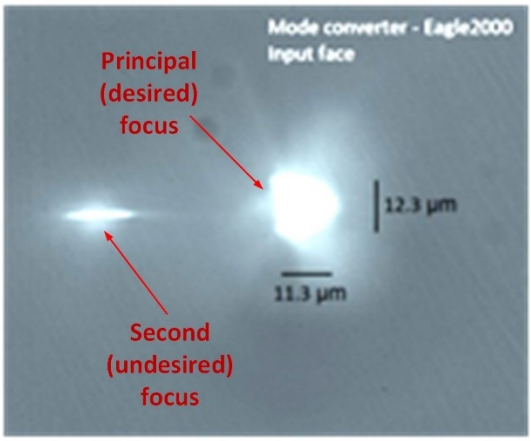

(b) Input face

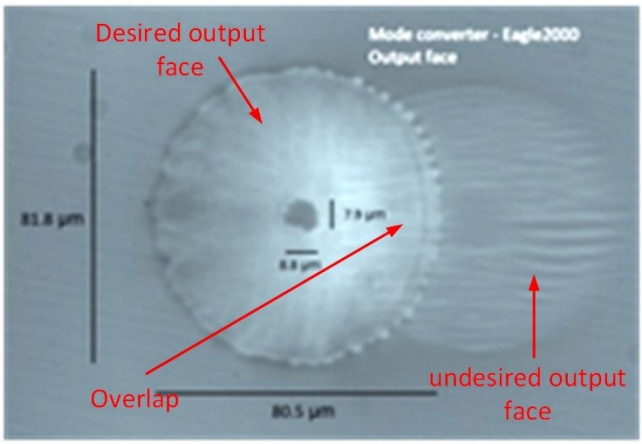

(c) Output face

Figure 3-15: Microscope image of (a) the top view, (b) the input face and (c) the output face of the fabricated mode converter.

Figure 3-16 depicts the output intensity profile of the resulting mode at four different wavelengths of 1510, 1540, 1550 and 1570 nm. Figure 3-16 demonstrates that despite the presence of the defects in the inscribed device, the output mode intensity profile is very close to an LP_{02}. All the intensity profiles in Figure 3-16 have an internal spot surrounded by an outer ring. In some wavelengths, the ring is not continuous due to the unwanted structure formed by the defect in the input laser beam. Figure 3-16 shows also that even though the converter was designed mainly for the C-band (from 1530 to 1565 nm), it covers a wider band, extending over both sides of the C-band.

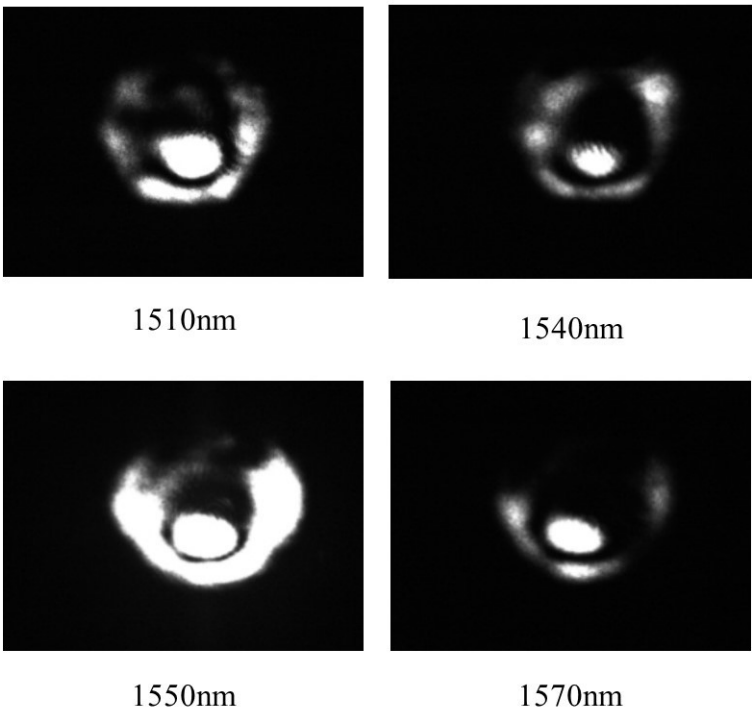

Figure 3-16: Intensity profile of the output LP_{02} mode at four different wavelengths.

The results shown in Figure 3-16 were obtained using the set-up illustrated in Figure 3-17. It consists of a tunable input laser, a 3-D adjustable stage for alignment and a high-resolution CCD camera. The input light beam from a single mode fiber (LP_{01} mode) connected to the tunable laser is directly injected into the input section of the mode converter (at air-glass interface as shown in Figure 3-15(a)). The output light from the converter (LP_{02} mode) is focused through lenses and then captured by the camera, which is connected to a computer. The 3-D adjustable stage is used to align the output light from the SMF into the input of the device. It has three degrees of freedom allowing a perfect alignment to insure minimum coupling losses between the light from the output of SMF into the input of the device under test.

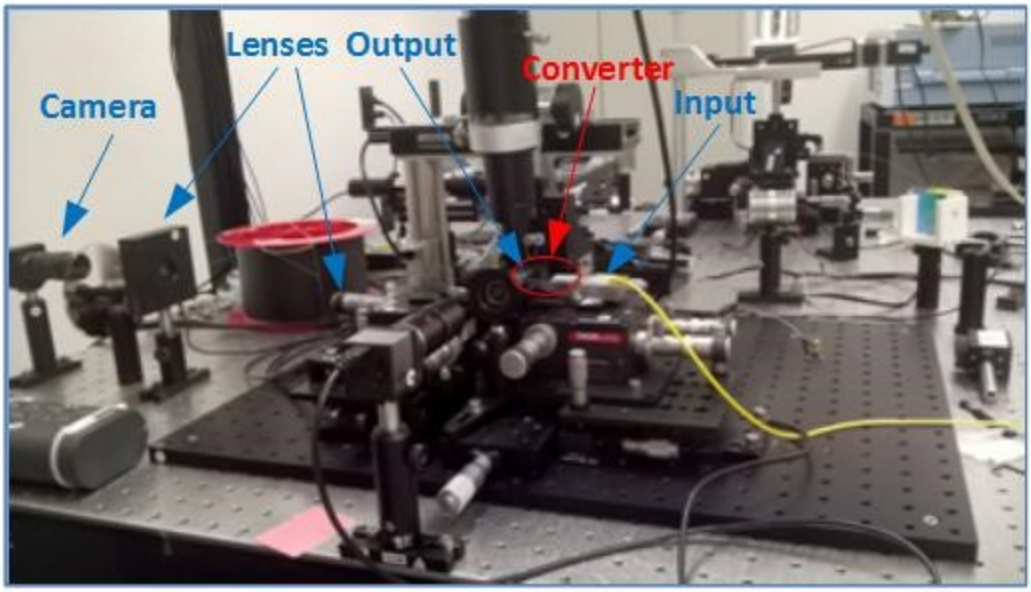

Figure 3-17: The set-up used to analyze the mode converter

Figure 3-18 illustrates the comparison between the simulated and measured insertion loss (conversion efficiency) of the fabricated converter. The simulation result shows a flat response of the converter over a wide range of wavelengths centered at 1550 nm, whereas the measured response has a minimum insertion loss at 1555 nm and the loss varies from 0.4 to 1.3 dB over the wavelength range from 1510 to 1575 nm. If only C-band is considered, the insertion loss is less than 1 dB, implying mode conversion efficiency of more than 80%.

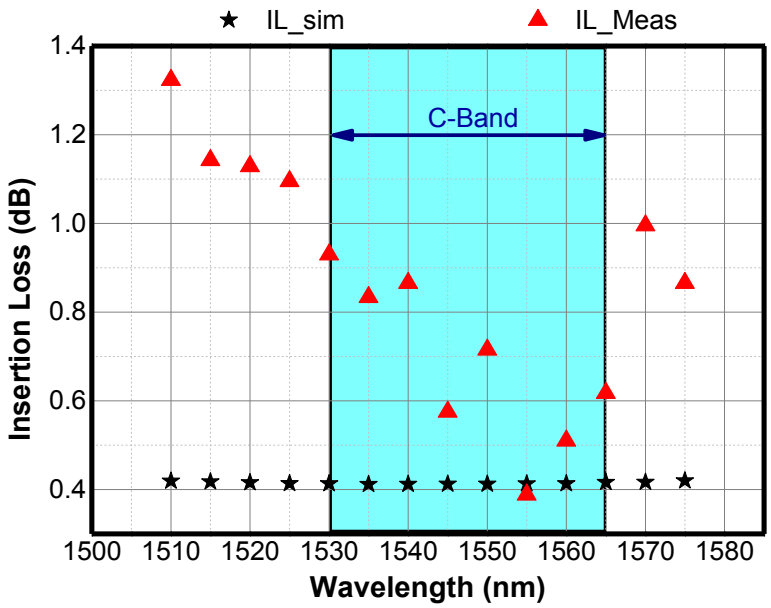

Figure 3-18: Insertion loss (IL) of the fabricated mode converter (sim: simulated, meas: measured)

3.8. Summary

In this chapter, we have proposed a broadband mode converter using two circular waveguide tapers to convert LP_{01} to LP_{02}, and vice versa. Over the entire O, S and C-band, more than 75% (O-band) and 98% (S- and C- band) conversion efficiency and higher than 10 dB (O-band) and 19 dB (S- and C-band) extinction ratio can be achieved. Furthermore, the dependence of conversion efficiency and extinction ratio on wavelength is not strong in C-band. The device can achieve more than 97% conversion efficiency and higher than 19 dB extinction ratio over the entire C-band. By the analysis, it has been found that the performance of the mode converter is not very sensitive to any small variations of the converter parameters.

For the reciprocal operation, the mode converter can have conversion efficiency of more than 99% and extinction ratio of more than 30 dB at the central wavelengths of the three bands. For the entire three bands, both conversion efficiency and extinction ratio show similar performance compared to the conversion from LP_{01} to LP_{02}.

In addition to the mode converter, a two-mode (de)multiplexer (for LP_{01} and LP_{02}) using the mode converter combined with symmetric directional coupler is designed. This (de)multiplexer has a small insertion loss (less than 0.5 dB over the entire C-band), suggesting more than 95% (de)multiplexing efficiency.

we have also reported the fabrication of an LP_{01} to LP_{02} mode converter using femtosecond laser 3D inscription on a borosilicate Corning Eagle 2000 glass. The fabricated converter length is 2.22 mm and has an insertion loss of less than 1dB over the entire C-band, implying mode conversion efficiency of more than 80%.

Chapter 4: LP_{01} to LP_{0m} Mode Converters

4.1. Introduction

In the previous chapter, we have presented the design, analysis and fabrication of an LP_{01} to LP_{02} mode converter. During the analysis of the converter performance, we have remarked that conversion can also be achieved to other higher order modes (especially LP_{0m} modes). In this chapter, we use the same structure, shown in Figure 4-1 to obtain LP_{01} to LP_{0m} mode converters by tuning the device parameters.

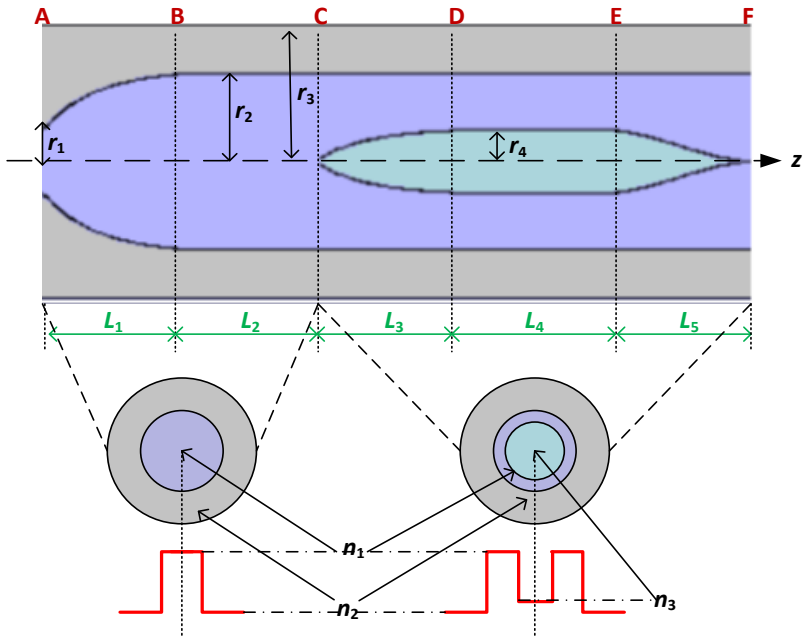

Figure 4-1: Schematic diagram of the proposed LP_{01} to LP_{0m} mode converter

4.2. The Performance Analysis of the Proposed LP_{01} to LP_{0m} Mode Converter Structure

We have carried out simulations to optimize the parameters of the mode converters from LP_{01} to LP_{0m} and the results for LP_{01} to LP_{0m}, m = 2 … 7 are summarized in Table 4-1. However, the same structure could be tuned for any LP_{01}–LP_{0m} conversion. For fabrication purposes, we have chosen n_1 = 1.4905 and $n_2 = n_3$ = 1.4877.

Table 4-1: Optimal parameters for the mode converters. Dimensions are in µm.

LP_{01} to	L_1	L_2	L_3	L_4	L_5	r_1	r_2	r_4	IL (at 1550nm)
LP_{02}	1179	114	167	95	1337	10	82	11	0.1
LP_{03}	1359	3	418	4	1833	12	115	15	1
LP_{04}	2898	373	105	1244	2000	12	80	71	1.2
LP_{05}	121	763	1424	300	542	12	147	47	2.5
LP_{06}	1414	388	557	53	589	12	163	100	2
LP_{07}	2482	26	100	290	917	12	213	92	2.5

Figure 4-2 shows the insertion loss (IL) of the different LP_{0m} modes. Figure 4-2(a), shows that the obtained mode converters can operate over a broad bandwidth. For instance, LP_{01}–LP_{03} mode converter can be used over the O-, E-, S-, C- and L-bands for an IL less than 3.5dB. The same bandwidth can be obtained for the LP_{01}–LP_{06} mode converter with a maximum IL of 6dB.

More interestingly, Figure 4-2(b) demonstrates that all the designed mode converters could span the C-band (from 1530nm to 1565nm) with an IL not exceeding 3dB.

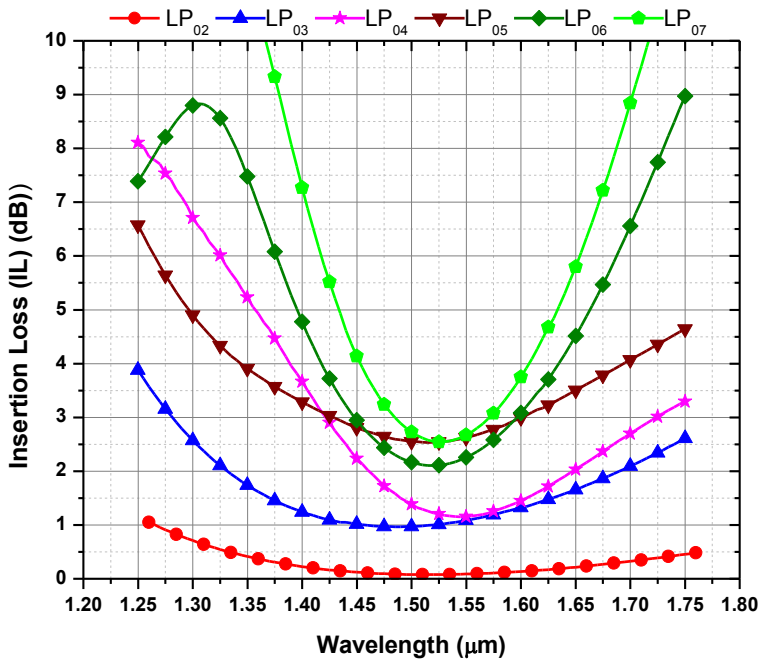

(a)

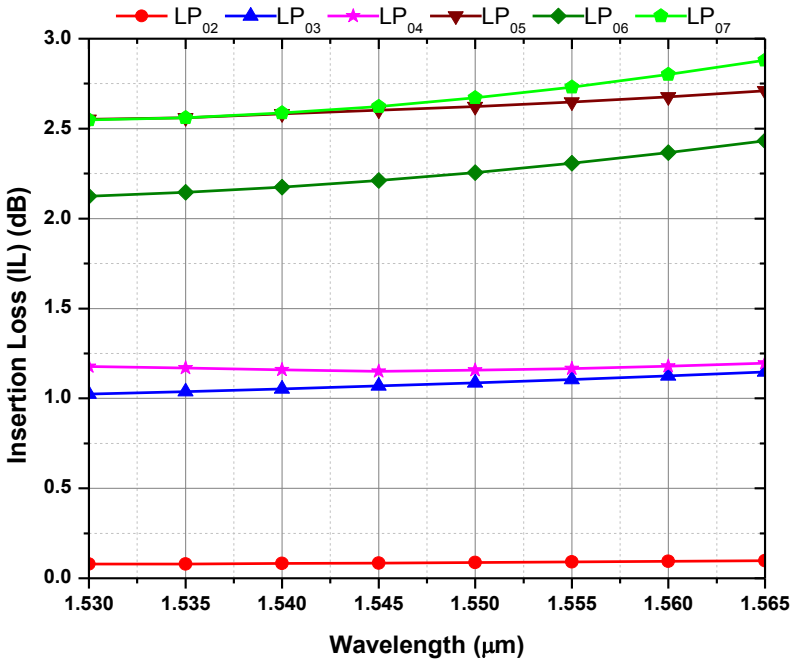

(b)

Figure 4-2: Insertion loss (IL) of LP_{0m} modes at the output of mode converter (a) over a broadband, (b) over the C-band

4.3. The Mode Multiplexer/Demultiplexer

After converting LP_{01} mode to the desired LP_{0m} modes, they need to be multiplexed on a single (few-mode) fiber at the transmitter and demultiplexed (and then reconverted back to LP_{01}) at the receiver. We have chosen to use directional couplers (DCs) for multiplexing and demultiplexing. A DC-based mode multiplexer is shown in Figure 4-3, in which multiplexing/demultiplexing of the first five LP_{0m} modes (m = 1, …, 5) is considered. However, multiplexing/demultiplexing of any number of modes can be applied in principle. The structural parameters of the multiplexer/demultiplexer are optimized based on minimizing the insertion loss of multiplexed/demultiplexed modes at the output.

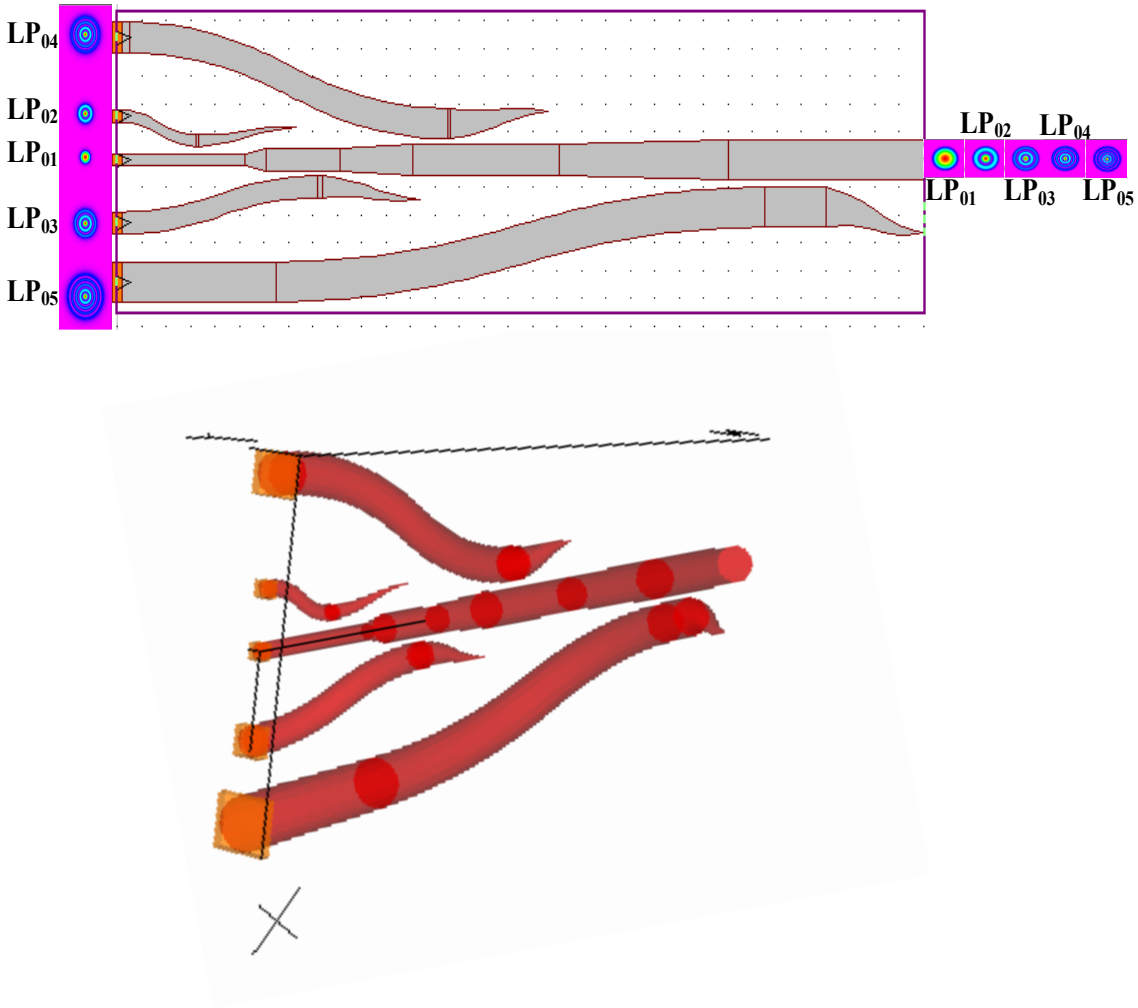

Figure 4-3: LP_{0m} (m = 1, 2, …, 5) mode multiplexer.

Figure 4-4 illustrates the insertion loss of the multiplexer and demultiplexer over the C-Band. It is shown that a worse case of 2.7 dB is obtained for demultiplexing LP_{04}. At the central wavelength of 1550 nm, all the five modes can be multiplexed/demultiplexed with an insertion loss of less than 2.3 dB.

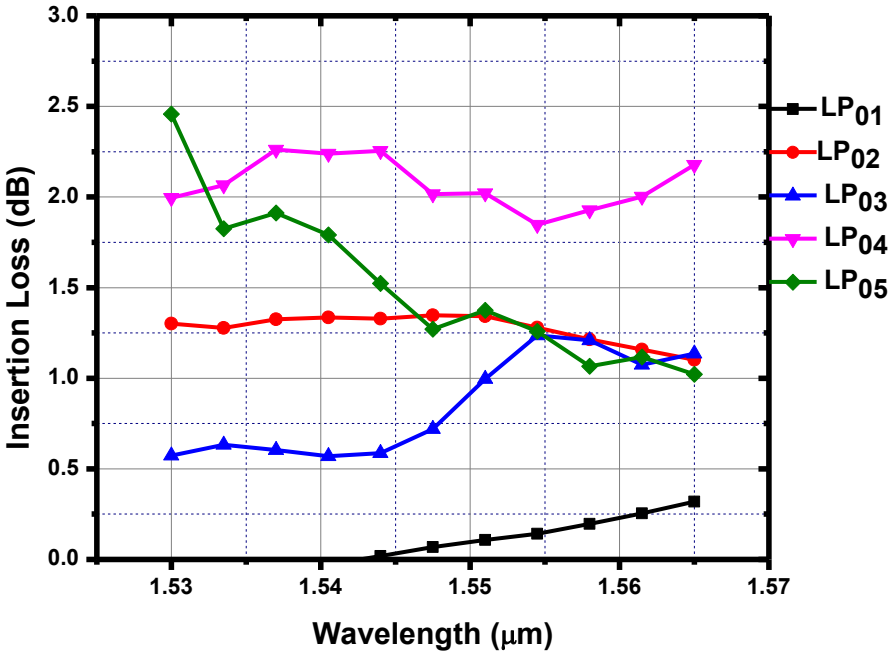

(a)

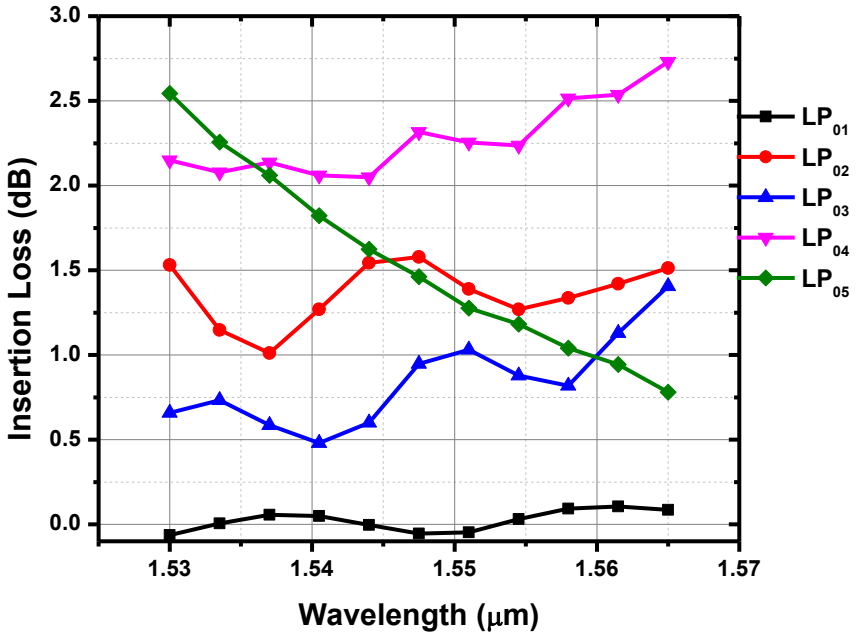

(b)

Figure 4-4: Insertion loss of LP_{0m} (m = 1...5) modes at the output of the mode (a) multiplexer and (b) demultiplexer.

Figure 4-5(a) and (b) illustrate the crosstalk of the multiplexer and demultiplexer for the C-band, respectively. Both have less than -15 dB crosstalk at the central wavelength (1550 nm) for the five modes. In general, it is shown that the crosstalk depends on the mode order, so higher order modes suffer from more crosstalk than lower order modes. Furthermore, the LP_{04} mode experiences the worst crosstalk between the modes.

In a systematic design, one can optimize the two structures (mode converter and mode multiplexer) to balance the insertion loss and crosstalk from both structures for all the modes.

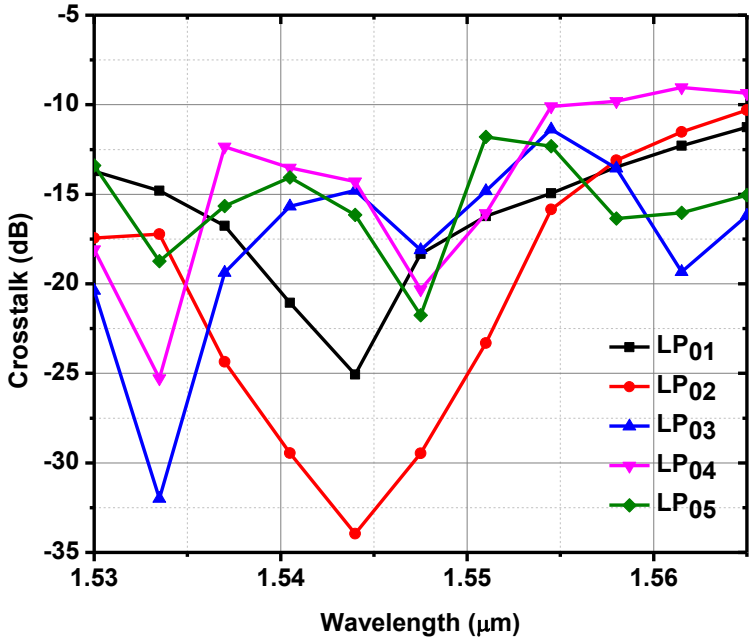

(a)

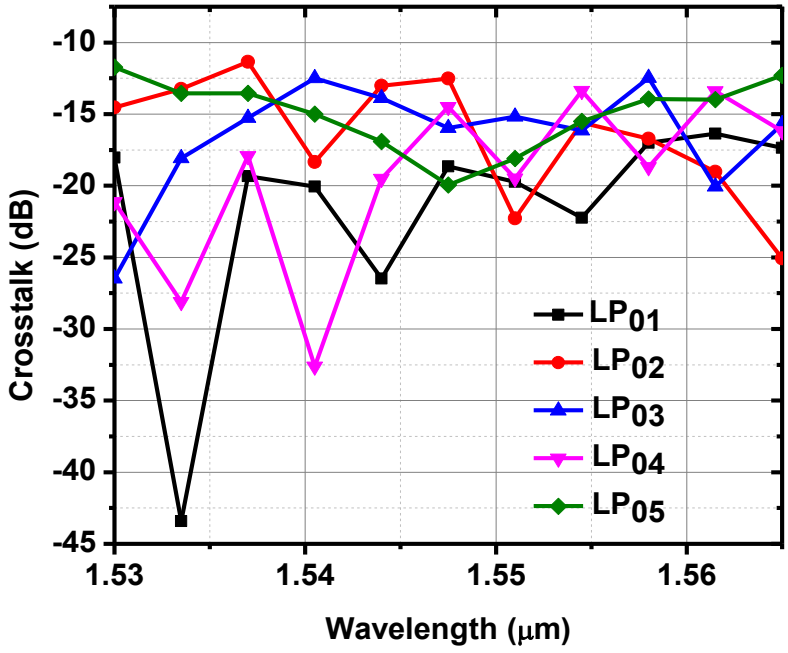

(b)

Figure 4-5: The crosstalk of the LP_{0m} (m = 1, 2, 3, 4, 5) modes at the output of (a)multiplexer and (b) demultiplexer.

4.4. Summary

In this chapter, we have proposed an LP_{01} to LP_{0m} mode converter structure. The converter structure is based on the structure proposed in chapter 3 for converting LP_{01} to LP_{02}. The proposed structure can convert LP_{01} mode to LP_{02}, LP_{03}, LP_{04}, LP_{05}, LP_{06} or LP_{07}, with an insertion loss (IL) ranging from 0.1 dB to 3 dB and an extinction ratio larger than 8 dB over the entire C-band. We have also proposed a mode (de)multiplexer based on directional couplers.

To our best knowledge, the proposed converter performances are better than the reported LP_{01} to LP_{0m} mode converters. The comparison of the insertion loss (IL) of the proposed mode converters with some reported devices in shown in Table 4-2.

Table 4-2: Comparison between the proposed mode converter with the previous works

Mode converter (MC)	IL of the proposed (MC)	IL of previous works	Features of the previous work
LP_{01}–LP_{02}	0.4 dB	0.6 dB [70]	Simulation, Photonic lanterns
		1.8 dB [44]	Simulation, MMI
		2.7 dB [87]	Simulation, MMI
		2.75 dB [88]	Experimental, Phase mask
LP_{01}–LP_{03}	1 dB	6.2 dB [87]	Simulation, MMI
LP_{01}–LP_{04}	1.2 dB	NA	
LP_{01}–LP_{05}	2.5 dB	NA	
LP_{01}–LP_{06}	2 dB	NA	
LP_{01}–LP_{07}	2.5 dB	NA	

Chapter 5: LP_{01} to LP_{lm} Mode Converters

5.1. Introduction

In the two previous chapters, the proposed structure was used to convert LP_{01} mode to any LP_{0m} mode. That was possible because of the concentric circular profiles of LP_{0m} modes. To convert LP_{01} mode to other LP_{lm} ($l \neq 0$) modes, we propose to modify the structure by inserting more inner elements. These elements provide more structural parameters and allow the conversion of the LP_{01} mode to any LP_{lm} mode. The structure is outlined in the next section.

5.2. The LP_{01} to LP_{lm} mode converter structure

To convert LP_{01} to LP_{lm} mode ($l \neq 0$), we propose to use the structure shown in Figure 5-1, where a single inner element (as was the case for LP_{0m} modes) is not sufficient.

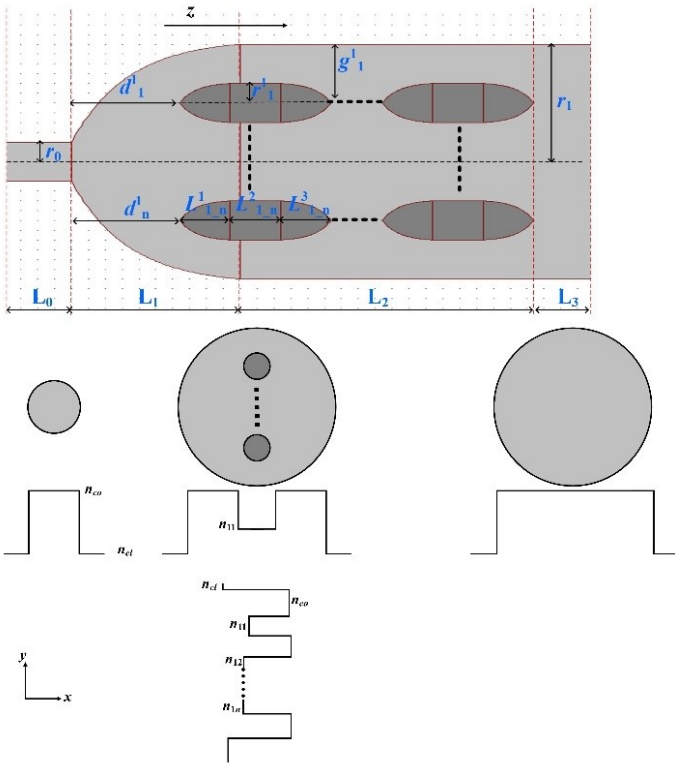

Figure 5-1: Schematic diagram of the proposed LP_{01} to LP_{lm} mode converter.

Inside the two outer circular sections, a matrix of small elements is inserted. Each element that is denoted by a row i and a column j, *i.e.* element (i, j), consists of three sections: a tapered section followed by a circular non-tapered section, and then followed by another tapered section. The beginning sections of the element (i, j) start with zero radius and taper to r^i_j with a length L^1_{ij}. The middle section is circular with a radius r^i_j and a length L^2_{ij}. The last section is circular with a radius r^i_j that is tapered to zero over a length L^3_{ij}. The refractive index of element (i, j) is n_{ij}. Elements (i, j) and $(i+1, j)$ (in the same column) are spaced by a gap g^i_j. Elements (i, j) and $(i, j+1)$ (in the same row) are spaced by a gap d^i_j. Table 5-1 illustrates the list of symbol definitions used in Figure 5-1

.

Table 5-1: List of symbol definitions used in Figure 5-1

Symbol	Definition
L_0	Beginning section length of the outer structure
L_1	Tapered section length of the outer structure
L_2	Circular (non-tapered) section length of the outer structure
L_3	Extra length for coupling to an MMF or an FMF
r_0	Beginning section radius of the outer structure
r_1	Circular section radius of the outer structure
L^k_{ij}	Length of the k^{th} section (k=1, 2 ,3) of the inner element (i,j)
r^i_j	Middle section radius of the inner element (i,j)
g^i_j	Vertical gap between two elements on column j
d^i_j	Horizontal gap between two elements on row i
n_{cl}	Refractive index of the cladding
n_{co}	Refractive index of the core (light-grey colored sections)
n_{ij}	Refractive index of element (i,j) (inner dark-grey colored sections)

5.3. The LP_{01} to LP_{11}, LP_{21}, LP_{31} converter structures

The number of the inner elements depends on the desired output LP_{lm} modes. As an example, we consider three modes only here, i.e. LP_{11}, LP_{21} and LP_{31}. Five inner elements were required to obtain LP_{11} and LP_{31}, whereas six inner elements were required for LP_{21} as shown in Figure 5-2. All three structures start with an initial radius r_0 of 5 μm for better coupling to a SMF. The LP_{01}-LP_{11} mode converter has a final radius r_1 of 30 μm, whereas the LP_{01}-LP_{21} and LP_{01}-LP_{31} mode converters both have r_1 = 26 μm. The inner elements have different radii ranging from 2 μm (element (2,2) in LP_{01}-LP_{11} MC) to 26 μm (element (2,1) in LP_{01}-LP_{31} MC) and different segment lengths ranging from 50 μm (end segment of element (1,2) in LP_{01}-LP_{21} MC) to 1500 μm (start segment of element (2,2) in LP_{01}-LP_{31} MC). For fabrication purposes, all inner elements have the same refractive index as the cladding (1.4877).

In order for these devices to be fabricated with available inscription technology requiring an input laser spot of 10 microns, the minimum vertical spacing between any two neighboring inner elements as well as between an inner element and the cladding should not be less than 10 microns.

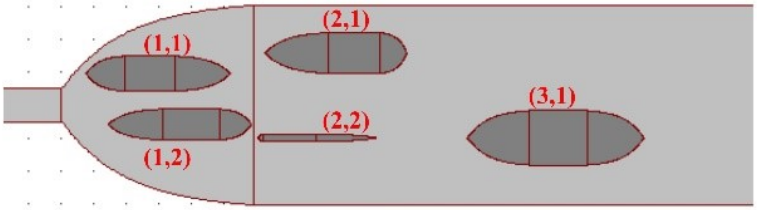

LP_{01} to LP_{11} MC

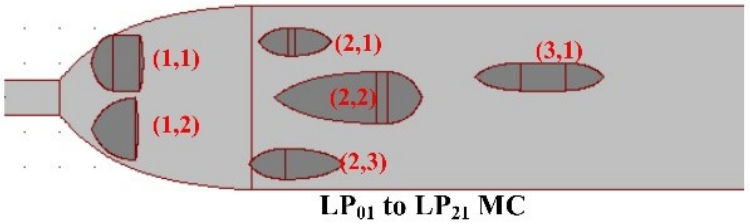

LP_{01} to LP_{21} MC

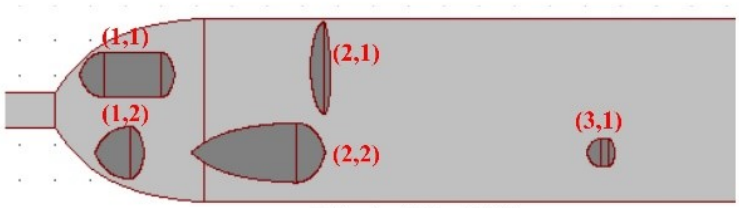

LP_{01} to LP_{31} MC

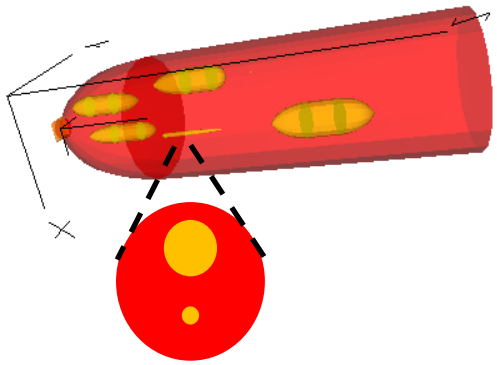

3D view of LP_{01} to LP_{11} MC

Figure 5-2: LP_{01} to LP_{11}, LP_{21} and LP_{31} mode converter structures.

Figure 5-3 shows the insertion loss of the three mode converters. Figure 5-3(a) shows the IL from 1300 to 1700 μm and Figure 5-3(b) presents the IL over the C-band. This figure shows that an IL of less than 2 dB is achieved over the entire C-Band for the three modes.

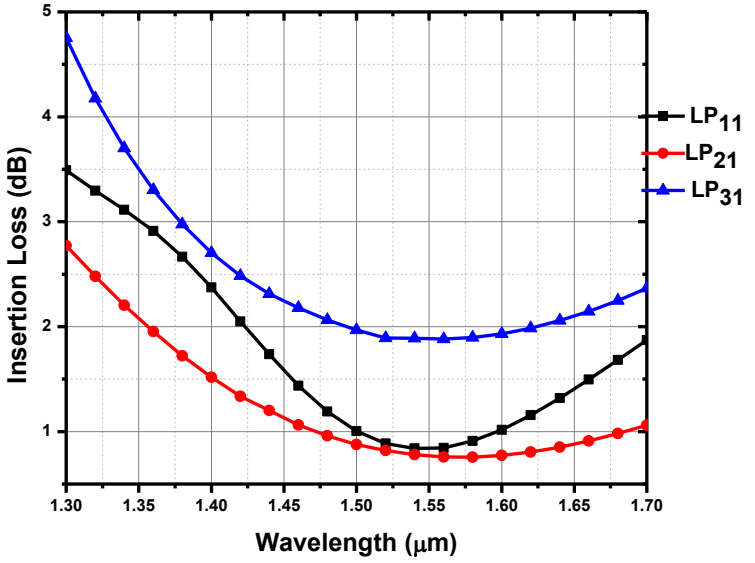

(a)

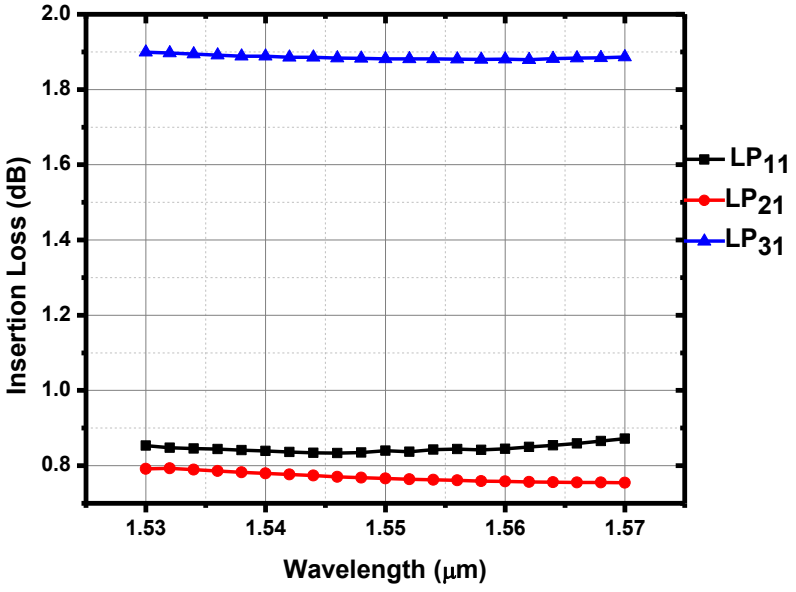

(b)

Figure 5-3: Insertion loss of LP_{11}, LP_{21} and LP_{31} modes over (a) a broadband, (b) the C-Band.

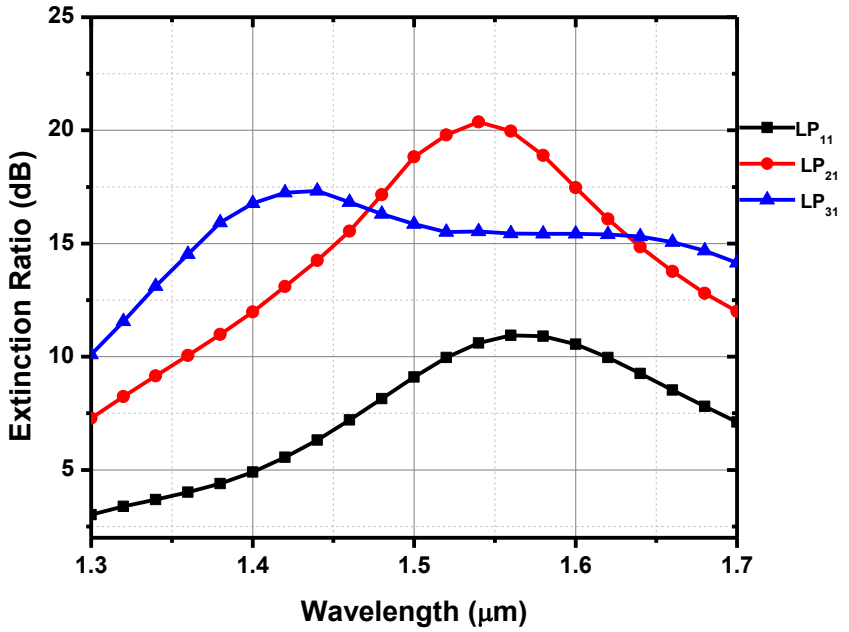

(a)

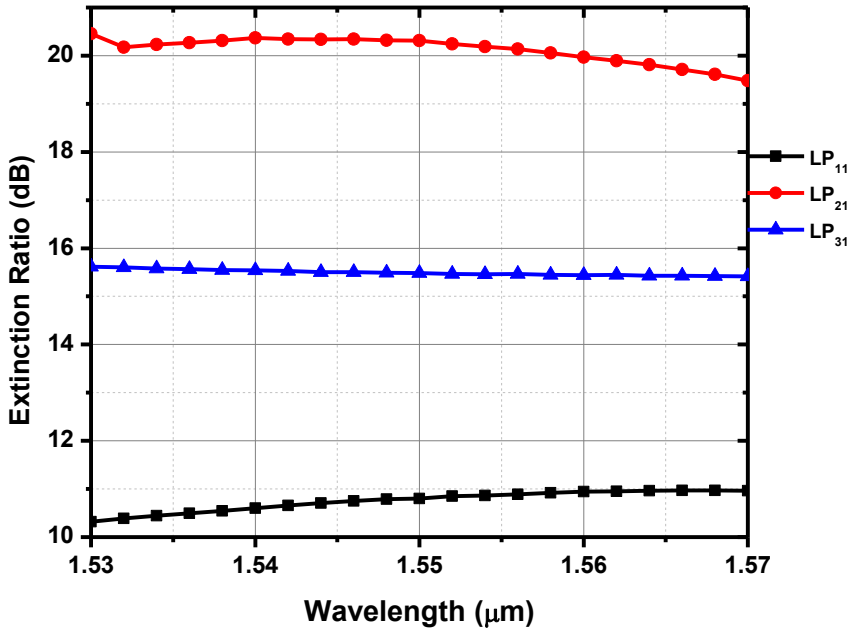

(b)

Figure 5-4: Extinction ratio for LP_{11}, LP_{21} and LP_{31} modes over (a) a broadband, (b) the C-Band.

Figure 5-4 shows the extinction ration (ER) of the three mode converters, where Figure 5-4(a) shows the ER over a broadband from 1300 to 1700 mm and Figure 5-4(b) presents the ER over the C-band and. Over this C-Band, an extinction ratio above 10 dB is achieved for the three modes. These results are obtained from brute-force simulation and optimization with numerical solvers and they can still be enhanced with some optimizations of the structure parameters and mode converters for any other LP_{lm} modes can be achieved using the structure in Figure 5-1.

5.4. The LP_{11}, LP_{21} and LP_{31} mode (de)multiplexer structure

To (de)multiplex the three obtained modes (LP_{11}, LP_{21} and LP_{31}), a (de)multiplexer structure based on parallel directional couplers like the one introduced in the previous chapter (see Figure 4-3) is used. The structure is shown in Figure 5-5. To simplify the structure design, all waveguides have the same radius (30 µm). This choice of using the same radius was motivated by the three radii (r_1) of the converters (LP_{01}~LP_{11}, LP_{01}~LP_{21} and LP_{01}~LP_{31}) which are 30 µm, 26 µm and 26 µm respectively. Furthermore, the same structure can be used at the transmitter side (for multiplexing) as well as at the receiver side (for demultiplexing) with similar performances.

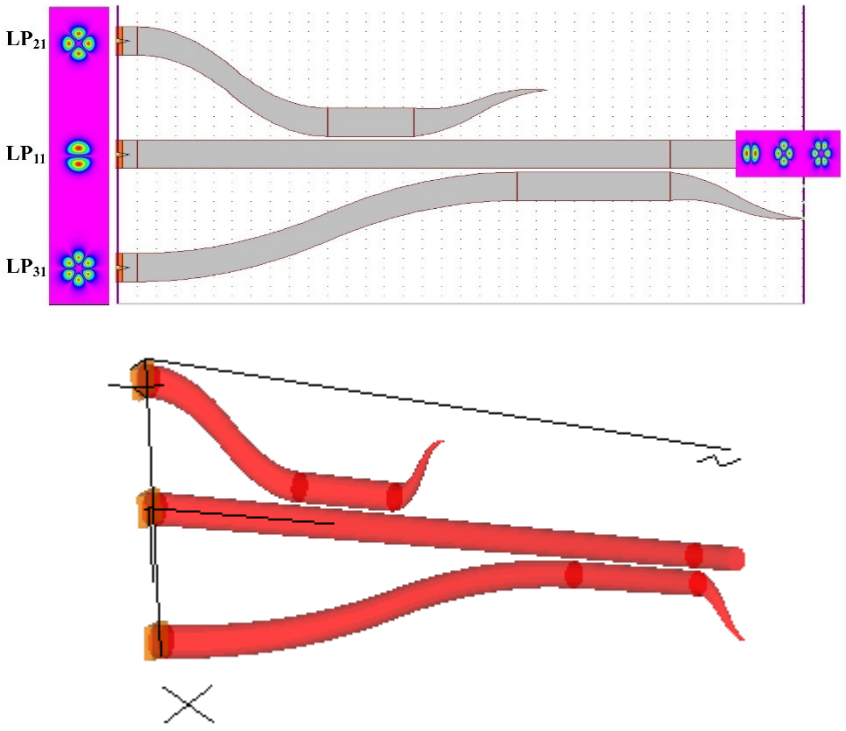

Figure 5-5: LP_{11}, LP_{21} and LP_{31} mode multiplexer

Figure 5-6 illustrates the insertion loss (IL) of the LP_{11}, LP_{21} and LP_{31} (d)multiplexer over the C-Band. Figure 5-6(a) shows that an IL of less than 1.9dB is achieved over the entire C-Band and less than 0.4dB at the design wavelength of 1550nm for the multiplexer. Figure 5-6(b) gives the simulation results of the demultiplexer over the C-Band. These results are similar to those of the multiplexer, therefore, the device is symmetrical, hence it can be used as multiplexer and demultiplexer.

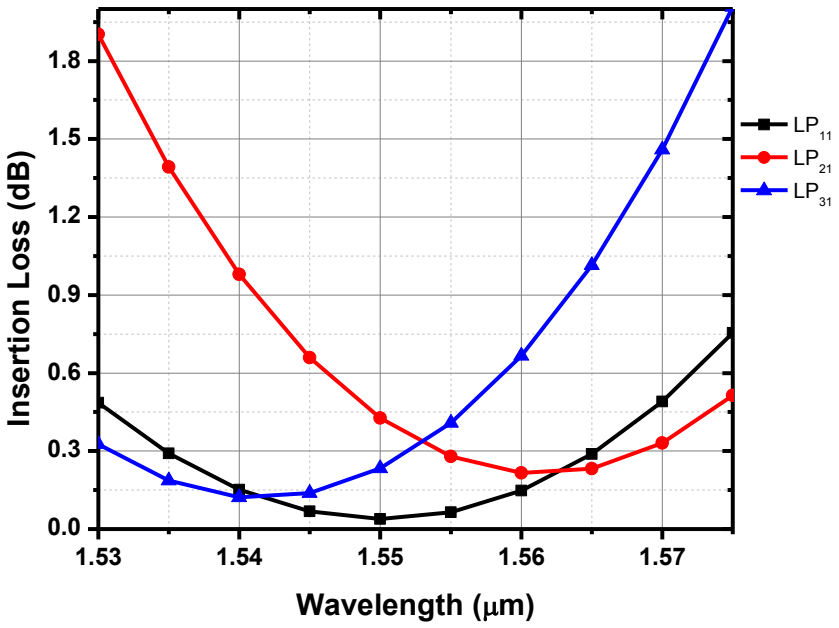

(a)

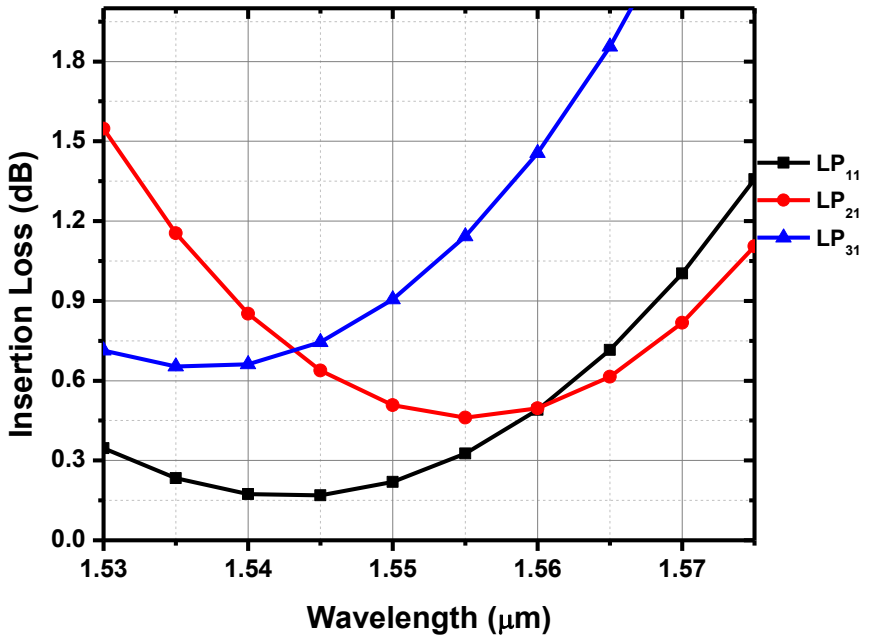

(b)

Figure 5-6: Insertion Loss over the C-Band for the LP_{11}, LP_{21} and LP_{31} (a) Multiplexer, (b) Demultiplexer.

In Figure 5-7, the crosstalk caused by the interferences between the three modes over the C-Band is presented. One can see from Figure 5-7(a) that a crosstalk below -13.8 dB is achieved over the entire C-Band and below -17.7 dB at the wavelength of 1550nm for the multiplexer. The demultiplexer results are given by Figure 5-7(b), where less than -18dB crosstalk is achieved for all three modes at the design wavelength (1550nm). Except for mode LP_{21}, the other modes have a crosstalk below -14dB over the entire C-band.

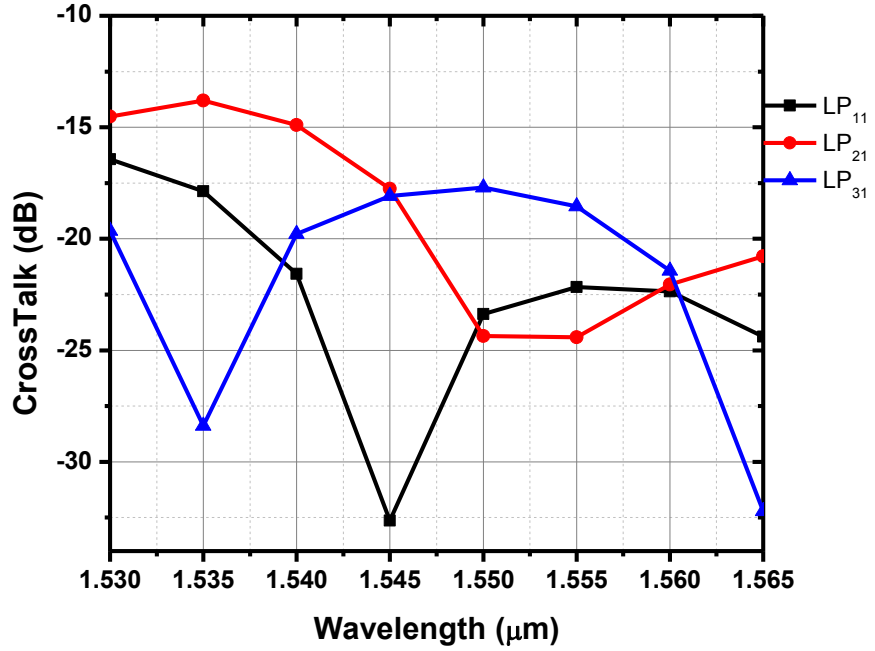

(a)

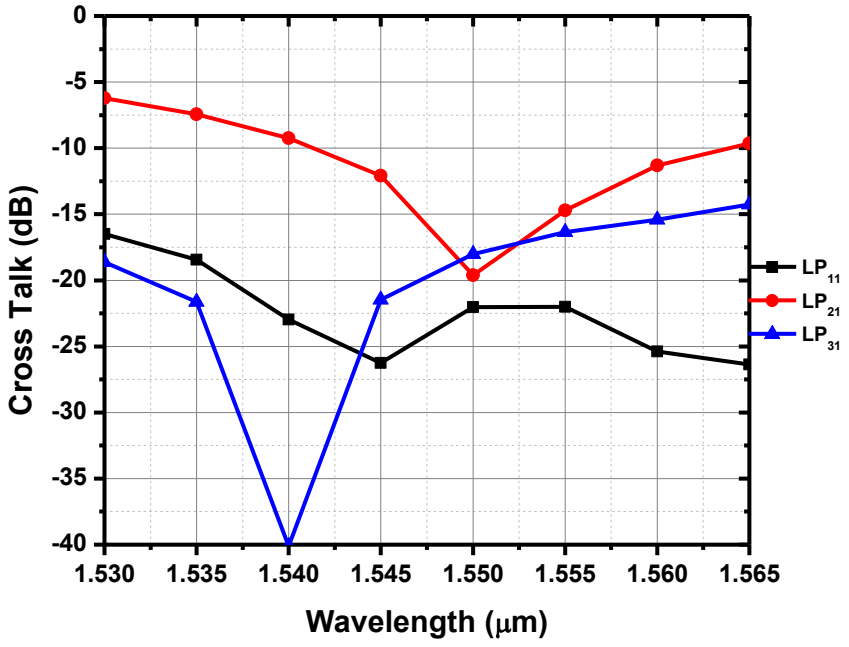

(b)

Figure 5-7: Cross Talk over the C-Band for the LP_{11}, LP_{21} and LP_{31} (a) Multiplexer, (b) Demultiplexer.

5.5. Summary

In this chapter, we have proposed an LP_{01} to LP_{lm} ($l \neq 0$) mode converter structure. The converter structure is a modified version of the structure proposed in chapters 3 and 4. The proposed structure can convert LP_{01} mode to any LP_{lm} with proper choice of its parameters. Furthermore, a case study of three converters (LP_{01} to LP_{11}, LP_{21} and LP_{31}) shows that these modes can be obtained with less than 2dB insertion loss and more than 10dB extinction ratio over the entire C-band. A (de)multiplexer based on directional couplers is also proposed. This device is symmetrical and has an insertion loss below 1.9dB for the entire C-Band. The comparison of these three converters with reported devices in shown in Table 4-2.

Table 5-2: Comparison between the proposed LP_{01} to LP_{11}, LP_{21} and LP_{31} mode converters with the previous works

Mode converter (MC)	IL of the proposed MC	IL of previous works	Features of the previous work
LP_{01}–LP_{11}	0.8 dB	0.3 dB [64]	Experimental, PCF
		0.5 dB [71]	Experimental, PLC
		1.5 dB [43]	Experimental, LPFG
		7.2 dB [31]	Experimental, Phase plates
		9 dB [32]	Experimental, LCOS
LP_{01}–LP_{21}	1.1 dB	0.7 dB [70]	Simulation, Photonic lanterns
		2 dB [89]	Experimental, PLC
		10 dB [51]	Experimental, PLC
LP_{01}–LP_{31}	1.9 dB	NA	

Chapter 6: Conclusion

6.1. Conclusion

Optical space and mode division multiplexing (SDM/MDM) is a promising technique to increase fiber link throughputs and overcome the capacity limitations of the single mode fiber (SMF) and enable the implementation of optical multiple-input and multiple-output (MIMO) systems. MDM transmission is based on few mode fibers (FMFs) and uses the orthogonal guided optical modes (such as the linearly polarized LP modes) to carry different optical signals (each mode is considered as an independent channel and can carry an independent signal). However, mode converters/(de)multiplexers are usually required for MDM systems at optical transmitters and receivers. In other words, mode conversion (from fundamental to higher order modes) and multiplexing are required at optical transmitters, while demultiplexing and mode conversion (from higher-order modes to the fundamental mode) are usually required at optical receivers. Mode conversion and multiplexing can be achieved using either free-space or waveguide-based optics. In this thesis, waveguide-based LP_{01} to LP_{lm} mode converters and (de)multiplexers are proposed to be used in MDM transmission systems. The details of the proposed mode converters and multiplexers are given below:

1. A broadband mode converter structure is proposed to convert the fundamental LP_{01} mode to the high order LP_{02} mode, and vice versa. The converter structure is based on circular waveguides and consists of two-stage tapers. The first stage has two sections: a tapered section followed by a non-tapered section. The tapered section has a starting radius r_1, an ending radius r_2 and a length L_1. The second section has a radius r_2 and a length L_2. The core has a refractive index n_1 and the cladding has a refractive index n_2. The second stage is obtained by inserting a doubly-tapered (from both sides) inner element. This inner element has a refractive index n_3 (n_3 is chosen to be same as n_2 to make the structure easily fabricable) and consists of three sections. The first section has a length L_3, starts with a zero radius and is tapered to an ending radius r_4. This first section is followed by a non-tapered section of length L_4. Then, another tapered section of length L_5 follows, with an ending radius of zero. All taper profiles follow an exponential function to make transition smooth and reduce loss.

The working principle of the proposed structure is as follows. The fundamental mode (LP_{01}) is injected at the left of the first stage. The adiabatically cross-sectional variations cause power to couple from LP_{01} mode to other higher order modes. Since the tapered fiber conserves circular symmetry, it will excite mainly local modes that have the same azimuthal dependence as the injected LP_{01} mode, and these modes are LP_{0m} modes. By careful tuning of the parameters of this stage (mainly r_1, r_2, L_1 and L_2), the power transfer can be forced to occur mostly from LP_{01} to the desired LP_{02}. However, other non-desired modes (LP_{0k}, $k > 2$) can still have a portion of power in this stage. The second stage of the converter is then used to further enhance the desired mode conversion and reduce the non-desired mode conversion. The converter can operate over a very wide band (the O, S and C-band), with less than 1.3 dB (O-band) and 0.1 dB (S- and C- band) insertion loss and higher than 10 dB (O-band) and 19 dB (S- and C-band) extinction ratio. Furthermore, the proposed mode converter is fabricated using femtosecond laser 3D inscription on a borosilicate Corning Eagle 2000 glass. This converter has a total length of 2.22 mm and an insertion loss less than 1 dB over the entire C-band. In addition to the mode converter, a two-mode (de)multiplexer (for LP_{01} and LP_{02}) using a symmetric directional coupler is designed. This (de)multiplexer has an insertion loss of less than 0.5 dB over the entire C-band.

2. With proper parameters selection, the proposed LP_{01} to LP_{02} mode converter structure can convert LP_{01} to any LP_{0m} mode. The structures that convert LP_{01} mode to LP_{02}, LP_{03}, LP_{04}, LP_{05}, LP_{06} and LP_{07} are presented. The insertion losses (IL) of these structures range from 0.1 dB to 3 dB and the extinction ratios are larger than 8 dB over the entire C-band. A mode (de)multiplexer based on directional couplers for the first five modes ($m = 1 \ldots 5$) has also been proposed and analyzed. The performance of this (de)multiplexer shows that all five modes can be multiplexed with an insertion loss ranging from 0.01 dB to 2.7 dB and cross talk below -9 dB over the entire C-Band. To the best of our knowledge, the proposed mode converter outperforms most of the reported LP_{01} to LP_{0m} mode converters.
3. A universal LP_{01} to LP_{lm} mode converter is also proposed. It is based on a modified LP_{01} to LP_{0m} mode converter (MC) structure. The MC is based on tapered circular waveguide which contains several inner structural elements that can be tuned to convert LP_{01} to any desired LP_{lm} mode. As a case study, three converters LP_{01}~LP_{11}, LP_{01}~LP_{21} and LP_{01}~LP_{31} for the

C-band are presented and analyzed. Simulation results show that all three MCs can achieve conversion with an insertion loss between 0.8 dB and 1.9 dB over the entire C-Band. The three obtained modes (LP_{11}, LP_{21} and LP_{31}) are (de)multiplexed using symmetric directional couplers with an insertion loss below 1.9 dB over the entire C-Band.

6.2. Future Work

As a future work, one can enhance the parameters of the proposed mode converters, especially the universal LP_{01}~LP_{lm} MC to decrease the insertion loss and increase the extinction ratio. Instead of relying on brute-force simulation and optimization with numerical solvers to obtain each structure, a strategy or easy-to-follow rule on how the index modulating elements need to be designed and placed in order to achieve a certain mode conversion.

The focus of this thesis was put on the design and performance evaluation of mode converters; however, less effort was given to mode (de)multiplexers, therefore, more study on mode (de)multiplexers is needed to propose a device with less losses and crosstalk. Furthermore, interference between modes (crosstalk) could be deeply studied to identify which modes, among all possible LP_{lm} modes, can be multiplexed together with less losses and crosstalk.

Another research direction complementary to this research is the study of Few-Mode Fibers (FMF). These fibers are the enabling transmission medium for MDM and therefore their impact on the overall performance of the MDM transmission systems should be lit on.

Moreover, adequate MIMO-DSP algorithms should be developed to correctly detect and restore the different signals at the receiver side.

References

[1] R. Essiambre and A. Mecozzi, "Capacity limits in single mode fiber and scaling for spatial multiplexing," in *Optical Fiber Communication Conference*, 2012.

[2] R.-J. R.-J. Essiambre *et al.*, "Capacity Limits of Optical Fiber Networks," *J. Light. Technol.*, 2010.

[3] R. J. Essiambre and R. W. Tkach, "Capacity trends and limits of optical communication networks," in *Proceedings of the IEEE*, 2012.

[4] J. H. Lin, A. Ellis, and D. Rafique, "Capacity Limits of Optical Fibre Based Communications," *Adv. Photonics*, 2011.

[5] D. J. Richardson, J. M. Fini, and L. E. Nelson, "Space-division multiplexing in optical fibres," *Nature Photonics*, vol. 7, no. 5. 2013.

[6] Y. Weng, X. He, and Z. Pan, "Space division multiplexing optical communication using few-mode fibers," *Opt. Fiber Technol.*, 2017.

[7] J. M. Kahn and Keang-Po Ho, "Mode-division multiplexing systems: Propagation effects, performance and complexity," in *OFC*, 2013.

[8] T. Morioka, "Recent progress in space-division multiplexed transmission technologies," in *Optical Fiber Communications Conference (OFC/NFOEC)*, 2013.

[9] G. Li, N. Bai, N. Zhao, and C. Xia, "Space-division multiplexing: the next frontier in optical communication," *Adv. Opt. Photonics*, vol. 6, no. 4, 2014.

[10] T. Mizuno and Y. Miyamoto, "High-capacity dense space division multiplexing transmission," *Opt. Fiber Technol.*, 2017.

[11] S. Randel, "Space-division multiplexed transmission," in *Optical Fiber Communications Conference (OFC/NFOEC)*, 2013.

[12] L. Wang *et al.*, "Linearly polarized vector modes: enabling MIMO-free mode-division multiplexing," *Opt. Express*, 2017.

[13] K. Shi, G. Gordon, M. Paskov, J. Carpenter, T. D. Wilkinson, and B. C. Thomsen, "Degenerate mode-group division multiplexing using MIMO digital signal processing," in *2013 IEEE Photonics Society Summer Topical Meeting Series, PSSTMS 2013*, 2013.

[14] S. O. Arik and J. M. Kahn, "Adaptive MIMO signal processing in mode-division multiplexing," in *Proceedings - 2014 Summer Topicals Meeting Series, SUM 2014*, 2014.

[15] A. Al Amin, A. Li, X. Chen, and W. Shieh, "Mode division multiplexing MIMO-OFDM optical transmission," in *Technical Digest - 2012 17th Opto-Electronics and Communications Conference, OECC 2012*, 2012.

[16] S. O. Arik, D. Askarov, and J. M. Kahn, "MIMO DSP Complexity in Mode-Division Multiplexing," in *Optical Fiber Communication Conference*, 2015.

[17] I. P. Giles, R. Chen, and V. Garcia-Munoz, "Fiber based multiplexing and demultiplexing devices for few mode fiber space division multiplexed communications," in *Conference on Optical Fiber Communication, Technical Digest Series*, 2014.

[18] Y. Xie, S. Fu, M. Zhang, M. Tang, P. Shum, and D. Liu, "Optimization of few-mode-fiber based mode converter for mode division multiplexing transmission," *Opt. Commun.*, 2013.

[19] P. Sillard, D. Molin, M. Bigot-Astruc, K. De Jongh, and F. Achten, "Rescaled Multimode Fibers for Mode-Division Multiplexing," *J. Light. Technol.*, 2017.

[20] M. Kasahara *et al.*, "Design of few-mode fibers for mode-division multiplexing transmission," *IEEE Photonics J.*, 2013.

[21] Y. Sun, R. Lingle, A. McCurdy, D. Peckham, R. Jensen, and L. Gruner-Nielsen, "Few-mode fibers for mode-division multiplexing," in *2013 IEEE Photonics Society Summer Topical Meeting Series, PSSTMS 2013*, 2013.

[22] P. Sillard, M. Bigot-Astruc, D. Boivin, H. Maerten, and L. Provost, "Few-Mode Fiber for Uncoupled Mode-Division Multiplexing Transmissions," *Eur. Conf. Exhib. Opt. Commun.*, 2011.

[23] M. Salsi, C. Koebele, G. Charlet, and S. Bigo, "Mode Division Multiplexed Transmission

with a weakly-coupled Few-Mode Fiber," *Opt. Fiber Commun. Conf.*, 2012.

[24] H. Kubota and T. Morioka, "Few-mode optical fiber for mode-division multiplexing," *Opt. Fiber Technol.*, 2011.

[25] S. Matsuo, Y. Sasaki, I. Ishida, K. Takenaga, K. Saitoh, and M. Koshiba, "Recent Progress on Multi-Core Fiber and Few-Mode Fiber," *2013 Opt. Fiber Commun. Conf. Expo. Natl. Fiber Opt. Eng. Conf.*, 2013.

[26] Y. Sasaki, K. Takenaga, S. Matsuo, K. Aikawa, and K. Saitoh, "Few-mode multicore fibers for long-haul transmission line," *Opt. Fiber Technol.*, 2017.

[27] S. Matsuo, Y. Sasaki, I. Ishida, K. Takenaga, K. Saitoh, and M. Koshiba, "Recent Progress in Multi core and Few mode Fiber," in *Optical Fiber Communication Conference/National Fiber Optic Engineers Conference 2013*, 2013.

[28] K. Nakajima, Y. Goto, T. Matsui, and S. Tomita, "Multi-core fiber technologies for extremely advanced transmission," *16th Opto-Electronics Commun. Conf.*, 2011.

[29] B. J. Puttnam *et al.*, "High capacity multi-core fiber systems," in *2016 21st European Conference on Networks and Optical Communications (NOC)*, 2016.

[30] K. Nakajima, Y. Goto, and S. Tomita, "Recent progress on multi-core fiber," in *Opto-Electronics and Communications Conference (OECC), 2012 17th*, 2012.

[31] R. Ryf *et al.*, "Mode-division multiplexing over 96 km of few-mode fiber using coherent 6×6 MIMO processing," *J. Light. Technol.*, 2012.

[32] M. Salsi *et al.*, "Mode Division Multiplexing of 2 x 100Gb/s Channels using an LCOS based Spatial Modulator," *J. Light. Technol.*, 2011.

[33] N. K. Fontaine, "Devices and Components for Space-Division Multiplexing in Few-Mode Fibers," in *Optical Fiber Communication Conference/National Fiber Optic Engineers Conference 2013*, 2013.

[34] J. Carpenter, B. J. Eggleton, and J. Schröder, "Applications of spatial light modulators for mode-division multiplexing," in *European Conference on Optical Communication,*

ECOC, 2014.

[35] M. Salsi *et al.*, "Mode-division multiplexing of 2 × 100 Gb/s channels using an LCOS-based spatial modulator," *J. Light. Technol.*, 2012.

[36] J. A. Carpenter, B. J. Eggleton, and J. B. Schroeder, "LCOS Based Devices for Mode-division Multiplexing," in *Optical Fiber Communication Conference*, 2015.

[37] D. Askarov and J. M. Kahn, "Long-period fiber gratings for mode coupling in mode-division-multiplexing systems," *J. Light. Technol.*, 2015.

[38] H. Mellah, X. Zhang, and D. Shen, "LP01 to LP0m mode converters using all-fiber two-stage tapers," *Opt. Commun.*, vol. 354, 2015.

[39] S. G. Leon-Saval, "Photonic lanterns for mode division multiplexing," in *MOC 2015 - Technical Digest of 20th Microoptics Conference*, 2016.

[40] K. Saitoh *et al.*, "PLC-based mode multi/demultiplexers for mode division multiplexing," *Opt. Fiber Technol.*, 2017.

[41] J. B. Driscoll, R. R. Grote, B. Souhan, J. I. Dadap, M. Lu, and R. M. Osgood, "Asymmetric Y junctions in silicon waveguides for on-chip mode-division multiplexing," *Opt. Lett.*, 2013.

[42] H. Mellah, X. Zhang, and D. Shen, "Analysis of optical fiber-based LP01<--> LP02 mode converters for the O-, S-, and C-Band," *Appl. Opt.*, vol. 54, no. 17, 2015.

[43] A. Li, X. Chen, A. Al Amin, J. Ye, and W. Shieh, "Space-division multiplexed high-speed superchannel transmission over few-mode fiber," *J. Light. Technol.*, 2012.

[44] C. P. Tsekrekos and D. Syvridis, "All-fiber broadband LP 02 mode converter for future wavelength and mode division multiplexing systems," *IEEE Photonics Technol. Lett.*, 2012.

[45] D. Dai, "Silicon-based Multi-channel Mode (de)multiplexer for On-chip Optical Interconnects," in *Advanced Photonics for Communications*, 2014.

[46] N. Riesen, J. D. Love, and J. W. Arkwright, "Few-core spatial-mode

multiplexers/demultiplexers based on evanescent coupling," *IEEE Photonics Technol. Lett.*, 2013.

[47] J. Xing, Z. Li, X. Xiao, J. Yu, and Y. Yu, "Two-mode multiplexer and demultiplexer based on adiabatic couplers," *Opt. Lett.*, 2013.

[48] Y. Ding, H. Ou, J. Xu, and C. Peucheret, "Silicon photonic integrated circuit mode multiplexer," *IEEE Photonics Technol. Lett.*, 2013.

[49] S. H. Chang *et al.*, "Mode division multiplexed optical transmission enabled by all–fiber mode multiplexer," *Opt. Express*, 2014.

[50] M. Yin, Q. Deng, Y. Li, X. Wang, and H. Li, "Compact and broadband mode multiplexer and demultiplexer based on asymmetric plasmonic–dielectric coupling," *Appl. Opt.*, 2014.

[51] N. Hanzawa *et al.*, "Two-mode PLC-based mode multi/demultiplexer for mode and wavelength division multiplexed transmission," *Opt. Express*, 2013.

[52] N. Hanzawa *et al.*, "Mode multi/demultiplexing with parallel waveguide for mode division multiplexed transmission," *Opt. Express*, vol. 22, no. 24, 2014.

[53] W. Chang *et al.*, "Ultra-compact mode (de) multiplexer based on subwavelength asymmetric Y-junction," *Opt. Express*, 2018.

[54] Z. Zhang, Y. Yu, and S. Fu, "Broadband On-Chip Mode-Division Multiplexer Based on Adiabatic Couplers and Symmetric Y-Junction," *IEEE Photonics J.*, 2017.

[55] H.-C. Chung, K.-S. Lee, and S.-Y. Tseng, "Short and broadband silicon asymmetric Y-junction two-mode (de)multiplexer using fast quasiadiabatic dynamics," *Opt. Express*, 2017.

[56] M. Lan, S. Yu, S. Cai, L. Gao, and W. Gu, "Mode multiplexer/demultiplexer based on tapered multi-core fiber," *IEEE Photonics Technol. Lett.*, 2017.

[57] S. G. Leon-Saval, N. K. Fontaine, and R. Amezcua-Correa, "Photonic lantern as mode multiplexer for multimode optical communications," *Opt. Fiber Technol.*, 2017.

[58] Z. S. Eznaveh, J. E. Antonio-Lopez, J. C. A. Zacarias, A. Schülzgen, C. M. Okonkwo, and

R. A. Correa, “All-fiber few-mode multicore photonic lantern mode multiplexer,” *Opt. Express*, 2017.

[59] D. Dai, Y. Tang, and J. E. Bowers, “Mode conversion in tapered submicron silicon ridge optical waveguides,” *Opt. Express*, 2012.

[60] S. Gross, N. Riesen, J. D. Love, and M. J. Withford, “Three-dimensional ultra-broadband integrated tapered mode multiplexers,” *Laser Photonics Rev.*, vol. 8, no. 5, 2014.

[61] N. Riesen, S. Gross, J. D. Love, and M. J. Withford, “Femtosecond direct-written integrated mode couplers,” *Opt. Express*, vol. 22, no. 24, 2014.

[62] R. Ryf *et al.*, “Photonic-lantern-based mode multiplexers for few-mode-fiber transmission,” in *Conference on Optical Fiber Communication, Technical Digest Series*, 2014.

[63] a Witkowska, S. G. Leon-Saval, A. Pham, and T. a Birks, “All-fiber LP11 mode convertors.,” *Opt. Lett.*, 2008.

[64] K. Lai, S. G. Leon-Saval, a Witkowska, W. J. Wadsworth, and T. a Birks, “Wavelength-independent all-fiber mode converters.,” *Opt. Lett.*, 2007.

[65] S. Yerolatsitis and T. A. Birks, “Three-mode multiplexer in photonic crystal fibre,” in *39th European Conference and Exhibition on Optical Communication (ECOC 2013)*, 2013.

[66] M. Skorobogatiy *et al.*, “Quantitative characterization of higher-order mode converters in weakly multimoded fibers.,” *Opt. Express*, 2003.

[67] A. Al Amin, A. Li, S. Chen, X. Chen, G. Gao, and W. Shieh, “Dual-LP_11 mode 4x4 MIMO-OFDM transmission over a two-mode fiber,” *Opt. Express*, 2011.

[68] N. Riesen and J. D. Love, “Tapered velocity mode-selective couplers,” *J. Light. Technol.*, 2013.

[69] S. Yerolatsitis and T. a Birks, “Tapered Mode Multiplexers for Single Mode to Multi Mode Fibre Mode Transitions,” *Opt. Fiber Commun. Conf.*, 2015.

[70] A. M. Velazquez-Benitez *et al.*, "Six Spatial Modes Photonic Lanterns," in *Optical Fiber Communication Conference*, 2015.

[71] T. Uematsu *et al.*, "Low-loss and broadband PLC-type mode (de)multiplexer for mode-division multiplexing transmission," in *Optical Fiber Communication Conference/National Fiber Optic Engineers Conference 2013*, 2013.

[72] N. Hanzawa *et al.*, "PLC-based four-mode multi/demultiplexer with LP11 mode rotator on one chip," *J. Light. Technol.*, 2015.

[73] J. Wang *et al.*, "Ultrabroadband silicon-on-insulator polarization beam splitter based on cascaded mode-sorting asymmetric Y-junctions," *IEEE Photonics J.*, 2014.

[74] C. P. Tsekrekos and D. Syvridis, "Symmetric few-mode fiber couplers as the key component for broadband mode multiplexing," *J. Light. Technol.*, vol. 32, no. 14, 2014.

[75] W. Klaus *et al.*, "Advanced Space Division Multiplexing Technologies for Optical Networks," *J. Opt. Commun. Netw.*, 2017.

[76] K. N. Fontaine, "Devices and components for space-division multiplexing in few-mode fibers," in *Optical Fiber Communications Conference (OFC/NFOEC)*, 2013.

[77] J.-P. Bérubé and R. Vallée, "Femtosecond laser direct inscription of surface skimming waveguides in bulk glass," *Opt. Lett.*, 2016.

[78] J.-P. Bérubé *et al.*, "Femtosecond laser direct inscription of mid-IR transmitting waveguides in BGG glasses," *Opt. Mater. Express*, 2017.

[79] D. Marcuse, "Coupled-Mode Theory for Anisotropic Optical Waveguides," *Bell Syst. Tech. J.*, 1975.

[80] J. R. Grenier, L. A. Fernandes, and P. R. Herman, "Femtosecond laser inscription of asymmetric directional couplers for in-fiber optical taps and fiber cladding photonics," *Opt. Express*, 2015.

[81] a. Fuerbach *et al.*, "Direct writing of photonic devices using femtosecond laser pulses," *Transparent Opt. Networks (ICTON), 2010 12th Int. Conf.*, 2010.

[82] C. Florea and K. A. Winick, “Fabrication and characterization of photonic devices directly written in glass using femtosecond laser pulses,” *J. Light. Technol.*, 2003.

[83] R. Osellame *et al.*, “Femtosecond laser writing of symmetrical optical waveguides by astigmatically shaped beams,” *Integr. Opt. Photonic Integr. Circuits*, 2004.

[84] R. Osellame *et al.*, “Femtosecond writing of active optical waveguides with astigmatically shaped beams,” *J. Opt. Soc. Am. B*, 2003.

[85] S. Ghosh, B. P. Pal, R. K. Varshney, and G. P. Agrawal, “Transverse localization of light and its dependence on the phase front curvature of the input beam in a disordered optical waveguide lattice,” *J. Opt.*, 2012.

[86] S. Ghosh, B. P. Pal, and R. K. Varshney, “Role of optical nonlinearity on transverse localization of light in a disordered one-dimensional optical waveguide lattice,” *Opt. Commun.*, 2012.

[87] N. Bhatia, K. C. Rustagi, and J. John, “Single LP(0,n) mode excitation in multimode fibers.,” *Opt. Express*, 2014.

[88] J. Carpenter, B. C. Thomsen, and T. D. Wilkinson, “Mode division multiplexing of modes with the same azimuthal index,” *IEEE Photonics Technol. Lett.*, 2012.

[89] N. Hanzawa; K. Saitosh; T. Sakamoto; K. Tsujikawa; T. Uematsu; M.Koshiba; F. Yamamoto, “Three-mode PLC-type multi/demultiplexer for mode-division multiplexing transmission,” *9th Eur. Conf. Exhib. Opt. Commun. (ECOC 2013)*, pp. 1–3, 2013.

[90] D. Gloge, “Weakly guiding fibres,” *Appl. Opt.*, 1971.

[91] A. W. Snyder, “Weakly guiding optical fibers,” *J. Opt. Soc. Am.*, 1980.

[92] J. Arnaud, “Optical waveguide theory,” *Optical and Quantum Electronics*. 1980.

[93] K. Okamoto, “Wave Theory of Optical Waveguides,” in *Fundamentals of Optical Waveguides*, 2006.

[94] C. Freude, Wolfgang; Koos, “Optical Waveguides and Fibers,” *Fundam. Photonics*, 2000.

[95] R. Lingle, D. W. Peckham, A. McCurdy, and J. Kim, “Light-Guiding Fundamentals and Fiber Design,” in *Specialty Optical Fibers Handbook*, 2007.

[96] K. Okamoto, *Fundamentals of Optical Waveguides*. 2006.

[97] K. Okamoto, “Optical Fibers,” in *Fundamentals of Optical Waveguides*, 2006.

[98] S. Pillay, D. Kumar, H. Azhar, and A. B. Rashid, “Weakly Guiding Fibers and LP Modes in Circular and Elliptical Waveguides,” *J. Electromagn. Anal. Appl.*, 2013.

[99] A. W. Snyder and W. R. Young, “Modes of optical waveguides,” *J. Opt. Soc. Am.*, 1978.

[100] J. R. Qian and W. P. Huang, “LP Modes and Ideal Modes on Optical Fibers,” *J. Light. Technol.*, 1986.

[101] J. R. Qian and W. P. Huang, “Coupled-Mode Theory for LP Modes,” *J. Light. Technol.*, 1986.

[102] D. G. Hall, “Vector-beam solutions of Maxwell’s wave equation,” *Opt. Lett.*, 1996.

[103] C. Yeh, “Guided-Wave modes in cylindrical optical fibers,” *IEEE Trans. Educ.*, 1987.

[104] X. Q. Jin, R. Li, D. C. O’Brien, and F. P. Payne, “Linearly polarized mode division multiplexed transmission over ring-index multimode fibres,” in *2013 IEEE Photonics Society Summer Topical Meeting Series, PSSTMS 2013*, 2013.

[105] J. Bures, “1 Vector Wave Equations,” *Guid. Opt.*, 2009.

[106] “LP modes.” [Online]. Available: https://www.rp-photonics.com/lp_modes.html. [Accessed: 20-Aug-2004].

[107] K. Thyagarajan, A. K. Ghatak, and A. Sharma, “Vector modes of an optical fiber in the weakly guiding approximation,” *J. Light. Technol.*, 1989.

[108] I. Gómez-Castellanos, “Intensity distributions and cutoff frequencies of linearly polarized modes for a step-index elliptical optical fiber,” *Opt. Eng.*, 2007.

[109] A. W. Snyder and J. D. Love, *Optical Waveguide Theory*. 1983.

APPENDIX: Linearly Polarized (LP) Modes

A.1. Introduction

In optical communication systems, the used waveguides are generally weakly guiding [90]–[97], which means the difference between the refractive index of the core to the cladding is typically less than 1%. In addition to that, the profile of transverse refractive index is radially symmetric and depends only on the radial coordinate r and not on the azimuthal coordinate ϕ as shown by Figure A-1. This fact simplifies the solution of the fiber modes, resulting in linearly polarized (LP) modes [98]–[104].

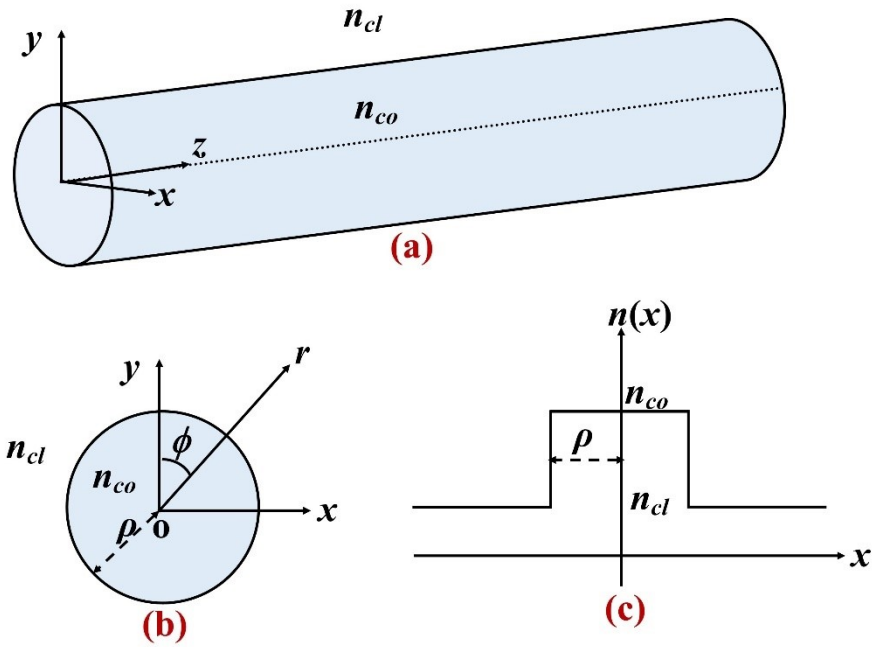

Figure A-1: (a) An optical fiber, (b) the cross-section, (c) the refractive index profile.

Therefore, the wave equation for the complex electric field profile $E(r,\phi)$ in cylindrical coordinates is given by [105][106]:

$$\frac{\partial^2 E}{\partial r^2} + \frac{1}{r}\frac{\partial E}{\partial r} + \frac{1}{r^2}\frac{\partial^2 E}{\partial \phi^2} + \beta E = 0 \qquad (A.1)$$

where β is the imaginary part of the propagation constant.

Due to the radial symmetry, $E(r,\phi)$ can be given by:

$$E(r,\phi) = \Psi(r)\begin{Bmatrix}\cos(l\phi)\\ \sin(l\phi)\end{Bmatrix} \qquad (A.2)$$

where l is called the mode azimuthal number, which must be an integer. The cosine and sine solutions refer to even and odd modes respectively. The resulting scalar radial equation will be:

$$\frac{d^2\Psi_l(r)}{dr^2} + \frac{1}{r}\frac{d\Psi_l(r)}{dr} + \left(n^2(r)k^2 - \frac{l^2}{r^2} - \beta^2\right)\Psi_l(r) = 0 \qquad (A.3)$$

where k is the vacuum wavenumber given by $k = \frac{2\pi}{\lambda}$ and $n(r)$ is the refractive index.

For a two-layer step-index fiber, such as the one shown in fig. A-1, the refractive index $n(r)$ is given by:

$$n(r) = \begin{cases} n_{co}; & r \le \rho \\ n_{cl}; & r > \rho \end{cases} \qquad (A.4)$$

Where ρ is the radius of the fiber core delimiting the core-cladding interface.

In this case, the effective index n_{eff} defined as:

$$n_{eff} = \frac{\beta}{k} \qquad (A.5)\ ;$$

for guided modes is:

$$n_{cl} < n_{eff} \le n_{co} \qquad (A.6)$$

For a given wavelength λ, solutions for the fiber guided modes (solutions that tend to zero for r going to infinity) exist for certain discrete values of β [107]. These values are noted as β_{lm}, where l is the azimuthal index (starting from 0) and m starts from 1 to some maximum value.

In the case of step-index fibers, solutions for the core and cladding part of the radial equation involve a Bessel function $J_l(Ur)$ and a modified Bessel function $K_l(Wr)$ respectively [102][108], where

$$U = \rho\sqrt{n_{co}^2 k^2 - \beta^2} \qquad (A.7)$$

And

$$W = \rho\sqrt{\beta^2 - n_{cl}^2 k^2} \qquad (A.8)$$

With:

$$V^2 = U^2 + W^2 = \rho^2(n_{co}^2 - n_{cl}^2)k^2 = (k\rho NA)^2 \qquad (A.9)$$

Where V is the normalized frequency and NA is the numerical aperture.

Now, the solutions the$\Psi_l(r)$ can be given by:

$$\Psi_l(r) = \begin{cases} \dfrac{J_l\left(\dfrac{Ur}{\rho}\right)}{J_l(U)} & r \le \rho, \\ \dfrac{K_l\left(\dfrac{Wr}{\rho}\right)}{K_l(W)} & r > \rho \end{cases} \qquad (A.10)$$

Applying the continuity of $\Psi_l(r)$ in $r = \rho$, we get the following eigenvalue equation:

$$U\frac{J_{l-1}(U)}{J_l(U)} = -W\frac{K_{l-1}(W)}{K_l(W)} \qquad (A.11)$$

Since equation (A.9) sets a relationship between W, U and V, therefore, for a given value of V and l, the solutions for equation (A.11) are discrete values U_{lm} (m is a non-zero integer) representing a guided mode LP_{lm}. Every value of U_{lm} of guided mode LP_{lm} lies between two limiting values: U_{min} (which is the cut-off value) and U_{max}. These two limiting values are the zeros

Indeed, there are two distinct cases to consider: $l = 0$ and $l > 0$.

$l = 0$: zeros of $J_1(U) < U_{0m} <$ zeros of $J_0(U)$.

$l > 0$: zeros of $J_{l-1}(U) < U_{lm} <$ zeros of $J_l(U)$.

Table A-1 gives the bounding values of the first few U_{lm} and Figure A-2 shows the first four Bessel functions of the first kind J_l showing their first few zeros.

Table A-1: The bounding values of the first few U_{lm}.

l	m	U_{min}	U_{max}	LP Mode
0	1	0	2.4048	LP_{01}
	2	3.8317	5.5201	LP_{02}
	3	7.0156	8.6537	LP_{03}
1	1	2.4048	3.8317	LP_{11}
	2	5.5201	7.0156	LP_{12}
	3	8.6537	10.1735	LP_{21}
2	1	3.8317	5.1356	LP_{31}
	2	7.0156	8.4172	LP_{32}
	3	10.1735	11.6198	LP_{33}
$l > 2$	m	$(m+1)^{th}$ Zero of J_{l-1}	$(m+1)^{th}$ Zero of J_l	LP_{lm}

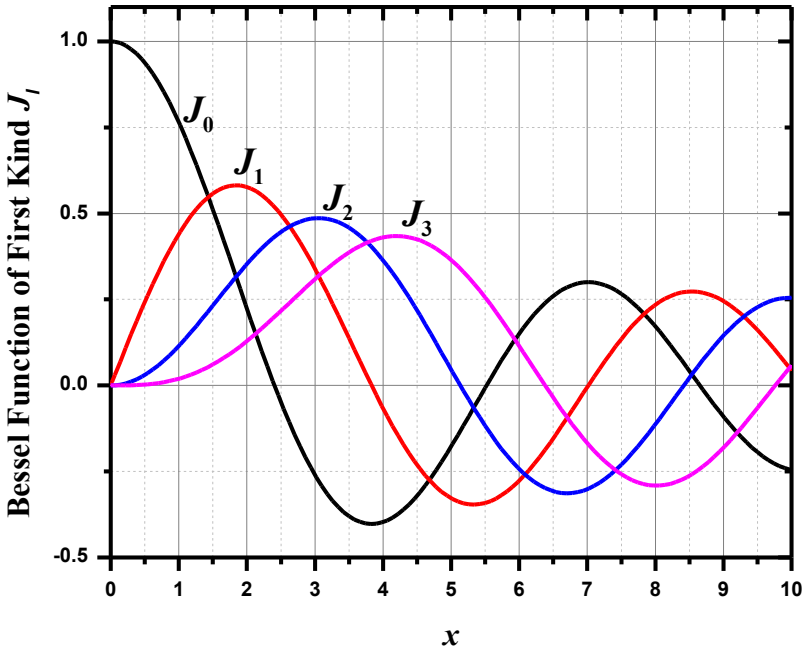

Figure A-2: The first four Bessel functions of the first kind

The value of the normalized frequency V determines the number of LP modes existing in the fiber. The higher the V number of the fiber, the more guided modes exist. For V below 2.405, there is only a single guided mode (the fundamental LP_{01} mode) and the fiber is a single-mode fiber. For large V, the fiber becomes multimode fiber and the number of supported LP modes is proportional to V^2[109]. Table A-2 gives the minimum V for each mode to be supported in the fiber. LP_{01} is not in the table because it always exists.

Table A-2: The V number for the first few LP_{lm} modes

V	2.405	3.832	5.136	5.520	6.380	7.016	7.588	8.417	8.654	8.771
Mode	LP_{11}	LP_{21} LP_{02}	LP_{31}	LP_{12}	LP_{41}	LP_{22} LP_{03}	LP_{51}	LP_{32}	LP_{13}	LP_{61}
V	9.761	9.936	10.173	11.065	11.086	11.619	11.792	12.225	12.339	13.015
Mode	LP_{42}	LP_{71}	LP_{04} LP_{23}	LP_{52}	LP_{33}	LP_{81}	LP_{14}	LP_{91}	LP_{62}	LP_{43}

A.2. Polarization of the LP modes

LP modes of nonzero azimuthal index ($l > 0$) have two independent solutions: an even solution one with $cos(l\phi)$ and an odd solution with $sin(l\phi)$. Each of these two solutions can have two possible polarization: x and y, resulting in four-fold degenerate modes: $LP_{lm}^{e,x}, LP_{lm}^{e,y}, LP_{lm}^{o,x}, LP_{lm}^{o,y}$. Modes with zero azimuthal index ($l = 0$) are two-fold degenerate: LP_{0m}^{x}, LP_{0m}^{y}. **Error! Reference s ource not found.** shows an illustration of these two polarizations of the electric field of some LP_{lm} modes and Figure . represents the 2-D intensity profile of some modes.

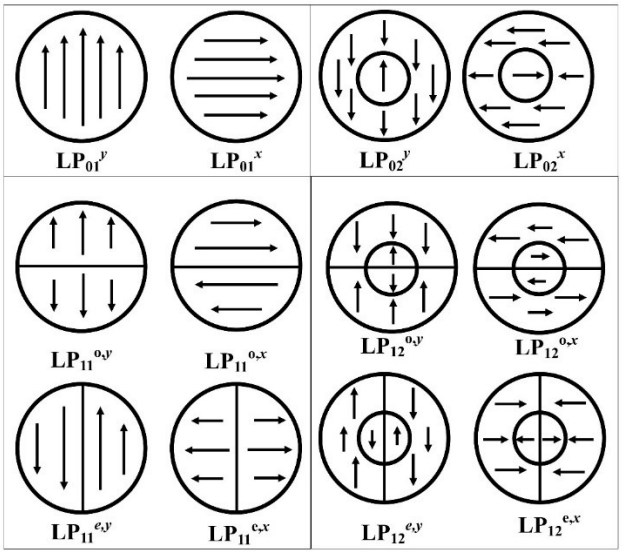

Figure A-3: The polarization of some LP_{lm} modes.

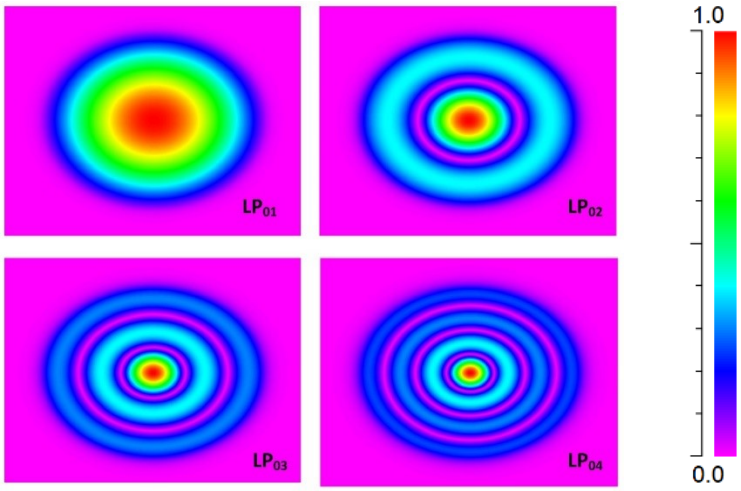

(a)

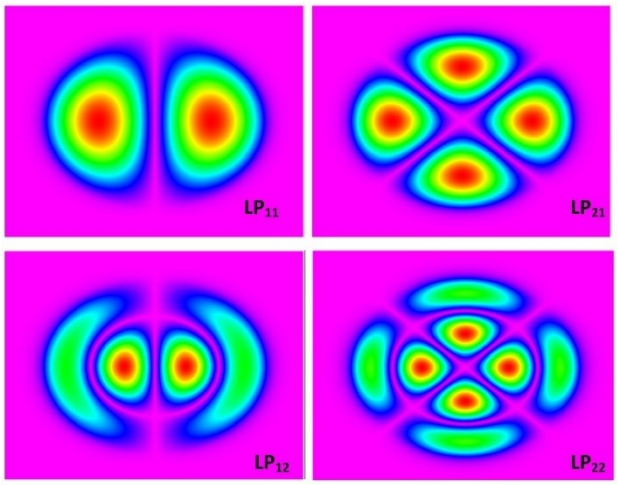

(b)

Figure A-4: Intensity profile of some LP_{lm} modes (a) $l = 0$, (b) $l \neq 0$

Publications

Journals:

1. **H. Mellah** and X. Zhang, "A Universal LP_{01} to LP_{lm} Mode Converter Based on a Bulk Circular Waveguide," OSA Continuum, 1(2), pp. 426–437, 2018.

2. **H. Mellah**, S. M. Mirjalili and X. Zhang, "Design Optimization of a Waveguide-Based LP01 to LP0m Mode Converter by using artificial intelligence technique," Electronics Letters, 54(11), pp.703–705, 2018.

3. D. Shen, C. Wan, C. Ma, **H. Mellah**, X. Zhang, H. Yuan and W. Ren, "A Novel Optical Waveguide LP01/LP02 Mode Converter," Optics Communications, 418, pp. 98–105, 2018

4. **H. Mellah**, J.-P. Bérubé, R. Vallée and X. Zhang, "Fabrication of a LP01 to LP02 Mode Converter Embedded in Bulk Glass Using Femtosecond Direct Inscription." Optics Communications, 410, pp. 475-478, 2018.

5. **H. Mellah**, X. Zhang and D Shen, "Analysis of optical fiber-based LP01↔ LP02 mode converters for the O-, S-, and C-Band." Applied optics, 54(17), pp.5568–5575, 2015.

6. **H. Mellah**, X. Zhang and D. Shen, "LP01 to LP0m mode converters using all-fiber two-stage tapers". Optics Communications, 354, pp.148–153, 2015.

Conferences:

1. **H. Mellah**, X. Zhang, and D. Shen, "Mode multiplexers/demultiplexers for space division multiplexed optical fiber communications". In 14th International Conference on Optical Communications and Networks (ICOCN 2015) [invited], 2015.

2. **H. Mellah**, X. Zhang, and D. Shen, "Two-stage taper fiber-based mode converters between LP01 and LP0m". In 14th International Conference on Optical Communications and Networks (ICOCN 2015), pages 1–3, July 2015.